NATIONAL INSTITUTE OF IMMUNOLOGY

ANNUAL REPORT

2008-09

CONTENTS

RESEARCH REPORTS

IMMUNITY and INFECTION

IMMUNITY AND INFECTION

Biology of T lymphocytes

Principal Investigator: Vineeta Bal

Project Associates/Fellows: S Moanaro Biswas
Suparna Barua

PhD Students: Bharathi Vishwanathan
Hamid Mattoo
Rituparna Das
Shipra Thukral
Vidya Ranganathan

Collaborators: Anna George
Apurva Sarin, *NCBS, Bangalore*
B Ravindran *ILS, Bhubaneswar*
Jeannine M Durdik, *Univ Arkansas, USA*
Satyajit Rath

The theme of the ongoing projects for this reporting year is T cell and macrophage fate decisions encompassing differentiation, proliferation, survival and death.

Objectives

1. To understand the effect of ageing on T cell differentiation, function and survival.
2. To study the role of variation in cell surface marker density in T cell function.
3. To study the regulation of macrophage survival and death in response to various stimuli.

1. To understand the effect of ageing on T cell differentiation, function and survival

We have used two approaches to understand the effect of ageing on T cell differentiation, function and survival. In the first approach we have continued to use naive CD4 cells from young [YNCD4] and aged [ANCD4] mice; and in another approach we have transferred T cells to congeneic mice and allowed them to age *in vivo*. In the first approach we looked for the contribution of DNA repair mechanisms in cell survival versus death. During cell division cellular DNA develops strand breaks which are repaired by the cell as the cell division progresses. If these breaks are not repaired efficiently the cell might die. We observed that activated ANCD4 cells show higher proportion of DNA strand breaks over a 24 hour period as compared to YNCD4 cells. Using comet assay to score individual T cell breaks we find a statistically significant increase in strand breaks. In support of this we see that the ANCD4 cells which receive activating stimulus and upregulate an early activation marker CD69 as early as 6 hours post-activation also show higher proportion of apoptotic cells as scored by Annexin V using flow cytometry. If the proportion of DNA breaks is further enhanced by gamma-radiation, ANCD4 cells which show CD69 upregulation are even more susceptible to apoptosis than YNCD4 cells are. Characterisation of the death of ANCD4 cells shows that mitochondrial membrane permeability is lost by larger proportion of these cells 12

hours post-activation and the trend continues upto 24 hours. Fewer ANCD4 cells enter cell cycle and continue towards completion, thus showing higher proportion of subdiploid cells and lower proportion of cells with >2n DNA content as compared to YNCD4 cells. All these changes are observed in ANCD4 cells even before they undergo their first division as scored by the CFSE dye-dilution method. In contrast ANCD4 cells which do not receive activating stimuli survive much better than their YNCD4 counterparts. These results indicate that ANCD4 cells start dying soon after they receive the activation signal and even before they undergo first cell division.

Results from our collaborators [Prof Durdik's Lab] showed that ANCD4 cells show two peculiar defects; firstly, their ability to produce lactate in response to metabolic stress imposed by activating signal is poor and secondly, LC3, a microtubule associated protein which is a marker of autophagic vacuoles inside the cells, is very minimally detectable in activated ANCD4 cells. We further showed that indeed autophagy is poorly used by ANCD4 cells as a survival mechanism. For this we blocked autophagy in activated ANCD4 and YNCD4 cells by 3-methyl adenine [3-MA] and looked for cell survival. While YNCD4 cells showed enhanced death in presence of 3-MA, making the death comparable to that observed in ANCD4 cells in absence of 3-MA, ANCD4 cells showed no further enhancement in death in presence of 3-MA. Thus indicating that YNCD4 cells use autophagic mechanisms as a survival strategy and prevent cellular death in conditions of stress, ANCD4 cells seem to be particularly ineffective in using this mode of cell survival. Results so far indicate that relatively compromised metabolic competence, inability to use autophagy as a survival mechanism, poor DNA damage repair process and leaky mitochondria make ANCD4 cells more susceptible to death on activation mediated stress than YNCD4 cells.

We also observed that this compromised ability to face activation related stress is not restricted to the first cell division period, but continues with succeeding cell divisions as well. Thus, upto 72 hours a somewhat larger proportion of ANCD4 cells continue to die at higher frequency with successive cell divisions as shown by cell cycle analysis, CFSE dilution, mitochondrial membrane permeabilisation assays and viable cell counts. However, not all ANCD4 cells appear equally susceptible to death and a subset of them seems to survive even beyond 96 hours of stimulation. When these surviving cells from aged mice are compared to similarly treated cells from young mice there is no difference in their ability to proliferate, upregulate early and late activation markers as well as survive. Thus ANCD4 cells *ex vivo* appear to consist of two subsets - one with higher susceptibility to death and the other normal. We have sorted naive and EM cells from young and aged mice and checked for their characteristics in view of the above findings showing existence of potential subsets. We find that *ex vivo* EM cells continue to show poor proliferation but lose their susceptibility to death. These data seem to indicate that the *in vivo* environment in young and aged mice affects the cells slowly and variably. It is likely that individual age of naive cells in the host and hence the duration over which it is exposed to the *in vivo* environment before being taken out and tested might determine its outcome. It is thus likely that relatively newly born naive CD4 cells in aged mice might behave similar to those from young mice and naive cells hanging around for longer duration in mice may get more adversely affected by the aged environment.

If it is the environment in aged/ageing mice which is adversely affecting the function and differentiation of naive T cells, we have initiated experiments to test this where we have transferred T cell receptor transgenic T cells in congeneic mice and parked them for

various durations. The effect of such ageing of T cells is of interest and will be followed for evaluating ageing effects.

2. To study the role of variation in cell surface marker density in T cell function

Most of the surface markers on a defined subset of immune cells show a normal distribution - when analysed by flow cytometry it is seen to be spanning over one log or more. For example staining of T cell receptor, CD4 or CD8 on T cells shows such a distribution. Even TCR transgenic cells show a similar pattern. The question we are attempting to address is whether there is any variation in the function and differentiation ability of cells which are near outliers in the normal distribution curves for such markers on a given cell type. If so, what is the developmental and/or functional significance of such findings. Our preliminary data on sorted naive CD4low and CD4high cells, which have nearly 10-fold difference in their staining intensity of CD4, show that the CD4 high naive cells respond better to activating stimuli as compared to CD4 low cells.

3. *To study the regulation of macrophage survival and death in response to various stimuli*

In addition to some progress in characterising signalling events contributing to enhanced death of macrophages from Xid mice activated with lipopolysaccharide and interferon-gamma, we have some data on another aspect of macrophage death now. It is known that macrophages which phagocytose infectious agents are capable of killing them but many macrophages also die in the process of pathogen clearance. A balance between survival of pathogen and survival of macrophages is crucial in the equation of host resistance to pathogen invasion, infection and disease. We have confirmed published reports which show that macrophages expressing Nef protein of HIV survive better when exposed to apoptosis inducing stimuli such as TNFa. We are working on the hypothesis that co-infection of macrophages contributes to the synergistic interactions between HIV and mycobacterial disease. Using *M.smegmatis* as a model pathogen we have initiated this work.

Publications

Original peer-reviewed articles

1. Chaudhry A, Das SR, Jameel S, George A, Bal V, Mayor S and Rath S (2008) HIV-1 Nef induces a Rab 11-dependent routing of endocytosed immune costimulatory proteins CD80 and CD86 to the Golgi. *Traffic* **9**:1925-1935.

Reviews / Proceedings

1. Bal V, Subramanian V and Murthy L (2008) Contraceptive research: Is there a gender-neutral approach? **In**: *Women's studies in India: a reader* (Ed: John ME), Penguin Books India, New Delhi, 371-380.

2. Bal V and Sharma V (2008) Women scientists meet in Delhi on international women's day. *Current Science* **95**:709-711.

3. Bal V (2008) Why women scientists in India need affirmative action. *Nature India* doi:10.1038/nindia.2008.322; Published online 20 November 2008.

Biology of animal viruses

Principal Investigator: Sudhanshu Vrati

Project Associates/Fellows: Mohan Babu Appaiahgari
Himani Sharma
APS Rathore

PhD Students: Manu Anantapadma
Jayita
Deepika

Collaborators: Rajni Rani
Nita Bhandari *SAS, New Delhi*

A. Japanse encephalitis virus

Japanese encephalitis virus (JEV) is a member of the *Flaviviridae* family of animal viruses that contains several other medically important viruses such as Dengue and Yellow fever. JEV is a major cause of human encephalitis and is responsible for considerable mortality and morbidity in India. Frequent epidemics of Japanese encephalitis (JE) are being reported from various parts of India and JEV has become endemic in several parts of the country. We are studying virus replication and developing novel vaccine candidates against JE.

We have previously described DNA vaccine candidates against JEV that were immunogenic in mice. We have now evaluated their immunogenicity in rhesus monkeys (*Macaca mulatta*) and compared it with the commercial mouse brain-derived, formalin-inactivated vaccine. Groups of four monkeys were immunized with either pMEa (expressing the anchored form of the envelope protein along with the pre-membrane protein of JEV) or pMEs (expressing the secretory form of the envelope protein along with pre-membrane protein of JEV) by intra-muscular (IM, using needle) or intra-dermal (ID, using gene gun) routes. Following primary immunization with 1 mg plasmid DNA given IM, or 5 microgram plasmid DNA given ID, the monkeys were boosted after 1 and 2 months with 0.5 mg DNA given IM or 5 microgram DNA given ID, and observed for a period of 6 months. After the second booster, most of the monkeys sero-converted and developed JEV neutralizing antibodies, albeit of low titer. Importantly however, following a sham challenge with the mouse brain-derived inactivated JEV vaccine given 6 months after immunization, the neutralizing antibody titers rose rapidly indicating a vigorous anamnestic response. Based on the JEV neutralizing antibody response following the vaccination and the extent of anamnestic response generated in the immunized monkeys, plasmid pMEa was superior to pMEs. This study indicates that the JEV candidate DNA vaccine is capable of generating protective levels of JEV neutralizing antibodies in rhesus monkeys and prime the immune system effectively against a subsequent exposure to JEV.

We have previously shown that three proteins of 32, 35 and 50 kDa bind the 3'-stem-loop (SL) structure of JEV 3'-NCR, and one of these was identified as 36-kDa Mov34 protein. Using electrophoretic mobility-shift and UV-cross-linking assays, and yeast three-hybrid system, we now show that La protein binds the 3'-SL of JEV. The binding was stable under

high salt condition (300 mM KCl) and affinity of RNA protein interaction was high; dissociation constant (K_d) for La binding with 3'-SL was 12 nM, indicating that this RNA-protein interaction is physiological plausible. Only N-terminal half of La protein containing RNA-recognition motifs 1 and 2 interacted with JEV RNA. RNA toe-printing assay followed by deletion mutagenesis showed that La protein bound to predicted loop structures in 3'-SL RNA. Further, we showed that siRNA-mediated down regulation of La protein resulted in repression of JEV replication in cultured cells. These data suggest that La protein is involved in JEV replication.

We have constructed recombinant adenoviruses expressing siRNAs to defferent sections of JEV genome. An adenovirus recombinant expressing siRNA directed against the genome circularization sequence was shown to significantly inhibit JEV replication in cultured cells. Additionally, antisense molecule directed to this sequence in JEV genome also inhibited virus replication in cultured cells.

B. Rotavirus

Rotavirus infections are estimated to cause approximately 500,000 deaths annually, predominantly in developing countries. In India, one child in 250 will die from rotavirus diarrhea and nearly 125,000 rotavirus attributable deaths occur among children under fives annually. The development and introduction of a rotavirus vaccine, therefore, has been accorded high priority globally.

A neonatal rotavirus candidate vaccine 116E, cGMP produced by M/s Bharat Biotech International (BBIL), Hyderabad, was tested in a double blind, placebocontrolled dose escalation trial. Two dosages of the Vero-cell adapted vaccine were evaluated. 187 infants were enrolled in the 10^4 ffu and 182 in the 10^5 ffu dosage study, in a 1:1 randomization with placebo. Infants received the vaccine at 8, 12 and 16 weeks, separately from routine vaccines. No significant differences in clinical adverse events or laboratory toxicity were observed between vaccine and placebo recipients. There were no vaccine related serious adverse events. A four-fold increase in rotavirus IgA titer was observed in 66.7% and 64.5% of infants after one administration and 62.1% and 89.7% of infants after three administrations of the 10^4 ffu and 10^5 ffu dosages, respectively; the differences with placebo were statistically significant. These data indicate that the three administrations of 10^4 ffu and 10^5 ffu dosages were safe and the 10^5 ffu dosage of 116E demonstrated a robust immune response after three administrations.

C. Chikungunya virus

Chikungunya fever, caused by alphavirus named Chikungunya virus (CHIKV), is spread by the bite of virus-infected mosquitoes. The disease resembles dengue fever, and is characterized by severe, sometimes persistent, joint pain (arthritis), as well as fever and rash. It is rarely life-threatening. Nevertheless widespread occurrence of diseases causes substantial morbidity and economic loss. We are interested in studying CHIKV replication and development of novel vaccine candidates against the virus.

CHIKV was isolated from clinical material obtained from an epidemic of Chikungunya fever in Ahmedabad. The virus was plaque purified and its complete genome sequenced. Based on the nucleotide sequence, this virus was found to be closely related to the Maharashtra isolate of the virus. We have adapted the virus to grow in WHO certified Vero

cells and have purified it by ultracentrifugation. Virus inactivation by chemical means generated immunogen that induced CHIKV neutralizing antibodies in mice.

Publications

Original peer-reviewed articles

1. Bharati K, Rani R and Vrati S (2009) Evaluation of Japanese encephalitis virus DNA vaccine candidates in rhesus monkeys [*Macaca mulatta*]. *Vaccine* **27**:10-16.

Reviews/Proceedings

1. Bharati K and Vrati S (2008) Development of recombinant vaccines against Japanese encephalitis. **In**: *Arthropode-borne viral infections: Current status and research* (Eds: Raghunath D and Durga Rao C), Tata McGraw-Hill, New Delhi, 259-283.

Patents

1. Vrati S and Appaiahgari MB (2009) DNAzymes for inhibition of Japanese encephalitis virus replication. *US patent application no. US-2009-0010907-A1* (published on January 8, 2009).

Genetic and functional analyses of host and HIV-1 genes that affect progression of HIV-1 and development of nucleic acids based antiviral approaches

Principal Investigator: Akhil C. Banerjea

Project Associates/Fellows: Vikas Sood
Rajesh Ranjan
Subodh Samrat
Vijay Shankar
Ujjwal Neogi
Rajesh Vyas
Snigdha Banerjee
Nilanjana Ghosh
Arpita Choudhry

PhD Students: Nidhi Gupta
Aalia S Bano
Yogeshwar Sharma
Sachin Verma
Sanket Ponia

Collaborators: Tapan Dhole, *SGPGI, Lucknow*
Ajay Wanchu, *PGIMER, Chandigarh*
Madhu Khanna, *V P Chest Institute, Delhi*
Saumitra Das, *IISc, Bangalore*
H Liu, *University of Miami, USA*

The major theme of research is to understand unique features of HIV-1 epidemic in North India and to develop nucleic acid based approaches (antisense, ribozymes, DNA-enzymes, siRNAs, micro-RNAs, etc). These approaches can be used to understand the functional implications of HIV-1 genes and other model genes and at the same time may be exploited to interfere with the replication of HIV-1 via retrovirus vectors. HIV-1 pathogenesis is a complex process that involves the host genes, the viral genes, presence of co-pathogens and several others. Detailed characterization of HIV-1 genes isolated from circulating HIV-1 will help identify targets and design more effective antiviral strategies.

We wish to carry out genetic analysis of host genes and HIV-1 genes from HIV-1 infected individuals from North India using modern genotyping tools. Since there are very significant changes in the sequences of all the HIV-1 genes between subtypes-B (found in USA and UK) and C (predominant subtype in India), we wish to find out the functional implications of these changes with respect to their known functions. Novel nucleic acid-based (ribozyme, DNA-enzynes, Si-RNAs, antisense, etc) combinatorial approaches will be developed against HIV-1, its coreceptors and other model genes.

DNA-enzymes against hepatitis C virus RNA inhibit viral RNA translation and replication

We identified several 10-23 catalytic motif containing DNA-enzymes (Dzs) against the IRES region which is a highly structured RNA region where ribosomes bind directly and initiate

translation. In a transient transfection system, these DNA-enzymes exhibited protection against virus challenge. Mutant Dz failed to show any significant protection. This study suggested that these DNA-enzymes can be used as selective and effective inhibitor of virus replication. Two conserved Dzs were obtained after screening several targets and were shown to act against more than one subtypes.

Bispecific si-RNA-Rz construct and Dzs against the CXCR4, HBx and CCR5 genes

A bi-specific construct consisting of siRNA and hammerhead ribozyme was constructed against several important target RNAs (CXCR4, HBx and HIV-1 co-receptors-CCR5). The selectively disabled mutant constructs were also generated that possessed either a point mutation in the hammerhead catalytic motif or a 4 point mutation in siRNA stem-region of the shRNA. A construct was also made that possessed completely inactive ribozyme and siRNA. With each target gene, in a transient expression system, we show that the target gene expression was significantly reduced but not with with the double mutant. Furthermore, selectively disabled mutants were less effective. This kind of chimeric construct was described by our group for the first time. We identified potent Dzs that act against HIV-1 Tat B and C subtypes, X RNA of hepatitis B virus and HIV-1 coreceptors (CXCR4 and CCR5) and in presence of antisense, the *in vitro* cleavage was significantly enhanced. Si-RNA and Dzs or antisense were shown to interfere with the replication of HIV-1, very often in a synergistic manner.

Genetic characterization of HIV-1 LTR regions from North India

HIV-1 LTR region governs transcription and is extremely rich with various transcription factor binding sites (TFBS), notably, the NFAT, Sp1, Nf-kbs, the Tar etc. We genetically characterized LTR regions from HIV-1 infected individuals from North India (Punjab-Haryana regions) and report for the first time the presence of a unique mosaic intra- and inter B/C recombinant. This recombinant possessed 3 complete copies of Nf-Kbs as compared to subtype B LTR that usually possesses 2 copies of it. Polymorphisms were observed at many other TFBS that may impact both on the basal as well as Tat-mediated LTR-reporter gene activation. These LTR promoter regions are in the process of being cloned upstream of a reporter gene to assess their relative promoter strength with respect to their ability to activate gene expression. This finding suggests that novel B/C recombinants may be formed due to the presence of subtype B and C subtypes in this region.

Genetic analysis of Tat and Vpr, Vif gene analysis

HIV-1 Tat exon 1 is sufficient in activating HIV-1 LTR promoter and the same is achieved by the Vpr protein also. These two proteins play an important role in gene expression, cell-cycle progression, apoptosis and in modulating several other reactions. Several variants from HIV-1 infected individuals have been cloned and are being genetically and functionally examined. Vif genes from subtype B and C (from -93IN905 – Indian isolate) were characterized for their ability to degrade APOBEC protein. We showed that the C-terminal of Vif C possesses the major determinant for APOBEC protein degradation. This has implications in generating diversity among HIV-1 subtypes.

Publications

Original peer-reviewed articles

1. Gupta, N., and Banerjea, AC (2009) C-terminal half of HIV-1 Vif C possesses major determinant for APOBEC3G degradation. *AIDS* **23**:141-143.

2. Neogi U, Sood V, Goel N, Wanchu A and Banerjea AC (2008) Novel HIV-1 long terminal repeat (LTR) sequences of subtype B and mosaic intersubtype B/C recombinants in North India. *Arch Virol* **153**:1961-1966.

3. Gupta N, Bano A, Sharma Y, Banerjea AC (2008) Potent knock down of the X RNA of hepatitis B by a novel chimeric-siRNA-ribozyme construct and modulation of intracellular target RNA by selectively disabled mutants. *Oligonucleotides* **18**:225-234.

4. Sood V, Ranjan R and Banerjea AC (2008) Functional analysis of HIV-1 subtypes B and C HIV-1 Tat Exons and RGD/QGD motifs with respect to Tat mediated transactivation and apoptosis. *AIDS* **22**:1683-1685.

5. Roy S, Gupta N, Nithya S, Mondal T, Banerjea AC and Das S (2008) Sequence specific cleavage of Hepatitis C virus RNA by DNA-enzymes: Inhibition of viral RNA translation and replication. *J Gen Virol* **89**:1579-1586).

Study of immunotherapeutic potential of *M.w* and the underlying mechanisms in animal models of tuberculosis and tumor model

Principal Investigator: Sangeeta Bhaskar

Co-Investigator: Pramod Upadhyay

Project Associates/Fellows: Ankan Gupta
Jiju Mani
Faiz Ahamad

PhD Students: Anirudha Roy
Pawan Kumar

Collaborators: VM Katoch, *JALMA Inst Leprosy, Agra*
M Natarajan, *JALMA Inst Leprosy, Agra*
UD Gupta, *JALMA Inst Leprosy, Agra*

One of the important vaccine strategies is whole bacterial vaccines which rely on multiple antigens and built-in-adjuvanticity. Mycobacterial strains which share cross-reactive antigens with *M.tuberculosis* are being considered as alternatives to *M.bovis* for vaccine use. *M.w* had been evaluated for its immunomodulatory properties in leprosy. *M.w* shares antigens not only with *M.leprae* but also with *M.tuberculosis* and initial studies had shown that vaccination with killed *M.w* induces protection against tuberculosis. Hence, we further studied the protective potential of *M.w* and the underlying immune responses.

The present study aims to investigate the protective efficacy of *M.w* immunisation in live or killed form, through parenteral route as well as by aerosol immunization, against subsequent infection with *M.tuberculosis* in animal models. Study of immune responses to *M.tuberculosis* in animals immunised with *M.w.* These responses are compared with those generated in BCG immunised mice. Another objective is to evaluate immunoprophylactic and immunotherapeutic activity of *M.w* in mouse syngeneic tumor model. Study of *M.w* as an adjunct to chemotherapy in combination with commercial anti cancer drug formulation in tumor bearing mice. Simultaneous study of mechanism of *M.w* mediated host immune activation.

Study of protective efficacy of M.w in animal models of tuberculosis

We have studied the protective efficacy of *M.w* given by aerosol route as well as by subcutaneous route at different doses and dose schedules in guinea pig model of tuberculosis since this is more susceptible to tuberculosis infection and pathology is closer to human disease. Protective efficacy of both live and killed *M.w* was evaluated and compared with BCG. The parameters used for the evaluation of protective efficacy following an aerosol challenge were bacillary load in lung, spleen and liver, and also pathological changes in these organs. We have used the challenge dose which resulted in early manifestation of disease, to get the clear comparison between different groups of immunized guinea pigs. Five groups of guinea pigs were immunized with live *M.w*/killed *M.w*/BCG/*M.w* by aerosol/control group. In one set of expt. these immunized guinea pigs were challenged with *M.tb*, 4 week post immunization. In the other set, to study the long term protective efficacy of *M.w*, animals were

challenged with *M.tb* H37Rv 16 week post immunization. In both sets, animals were euthanised at 4 week and 8 week post infection.

It was observed that 4 week post infection, in *M.w* aerosol immunized group there was about 2 log reduction in lung bacilli load, as compared to control group. As compared to BCG immunized guinea pigs, bacterial load was 5 times less in this group. When we compare the live *M.w*, s.c. group and BCG group, there was more than 2 fold reduction in the former (Table-1). This reduction in bacterial load was also reflected in total body weight and lung pathology. In another set of experiments where interval between immunization and infection was extended to 16 week, *M.w* immunized groups still gave higher protection. About 1.5 log reduction in lung bacilli count was observed. In spleen and liver, reduction was about 2.0 log.

Table-1.

Group	CFU / Organ x 10^5	
	Lung	Spleen
Unimmunised Control	2950 ± 389	30.7 ± 9.1
M.w by Aerosol	20.4 ± 4.6	2.3 ± 1.1
Live M.w by s.c. inj.	44.5 ± 5.0	5.0 ± 1.4
Killed M.w by s.c. inj.	59.0 ± 8.3	5.7 ± 0.5
BCG by s.c. inj.	106.5 ± 26	6.3 ± 0.2

In another set of experiments, we are also studying the therapeutic efficacy of *M.w* along with combination of three chemotherapeutic drugs viz. Rifampicin, Isoniazid & Pyrazinamide in *M.tb* infected guinea pigs. This is being compared with the group where only anti TB drugs are given. Both lung bacterial load and histological examination are being done at different time intervals after treatment. Body weights were also checked at regular time interval after infection which also reflected protection in *M.w* immunized guinea pigs.

Study of immunotherapeutic potential of m.w and the underlying mechanisms in mouse tumor model

Host Immune system plays a critical role in promoting host protection against cancer. However, the generation of antitumor immunity is often difficult in the tumor-bearing host because of various negative regulatory mechanisms. Activation of type-1 innate and acquired immunity is important to overcome immunosuppression in the tumor-bearing hosts. There are indications from different clinical studies that *M.w* may be useful as an immunomodulatory adjunct in some cancers. In animal model of tuberculosis we have found that *M.w* induces Th1 type response. As induction of Th1 type immune response and CTL activity is also important for host antitumor activity, we have started this study to evaluate the immunoprophylactic and immunotherapeutic activity of *M.w* in mouse syngeneic tumor model.

Different concentrations of tumor cells were implanted in syngeneic BL/6 mice to determine an appropriate tumor burden. Initial experiments were done to find out the optimum dose of

M.w. It was observed that high doses of *M.w* resulted in no regression or some aggravation in tumor. Hence, optimum dose was selected and then it was given by different dose schedules in different groups. In one group *M.w* injections were given at 14 days interval while in the other at 7 days interval. In the later group higher protection was seen. There was delay in tumor growth in 50% of the treated mice and 40-50% reduction in tumor size was observed in 50% of the *M.w* treated mice as compared to control untreated mice.

In the above experiments, *M.w* injections were given after the implantation of B16 cells (Immunotherapeutic). In another set of experiment two injections of *M.w* were given before implantation of tumor (Prophylactic dose) and then it was given at weekly interval after B16F10 (Melanoma cells) injection. This group was compared with the group where weekly *M.w* injections were given only after the implantation of tumor cells (Therapeutic dose). *M.w* both as therapeutic/prophylactic + therapeutic reduced the tumor growth as compared to control. But tumor growth was delayed and volume of tumor were significantly less in the group where it was given as prophylactic + therapeutic (Figure-1).

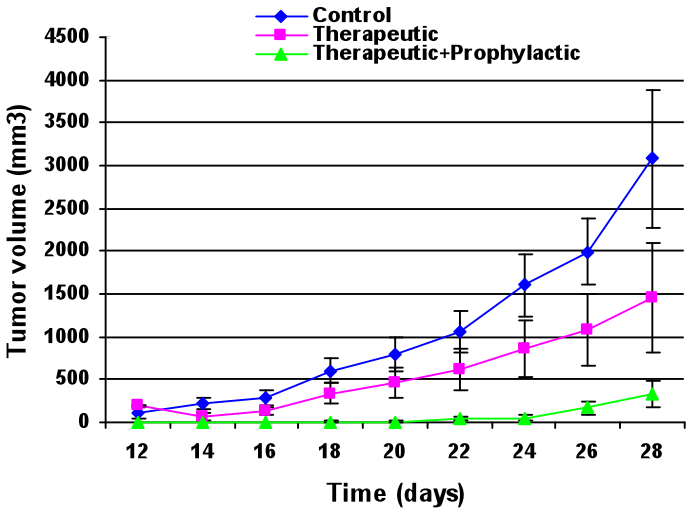

Figure-1: xxxxxxxxxxxx

In another set, when lower concentration of B16 was injected, it was observed that in control, unimmunised mice, tumor started appearing about 3 week after tumor implantation, while in mice vaccinated with *M.w*, it started appearing at 5-6 week and tumor appeared in only 50-60% of mice. In 15% of the mice it started reducing in size few days after appearance and it remained at stable size. While in the control group, all the mice died during the experimental observation period, only 25% of the vaccinated group died during that period.

To study the mechanism of *M.w* mediated host immune activation, we are also doing immunological studies. Induction of immune cells relevant for tumor control like T cells, NK cells and macrophages were studied in the tumor draining lymphnodes of *M.w* immunised mice and control mice. It was found that tumor draining lymphnode of immunised mice had higher expression of MHC-II, CD80 and CD86 as compared to control mice. There was some increase in the percentage of CD3 +ve cells also and particularly percentage of CD8 +ve cells increased.

To study the efficacy of *M.w* as an adjunct to chemotherapy, one week after implantation of tumor, drug Doxorubicin/DITC was given. When *M.w* was given along with i.v. Doxorubicin, it gave higher protection as tumor volume was less as compared to the group where drug was given alone, but it was not significant. In other set of experiment, drug DITC was given for 10

days, starting 7 days after B16 injection. Simultaneously, in other group *M.w* was given along with drug. Tumor growth and mortality was similar in both groups. We are repeating the experiments with other drugs.

Another important observation was that *M.w* injection even if given at the distant site of tumor, it gives protection as compared to control mice.

Publications

Original peer-reviewed articles

1. Gupta A, Geetha N, Mani J, Upadhyay P, Katoch VM, Natrajan M, Gupta UD and Bhaskar S (2009) Immunogenicity and protective efficacy of *Mycobacterium w* against *Mycobacterium tuberculosis* in mice immunized with live versus heat-killed *M.w* by the aerosol or parenteral route. *Infect Immun* **77**:223-231.

Studies on immune response from antigen loaded biodegradable polymer particles

Principal Investigator: Amulya K Panda

Project Associates/Fellows: Vikram Mishra
Simi Mathews
Bikash Mohapatra

PhD Students: G Rajmohan
Arun Kumar Upadhyay
CK Anish
Dinesh G Goswami
Prasad S Admane

Collaborators: Lalit C Garg
Om Singh
Rahul Pal
Pramod K Upadhyay
Ayub Qadri
Devinder Sehgal
Alok R Ray, *IIT, New Delhi*
SP Vyas. *DHG Vishwavidyalaya, Sagar, MP*
DK Majumdar, *DIPSAR, New Delhi*
Roop K Khar, *Jamia Hamdard, New Delhi*
PC Ghosh, *UDSC, New Delhi*
Vinod Labhasetwar, *LRI, USA*
Tapani Hovi, *KTL, Finland*
Merza Roivainen, *KTL, Finland*
Outi Vaarala, *KTL, Finland*

The theme of the project is to evaluate the immunostimulatory activities associated with polymer entrapped antigens such as Tetanus Toxoid (TT), Hepatitis B surface antigen (HBsAg); and viral, carbohydrate and DNA vaccines for the development of single dose formulation.

The main objective is to study the immune response from biodegradable polymer particles entrapping antigens and plasmid DNA. Immune response from polymer particles entrapping TT, HBsAg or plasmid DNA expressing HBsAg protein is being evaluated. The objectives of the project are:

1. Analysis of immune response from antigen loaded particles by employing different polymer composition, particle size and usage of various immunization protocols.
2. Evaluation of long term memory response using polymer particle based immunization.
3. Generation of cell mediated immune response using different sized antigen entrapped polymer particles.
4. Evaluation of immune response from polymer entrapped viral, carbohydrate and DNA based vaccines.5. Formulation and evaluation of large porous polymeric particles for three dimensional growths of animal cells *in vitro*.6. Solubilization and refolding of inclusion body proteins from *E.coli*.

A. *Memory antibody response from polymer particle based immunization*

Evaluation of memory response using TT/DT and HBsAg microparticles was carried out in Wistar rats. The animals were immunized with equal doses of polymer entrapped antigen, admixture of alum and polymer particles and antigen adsorbed on to alum. It was found that TT microparticles (TTP) + alum immunized animals when challenged with soluble TT elicited the highest secondary antibody titers (within one week) and sustained at higher level for three months. The secondary antibody response from polymer entrapped antigen was very high in comparison to that achieved with two doses of alum adsorbed TT immunization. It was also observed that memory antibody generation through polymer particle based immunization is antigen specific. High secondary antibody response could be detected in rats even after 18 months of primary immunization. These antibodies have high affinities and are mostly because of long lived memory B cells. Polymer particle having different release kinetics of antigen was used to evaluate the role antigen on memory antibody response. Normal PLA particles entrapping antigen both in the matrix and on the surface were used as a control. Porous particles (by optimization of formulation variable) could releases 100% antigen in 7 days where as dummy particles coated with antigen only on the surface (prepared by coating of antigen on dummy PLA particles) could release the antigen once. Surface adsorbed antigen on the particles was removed by *in vitro* release (IVR) and used as particles representing slow, continuous release profile. All these above particle formulations containing similar load of TT were immunized and challenged after six month for memory antibody response. Dummy particle with layer of antigen on the surface and the porous particle did not elicit improved secondary antibody titers. It was observed that only in formulation having continuous release of antigen could give rise to memory antibody titers. These results favor the hypothesis that continuous release/ presence of antigen for improved memory antibody response. The detail mechanisms of improved memory antibody response are under investigation.

B. *Entrapment of enterovirus in PLA particle and evaluation of its immunogenicity*

The objective of the project was to formulate enterovirus in polymer particles and evaluate its immunogenicity. PLA particle entrapping Coxsackie B5 virus was evaluated for immune response in mice from single dose immunization. It was observed that single dose of polymer entrapped viral particles elicit long lasting antibody response. However the antibody titer were not bio neutralizing indicating the possible denaturation of virus antigen during particles formulation. Formulation variable were optimized to take care of virus denaturation during particle formulation. These formulations gave rise to better antibody response from single point immunization. The neutralizing antibodies are being tested at KTL Finland. Recombinant outer membrane protein (VP1) of enterovirus has also been cloned and purified using *E. coli*. The protein will be used for formulation of particles for immunization and for T cell proliferation assay.

C. *Immune response from polymeric formulation entrapping candidate polysaccharide antigen*

Polymeric formulation entrapping Typhoid vaccine (Vi polysaccharide) and capsular polysaccharide from *S.pneumoniae* were evaluated for antibody titer in mice. Recombinant proteins/TT as T cell helper antigen were co-entrapped for improving the immunogenicity of carbohydrate antigen. For Typhoid vaccine, it was observed that entrapment of Vi polysaccharide in microparticle improved both primary and secondary antibody response from single dose. Nanoparticles did not give rise to improved antibody response. Even co-entrapment of Vi polysaccharide and TT did not elicited improved antibody titers from single point immunization. The antibody titers were comparable to PLA particles entrapping Vi only. This indicated that entrapment of polysaccharide antigen in PLA particle is more than sufficient to improve its immunogenicity. For capsular polysaccharide from *S.pneumoniae*, co-entrapment of protein antigens such as PspA, PsaA did not improve the antibody response. Surprisingly, nanoparticles entrapping capsular polysaccharides elicited higher antibody titer than microparticles. Polymer particle mimicking bacteria were also prepared. These particles contain carbohydrate in surface of the particle and protein antigen in core of the particles. These particles are being evaluated for improved antibody repose from single point immunization. Other recombinant S.*pneumoniae* proteins are being purified in the laboratory to be used in combination with polysaccharide for improved antibody response.

D. *Formulation of large porous PLA particles for tissue culture and formation of polymer membranes*

Large porous polymeric particles (>200 μm) made from composite polymers such as mixture of PLGA, PLA or chitosan were formulated for growth of animal cells *in vitro*. Due to the biodegradable nature, these polymeric scaffolds support three dimensional growths of animal cells *in vitro* and thus can be used as a model for cytotoxic evaluation of a drug or drug delivery system *in vitro*. Last year we have reported a process of making polymer membranes for wound healing using surfactant based fusion of polymer particles (PCT patent application pending). The polymer particles after fusion into higher order structures retain their characteristics and can be fabricated into different designs for various biomedical applications. This year we investigated in details the molecular mechanism of self-assembly of polylactide particles into membrane like structures at room temperature. In presence of ethanol, evenly spread surfactant coated polylactide particles fused immediately into membrane like structures at room temperature. Fusion regions were mostly formed at the point of contact between the surfaces of polymer particles in presence of alcohol. Zeta potential measurements and atomic force microscopy of the polylactide particles confirmed that desorption of surfactant molecules from the surface of the particles during ethanol treatment and solubility of the polymer in alcohol/surfactant mixture as the main reason behind the fusion of particles in to membrane like structure. FTIR, X-ray diffraction and calorimetric studies showed that there was no change in characteristics of the polymer particles after the fusion process. Polymer scaffolds of the desired shape and size were fabricated from polylactide particles using this surfactant mediated fusion process. In experimental animal wound models, the polylactide membranes showed faster wound closure with increased strength of the healed skin. This approach provides an easy and simple method for fabrication of biodegradable polymer membrane as skin substitute and scaffolds of different designs at room temperature for regenerative medicine. Currently we are fabricating polymer membrane from particle entrapping antibiotics for improved wound healing.

E. *Solubilization and refolding of inclusion body proteins*

We have been investigating the refolding of inclusion body proteins from *E. coli* using mild solubilization procedures. Last year we reported that many recombinant inclusion body proteins can be solubilized using high concentration of β-mercaptoethanol. It was observed that β-mercaptoethanol acts as a detergent which eventually helps in solubilization of protein aggregates. This was confirmed using surface tension and dielectric constant measurements of buffers containing β-mercaptoethanol. Many other organic solvent having above properties were investigated and it was also found that iso-propanol with 2 M urea also could solubilize inclusion body proteins. Human growth hormone was successfully solubilized and refolded in to bioactive conformation. The detailed mechanism of organic solvent based solubilization of protein aggregates are under investigation.

Publications

Original peer-reviewed articles

1. Singh SM, Upadhyay AK and Panda AK (2008) Solubilization at high pH results in improved recovery of proteins from inclusion bodies of *E coli. J of Chemical Technology and Biotechnology* **83**:1126-1134.

2. Naha PC, Kanchan V, Manna PK and Panda AK (2008) Improved bioavailability of orally delivered insulin using Eudragit L30D coated PLGA microparticles. *J Microencapsulation* **25**:248-256.

3. Horning JL, Sahoo SK, Vijayaraghavalu S, Dimitrijevic S, Vasir JK, Jain TK, Panda AK and Labhasetwar C (2008) 3-D tumor model for *in vitro* evaluation of anti-cancer drug. *Molecular Pharmaceutics* **5**:849-862.

4. Nayak B, Panda AK, Ray P and Ray AR (2009) Formulation, characterization and evaluation of rotavirus encapsulated PLA and PLGA particles for oral vaccination. *J Microecapsulation* **26**:154-165.

Patents/Trademark Product

1**.** Artskinii ^{TM} (A product for wound healing and burn treatment)

Analysis of *Salmonella typhi*-host cell interaction

Principal Investigator: Ayub Qadri

Project Associates/Fellows: Sheikh Mohd Atif
Naveen Sharma
Sushil Kumar

PhD Students: Naveen Sharma (till Jun 2008)
Rohini Garg
Neha Dikshit
Debjani Dutta

Collaborator: Amulya K Panda

Pathogenic *Salmonella* species produce systemic infection or localized gastroenteritis depending upon the *Salmonella* serovar and the host type. In humans, *S.typhi* causes systemic infection, typhoid, while *S.typhimurium* produces self-limiting gastroenteritis. In mice, on the other hand, infection with *S.typhimurium* results in a systemic infection that is analogous to human typhoid. The host-pathogen interactions which determine host specificity and bring about different manifestations have not been identified. Moreover, the mechanism by which pathogenic *Salmonella* might modulate immune responses at different stages of infection is not clear. Work in our laboratory focuses on these aspects of *Salmonella* infection.

The objectives of the project are to (i) understand modulation of immune responses during infection with pathogenic *Salmonella* and (ii) identify and characterize *S.typhi* - specific pathogen - immune cell interactions.

Vi produces inflammatory responses from mononuclear phagocytes

Studies carried out in our laboratory have shown that Vi capsular polysaccharide of *S.typhi* can inhibit inflammatory responses from IEC. Once past intestinal epithelium, *S.typhi* disseminates systemically and can be isolated from many organs including spleen, liver and bone marrow. Bacteria are carried from the gut to these organs by cargo cells such as macrophages, neutrophils and dendritic cells. We therefore investigated possible effects of Vi on inflammatory responses produced by macrophages. Vi suppressed chemokine secretion from macrophages activated with *Salmonella* flagellin which is a major proinflammatory determinant of this pathogen and produces inflammatory mediators through activation of Toll-like receptor-5 (TLR-5). This suppression was reduced in cells in which expression of prohibitin was knocked down by RNA interference demonstrating that prohibitin was required for Vi-mediated inhibitory effects. As seen with IEC, this inhibition was best obtained under serum-free conditions. Remarkably, further analysis revealed that Vi itself could induce secretion of chemokines and cytokines when presented to macrophages in presence of serum. The proinflammatory Vi activated secretion of cytokines from cells through engagement of TLR-2. These results suggest that Vi can differentially modulate inflammatory and innate immune responses during infection with *S.typhi* depending upon its interaction with host molecules. Vi might be anti-inflammatory in the gut due to low levels of serum-derived factor(s), thereby promote establishment of

infection. On the other hand, during systemic dissemination of *S.typhi* when serum factors would be readily available, Vi could bring about induction of inflammatory and innate immune responses.

Sphingosine 1 phosphate (S1P) inhibits flagellin- induced chemokine secretion from human T cells

We reported previously that IL-8 secretion produced by flagellin in IEC and human monocytes was increased in presence of serum or serum-borne lysophospholipids. Since TLR-5 is also expressed on human T cells, we investigated possible role of serum-derived factor(s) in the regulation of flagellin-induced inflammatory responses from this cell type. Interestingly, unlike the upregulation seen with IEC and macrophages, serum inhibited IL-8 secretion from human T cells activated with flagellin. This inhibition was seen with model human T cell line Jurkat as well as *ex vivo* T cells obtained from peripheral blood. The suppression was not due to cell death or blockade of flagellin-binding to T cells in presence of serum but due to modulation of intracellular signaling. Serum reduced flagellin-activated phosphorylation of JNK, p38-MAPK and CREB. The downregulation of flagellin-induced chemokine secretion mediated by serum could be reproduced with S1P. The effect of S1P was reversed with calcium channel blockers and intracellular calcium chelator BAPTA-AM, thus revealing a role for calcium in the suppression mediated by this lipid. The regulatory effect produced by serum was specific to the innate arm as it didn't inhibit flagellin co-stimulated IL-2 secretion from TCR-activated T cells. Notably the modulation of cellular responses by S1P was also seen during TLR-4-activated chemokine secretion from T cells. These results demonstrate a regulatory mechanism by which TLR-induced innate immune responses might be controlled in human T cells.

Regulation of inflammatory responses during infection with Salmonella

Work done in our laboratory has shown that sensing of IEC-derived lysophospholipids by pathogenic *Salmonella* can trigger *de novo* synthesis and release of monomeric flagellin which activates innate immune responses from different cell types through engagement of TLR-5. Further investigation demonstrated that the host factor capable of bringing about secretion of proinflammatory flagellin monomers from pathogenic *Salmonella* was also released during induction of macrophage cell death (pyroptosis) by this pathogen. This factor was not produced when infection of macrophages was carried out in presence of calcium-independent phospholipase A2 inhibitor bromoenol lactone suggesting that the stimulus might be lysophospholipid in nature. The activity in the supernatant from apoptotic macrophages capable of triggering release of flagellin from *Salmonella* was not affected by treatment with proteianse K. However, extraction of this supernatant with chloroform abrogated the flagellin-inducing capability again indicating that the host factor was most likely of a lipid nature. The establishment of identity of this molecule is currently in progress. Significantly, this stimulus was also produced from cells transfected with monomeric flagellin which brings about cell death and IL-1β release through Ipaf-dependent activation of the inflammasome. This finding suggests that flagellin-induced death during infection with *Salmonella* might serve as an amplification loop for the production of proinflammatory flagellin monomers from *Salmonella*.

The release of monomeric flagellin from *Salmonella* in response to pyroptosis-derived host stimulus if allowed to proceed could bring about clearance of bacteria due to potent

immunomodulatory abilities of flagellin. To neutralize this host response, we now show that with the progression of infection, *Salmonella* switches to a phenotype that is inefficient at bringing about cell death. We believe that this switch might be produced as a result of sensing of another host signal by the pathogen. The molecular details of this switch are currently being worked out. These results reinforce the importance of the two way host-pathogen cross-talk in the regulation of inflammatory and innate immune responses during infection with *Salmonella*.

Study of mucosal immune responses

Principal Investigator:	Anna George
PhD Students:	Priyadarshini Chatterjee Gautam Shenoy Sheetal Kaw Ritesh Kumar Tiwari
Collaborators:	Vineeta Bal Satyajit Rath Tushar Vaidya,*CCMB, Hyderabad*

The laboratory is currently dissecting signals that determine the activation, proliferation and differentiation of peripheral lymphoid cells.

The objectives comprise analysis of cell-intrinsic and cell-extrinsic factors that are likely to influence the outcome of B and T cell priming in systemic and mucosal lymphoid tissues. With the help of cellular, molecular, biochemical and *in vivo* approaches, we aim to dissect the role of various receptors, accessory molecules, cytokines, microbial flora and antigen processing pathways in determining the nature and duration of B and T cell priming.

Over the current reporting year, we have used cellular and molecular approaches to understand the mechanism by which CD40 ligation prevents terminal differentiation. Using the same panel of pharmacological inhibitors used in the CD27 study reported last year, we have tried to reverse the effect of CD40 ligation *in vitro*. We established that stimulating cells with LPS in the presence of increasing amounts of anti-CD40 leads to a dose-dependent inhibition of plasma cell generation. However, addition of JNK inhibitor to the assay does not reverse the effect, as was seen with CD27. Inhibition of PI-3 kinase, on the other hand, led to some reversal. Thus the two TNF receptors appear to affect B cell differentiation by different pathways.

Our major effort over the reporting year has been microarray analysis of differential gene expression between cells stimulated with LPS in the presence or absence of CD40 ligation. The array set contained 35,000 spots each containing 70mers which represent 29,000 mouse genes. Changes in gene expression were profiled at 24 h, 48 h and 72 h post-treatment. In addition, we have also compared resting vs. LPS-stimulated cells. Four independent hybridizations were carried out for each time point and the signal data were subjected to both Lowess- and Flip dye- normalizations. Gene spots were included in the analysis if the signal was non-zero and present on each slide, and if the directionality was the same in both normalizations. Combining the data from all the time points, we have generated a composite list of 9457 genes that are consistently detectable at one time point at least.

We then analyzed the list of valid genes in each experiment for their pattern of expression in response to the treatment. Criteria applied for induced or repressed genes: Induced = fold change >1.5; Repressed= Fold change <0.67; Unchanged= Fold change <1.5 AND >0.67.

Table-1: Distribution of induced or repressed genes at each time point

Experiment	Total valid genes	Induced genes	Repressed genes	Unchanged genes
Day 0 v/s LPS, 24h	1525	748	724	52
Anti-CD40/LPS v/s LPS, 24h	5080	2002	1737	1341
Anti-CD40/LPS v/s LPS, 48h	2978	706	515	1757
Anti-CD40/LPS v/s LPS, 72h	2313	1232	702	379

Thus, 1525 genes were differentially expressed upon activation of resting cells. Further, CD40 ligation led to the differential expression of 5080 genes at 24 h, 2978 genes at 48 h and 2313 genes at 72 h. In general, more genes were upregulated (than downregulated) in the CD40 group. We also found that most of the changes in the gene expression patterns appear to be taking place around 24 hours, post treatment. At later time points, there are limited changes from what has already happened in the initial 24 hour period. Thus, commitment to plasma cell generation may occur very early after B cell stimulation and it is possible that chromatin modifiers likely play a role in the process. We have initiated a pathway analysis of genes that are part of the composite list. The top ten pathways with maximal numbers of participating genes included antigen processing, cell adhesion, cell cycling, DNA replication, gap junction signaling, cytoskeletal regulation, MAPK- and PI-kinase signaling and ribosomal genes.

In addition to our microarray studies on global patterns of gene expression upon CD40 signaling, we have carried out a quantitative real-time PCR analysis of the expression pattern of 66 candidate genes. These genes were selected on basis of a combination of several criteria: their potential participation as reported in literature, their expression pattern during the time course analysis, their known function (transcription factors, receptors, cytokines, chemokines, signaling molecules, chromatin modifiers etc). Three housekeeping genes (L7, GAPDH and β2 microglobulin) were included. In all cases, the resulting amplicon was between 175 and 225 bases, the efficiency of the PCR amplification was between 90% and 105%, and all PCR reactions yielded a single amplicon with a reproducibly consistent thermal dissociation. In general, the PCR data mirrored the microarray data.

In our efforts to generate naive B cells overexpressing specific genes in peripheral lymphoid organs, we report the standardization of techniques for getting relatively high titers of retroviruses expressing either EGFP, CD27 or Enc-1. The retroviral supernatants have been successfully used for transduction of fibroblasts and primary B cells and some success has been obtained with transduction of bone marrow.

Table-2: Fold change in expression of selected genes, from the 66 analyzed, at various time points as determined by real-time RT-PCR

Gene	24h QRT-PCR	48h QRT-PCR	72h QRT-PCR
CD19	1.26	0.97	1.36
IL1a	2.15	0.72	0.22
Mitf	0.48	1.38	1.04
Bach2	1.32	0.64	1.36
Xbp1	0.78	0.47	1.17
Bcl6	0.52	0.37	0.43
Rnase6	0.31	0.35	0.38
Blimp1	0.58	0.33	0.15
IL10	0.01	0.26	0.04
Ig J chain	0.72	0.06	0.23
Fcer2a	2.18	1.57	3.29
IL6	2.93	1.69	0.58
Ccl22	2.62	31.93	10.98
IRF4	1.05	0.75	0.95
Jun	2.98	1.15	0.84

Over the current reporting year, we have also looked at the role of iNOS in T-independent responses. We report that iNOS-null B cell cultures make more IgM when stimulated at low cell densities with LPS in vitro. Further, iNOS-null mice make more NP-specific IgM responses following immunization with NP-Ficoll than WT mice do. Interestingly, when plated at higher densities in vitro, similar amounts of secreted Ig is detectable in culture supernatants from WT and iNOS-null B cell cultures and preliminary data indicate that this may correlate with a greater tendency of iNOS-null plasma cells to die in crowded cultures. We also report that the iNOS-null phenotype is reproduced in a dose-dependent manner when WT cells are cultured with the NO-inhibitor aminoguanidine.

Publications

Original peer-reviewed articles

1. Chaudhry A, Das SR, Jameel S, George A, Bal V, Mayor S and Rath S (2008) HIV-1 Nef induces a Rab11-dependent routing of endocytosed immune costimulatory proteins CD80 and CD86 to the Golgi. *Traffic* **9**:1925-1935.

Analysis of antigen processing and presentation

Principal Investigator: Satyajit Rath

Project Associates/Fellows: Deepak K Rathore

PhD Students: Divya Anna Verghese (till Jun 2008)
Hridesh Banerjee
T Krishnamurthy
Abhishek Das
Rupali

Collaborators: Vineeta Bal
Anna George
Shahid Jameel, *ICGEB, New Delhi*
Satyajit Mayor, *NCBS, Bangalore*
Apurva Sarin, *NCBS, Bangalore*
B Ravindran, *RMRC, Bhubaneswar*
Tushar Vaidya, *CCMB, Hyderabad*
Jeannine M Durdik, *Univ Arkansas, USA*
Ranjan Sen, *NIA-NIH, USA*

The aim of the ongoing programmes in this group is to examine the generation and activation of T, B and antigen-presenting myeloid cells using multiple interlinked experimental systems.

A variety of experimental approaches are taken to address the theme issues. The approaches in current use examine APCs and pathways involved in antigen presentation to MHC class I and class II-restricted T cells, and analyse the consequences of intracellular signal transduction modulation for both development and responses of B cells, T cells and macrophages using genetic as well as pharmacological tools.

Parameters controlling functional outcomes of CD8 T cell activation: the role of ligand density

CD8 T cells can be activated within 1-3 h of exposure to peptide-MHC class I (MHCI) ligand on antigen-presenting cells (APCs). Even if these activated CD8 T cells are then separated from the APCs, they undergo activation, proliferation and differentiation on their own. We have been using CD8 T cells from mice transgenic for T cell receptors (TCRs) specific for peptide-MHCI complexes to address the quantitative parameters of CD8 T cell responses. We have tracked the acquisition of early and late-arising cell-surface activation markers such as CD69, CD25, and CD44. Proliferation has been followed by CFSE dilution and by tracking cell numbers. Differentiation has been measured by the ability of the T cells to secrete interferon-gamma (IFNg) upon re-stimulation, and by their ability to kill peptide-MHCI-bearing target cells. Either P14 or OT-I TCR-transgenic mouse strains have been used. While P14 CD8 cells recognize an LCMV peptide bound to H-2D-b, OT-I CD8 cells recognize a chicken ovalbumin-derived peptide bound to H-2K-b.

Naïve CD8 T cells from these TCR-transgenic mice, when stimulated with peptide-pulsed APCs, initially downmodulated their cell-surface TCR levels and expressed CD69 within the first hour. Even when they were separated from APCs after 3 h and cultured further, the activation programme continued to be executed, with CD25 expression, followed by high levels of CD44. The cells underwent at least four cycles of cell division by ~60 h as judged by CFSE dilution. By this time, they became effective cytotoxic cells and could secrete IFNg in response to re-stimulation.

We have used adherent APCs, either epithelial cells, or adhered dendritic cells (DCs), for these experiments. Although costimulation is considered crucial for effective T cell activation, we observed that, as reported earlier, for the high-affinity TCR-bearing transgenic CD8 T cells in our system, the presence or absence of transfected CD80/CD86 molecules on the APCs did not substantially alter the extent or efficiency of the T cell response generated in vitro. This allowed us to concentrate our analysis on the levels of peptide-MHCI ligand available as a potential parameter regulating T cell responses.

In order to ensure that stimulation of T cells was restricted to the 3-h period of interaction with APCs, with no peptide carryover into post-stimulation cultures, we activated CFSE-labeled CD8 cells by a 3-h interaction with peptide-loaded APCs, and then separated these T cells and cultured them with fresh unlabeled naïve CD8 T cells for 24 h. The freshly added naïve CD8 T cells did not show any activation, indicating that no ligand was present in the post-separation cultures.

Since actin polymerization has been argued to be crucial for T cell activation, we tested if the presence of actin polymerisation inhibitors such as cytochalasin D during APC exposure blocked T cell activation. Activation was completely blocked by cytochalasin D and not by the microtubule inhibitor nocodazole; however, we observed that inhibition of actin polymerization blocked the formation of stable cell-cell conjugates between T cells and APCs. Thus, no interpretation could be offered for the possible effects of inhibition of actin polymerization in T cell signaling pathways per se in this assay system.

We next analysed the role of the levels of peptide-MHCI ligand available as a potential parameter regulating T cell responses. For this, TCR-transgenic CD8 cells were stimulated in 3-h cultures with adherent APCs that were pulsed with three titrating doses of the specific peptides. These peptide concentrations were tested in bulk 3H-thymidine incorporation assays, and were in the linear range of the dose-response curve. They were also tested, for the ovalbumin peptide, in an assay to detect the amount of peptide-MHCI complexes formed using a monoclonal antibody specific for the ovalbumin peptide-H-2-K-b complex, which showed that significantly differing levels of ligand were formed over this peptide dose range. At the end of 3 h of co-culture, the CD8 cells were separated and tested for activation by measuring CD69 induction. The three peptide concentrations tested showed a dose-response relationship with the frequency of CD8 cells showing induction of CD69. However, the intensity of CD69 levels on individual activated CD8 cells was not drastically altered by peptide dose. When put into culture post-separation, the CD8 cells activated at differing ligand densities underwent proliferation to the same extent. However, since the frequencies of cells activated and initiating proliferation differed, the absolute numbers of proliferated cells generated were lower in cultures from low-level ligand-exposed T cells. These proliferated and differentiated cells, when purified and tested, showed equivalent abilities to make IFNg upon re-stimulation. Thus, the frequency of responding CD8 T cells is sensitive to the

magnitude of signals transduced during the T cell-APC contact, while the completion of the program of proliferation and differentiation initiated in triggered T cells is more robust. These data suggest that individual T cells and T cell populations respond differently to modulations of ligand density, and have implications for the understanding of T cell responses to infections in vivo.

Bruton's tyrosine kinase (Btk) in myeloid cells: role in the eosinophil lineage

Btk, expressed in both lymphoid and myeloid lineage cells, has been shown to participate in macrophage and neutrophil effector functions and to modulate neutrophil development. Eosinophil leucocytes normally constitute a minority of circulating granulocytes and a majority of mucosal granulocytes, and while they can phagocytose and eliminate microbial pathogens, they differ from neutrophil leucocytes in the triggers that activate them and their mode of degranulation-based function. Hence, given the known role of Btk in modulating neutrophil functions, it was of interest to examine the possible role of Btk in the eosinophil lineage.

The low proportion of eosinophils in peripheral blood is one major limitation of eosinophil studies. We have used transgenic mice in which generation of IL-5, a major trigger for eosinophil development, is controlled by a metallothionein promoter that is constitutively active in mice given normal drinking water probably due to low levels of zinc in the water. A high proportion of the circulating granulocytes in these IL5Tg mice were eosinophils, and a high proportion of the granulocytes recruited to sites of acute inflammation were eosinophils.

To examine the role of Btk in the eosinophil lineage, X-linked immunodeficient (XID) mice lacking functional Btk were crossed with IL5Tg mice. Peripheral blood leukocytes from XID-IL5Tg mice showed high frequencies of eosinophils. However, compared to WT-IL5Tg mice, XID-IL5Tg mice showed compromised eosinophil recruitment to sites of inflammation, although Siglec-F levels were normally induced upon activation in XID-IL5Tg eosinophils. The LPS-induced generation of reactive oxygen species (ROS) was substantially compromised in the XID-IL5Tg eosinophils. Since protein kinase C (PKC) is required for ROS generation, and since Btk is known to associate with PKC in B cells and mast cells, it is possible that PKC activation is a major role mediated by Btk in the eosinophil lineage.

Publications

Original peer-reviewed papers

1. Tupperwar N, Vineeth V, Rath S and Vaidya T (2008) Development of a real-time polymerase chain reaction assay for the quantification of *Leishmania* species and the monitoring of systemic distribution of the pathogen. *Diagn Microbiol Infect Dis* **61**:23-30.

2. Chaudhry A, Das SR, Jameel S, George A, Bal V, Mayor S and Rath S (2008) HIV-1 Nef induces a Rab11-dependent routing of endocytosed immune costimulatory proteins CD80 and CD86 to the Golgi. *Traffic* **9**:1925-1935.

Analysis of anti-lymphocyte autoimmune antibody responses

Principal Investigator: Rahul Pal

Project Associates/Fellows: Harshita Bhatnagar
Latika Sharma

PhD Students: Pooja Arora
Alpana Satsangi

Humans are plagued by a large variety of autoimmune diseases. For most diseases, etiologies remain unknown and the diversity of observed immune responses is the subject of intense investigation. Systemic lupus erythematosus (SLE) is the prototypical organ non-specific autoimmune disease. The disease generally manifests a life-long, relapsing-remitting phenotype. Multiple organs are targeted; chronic renal failure is a serious consequence, and patients can also exhibit arthritis, neurological involvement and immune dysfunction. More than a hundred different autoantibody specificities have been described, with some reactivities associated with pathology. Drawing correlations of disease manifestations and with autoimmune specificity remains a high priority.

Interestingly, in both SLE patients and several disease-prone animals, aberrance in apoptotic processes has been observed. Excessive spontaneous apoptosis (or excessive susceptibility to apoptotic stimuli) as well as inefficient clearance of apoptotic debris, have been documented in lupus patients, and animals genetically modified to impair the uptake of apoptotic cells exhibit lupus-like pathology. Apoptotic debris may therefore be the source of antigenic material that initiates autoreactivity. It is conceivable that the specificity and characteristics of early immune responses to apoptotic cell in individuals genetically prone to autoimmune disease could influence pathological outcomes.

This project seeks to investigate the consequences of the aberrant recognition of cell death in systemic autoimmune diseases. Apoptotic cells, rather than individual molecules known to be externalized during apoptosis, would served as targets for the development of human or murine monoclonal antibodies from SLE patients and autoimmune-prone strains of mice. Antibody specificities would be determined and the biological roles they mediate would be ascertained. Their impact on the uptake of apoptotic debris and influence on elicited cytokines would be assessed. In addition, the impact of the antibodies on the migratory behaviour of phagocytes would be evaluated. The antibody variable regions would be sequenced in order to determine whether the humoral recognition of death in a pathological context is necessarily an antigen-driven process. Since many autoantigens externalized on apoptotic blebs are components of macromolecular complexes, the postulate that “internal image” anti-idiotypic antibodies could contribute to epitope spreading would be investigated.

Previous work had established the presence of auto-antibodies to hemoglobin (Hb) in patients of systemic lupus erythematosus, malaria and visceral leishmaniasis, as well as in aging auto-immune prone NZB/W F1 mice. That such antibodies could contribute to pathology was surmised by two finding: Firstly, anti-Hb antibody sequestration was observed in the lungs, kidneys and brains as NZB/W F1 (but not non-autoimmune prone BALB/c) animals aged and secondly, immune complexes of Hb with an autoimmune monoclonal anti-Hb antibody induced synergistic secretion of the pro-inflammatory

cytokines TNF-α, IL6 and IL8 from monocytic cells. Data from human SLE patients had suggested a putative association of anti-Sm and anti-Hb autoantibody responses. These and other studies led to the hypothesis that anti-Sm responses may be sufficient but not necessary for anti-Hb responses, and assumption that was tested in the murine system. NZB/W F1 and BALB/c animals were immunized with either Sm or Hb. Whilst Sm immunization elicited anti-Sm antibodies in both strains, Hb was essentially ineffective as an immunogen. Interestingly, anti-Hb antibodies were elicited in a percentage of NZB/W F1 animals upon immunization with Sm. BALB/c mice failed to respond in this manner, indicating the probable importance of an autoimmune milieu in the phenomenon. Absorption studies ruled out the possibility that frank cross-reactivity was responsible for the association of anti-Sm and anti-Hb responses, a conclusion also supported by the fact that commercial anti-Hb antisera against the alpha and beta subunits did not bind Sm, and Sm was not a dominant reactivity in murine anti-Hb monoclonal antibodies established from aging NZB/W F1 animals. Current data support the hypothesis that anti-Hb antibodies may arise by epitope spreading subsequent to the elicitation of anti-Sm antibodies and experiment are in progress to verify these claims. Clearly however, alternative etiologies for the generation of anti-Hb autoantibody responses exist. Establishing potential patho-physiological outcomes of their presence will form the focus of future investigation.

Aberrant apoptosis is considered one of the hallmarks of systemic autoimmune disease. Our lab has been investigating the hypothesis that antibodies targeting apoptotic cells, depending on isotype, specificity and V region usage, can influence on-going autoimmune responses. Previous work based on immunization of both human and murine monoclonal antibodies indicated increased diversification of elicited autoreactive antibody responses, as ascertained by Western blots, confocal microscopy and ELISAs on a panel of recombinant antigens. Independent immunizations with two IgG murine monoclonal antibodies (which specifically bound apoptotic cells) in NZB/W F1 animals resulted in a significant increase in circulating levels of the IgG1, IgG2a and IgG2b isotypes, with more modest increases in the IgM isotype. The spectrum of enhanced autoreactivity was consistent between individual animals immunized with a particular antibody. In some instances, immunization of six week old auto-immune prone animals led to the appearance in serum of autoantibody responses normally seen only at eight to ten months. Of significance was the observation that this enhancement in the kinetics of the appearance of autoantibodies upon immunization appeared to be restricted to auto-immune murine strains. While Sm complex appeared to be a favoured target for diversification, analysis revealed that individual antigens bound within the complex varied depending on the immunogen. Antigens externalized during the late stages of apoptosis appeared to be preferentially recognized by the elicited antibodies; induction of apoptosis in the presence of a pan-caspase inhibitor abolished reactivity. Further efforts will aim at more precise and comprehensive molecular characterization of target antigens. Additionally, two novel monoclonal antibodies have been generated; while V region usage and somatic mutations analysis has been completed, immunization studies are on-going. It is envisaged that cumulative data arising from such studies would help define and refine the rules which govern the nature and extent of idiotype-mediated antigenic diversification.

Several reports suggest that systemic autoimmune diseases appear to worsen during pregnancy, whereas organ-specific autoimmune diseases ameliorate. Though probably overly simplistically, these effects have often been ascribed to the observation that successful pregnancy appears to be associated with a Th1 to Th2 shift. In this context, human chorionic gonadotropin has been shown by other investigators to induce a

significant amelioration in spontaneous murine Type 1 diabetes in NOD mice, effects accompanied by an increase in T regulatory cell activity. The effects of the administration of hCG into young NZB/W F1 animals was assessed. Enhanced anti-self reactivity was observed as animals aged, accompanied by heightened circulating levels of IgG1 and IgM. Interestingly, levels of IgG2a, IgG2b and IgG3 were lowered. On-going efforts are aimed at characterizing the molecular targets of these responses, and to discern the extent to which the effects of hCG are mediated by its steroidogeneic actions.

Publications

Original peer-reviewed articles

1. Das J, Arora P, Gracias D, Praveen A, Raj BPJ, Martin E and Pal R (2008) Endogenous humoral autoreactive immune responses to apoptotic cells: Effects on phagocytic uptake, chemotactic migration and antigenic spread. *Eur J Immunol* **38**:3561-3574.
2. Vyas HK, Pal R, Vishwakarma R, Lohiya NK and Talwar GP (2009) Selective killing of leukemia and lymphoma cells expressing ectopically hCGβ by a conjugate of curcumin with an antibody against hCGβ subunit. *Oncology* **76**:101-111.

Molecular basis of B cell responses

Principal Investigator: Devinder Sehgal

Project Associates/Fellows: Gautam Kumar Saha
Soma Rohtagi (Jul-Dec 2008)
Minny Bhatty (since Feb 2009)
Parul Ganju (till Jun 2008)
Sriram Srivatsa (till Sep 2008)
Agnideep Mukherjee (since Feb 2009)
Naeem Khan (since Feb 2009)

PhD Students: Soma Rohatgi (till Jun 2008)
Nitika Kaushal
Kumari Sneha
Shweta Narang

Collaborator: Amulya K Panda

B cells critically control infections caused by extracellular bacteria. We use the extracellular bacterial pathogen *Streptococcus pneumoniae* as a model system to understand B cell responses against antigens present in the context of the pneumococcal cell surface. *S.pneumoniae* has several immunogenic protein (T-cell dependent) and polysaccharide (T-cell independent) antigens on its cell surface. Antibodies directed against these cell surface determinants confer protective immunity to *S.pneumoniae*. The research theme in the laboratory is to decipher the molecular and cellular basis of B cell responses against protein and polysaccharide antigens in the context of the pneumococcal cell surface.

The main objectives are (i) molecular analysis of B cell responses to Pneumococcal surface protein A, a protection eliciting antigen and (ii) evaluation of *S.pneumoniae* derived proteins for the development of a protein based pneumococcal vaccine.

Molecular analysis of B cell responses to Pneumococcal surface protein A

Lack of D_H gene-derived amino acids does not prevent anti-$PspA^{3-286}$ mAbs from attaining average relative avidity

In order to assess whether the lack of D_H gene-derived amino acids makes a difference to the binding ability, the relative avidities of 13 IgM and 23 IgG anti-$PspA^{3-286}$ mAbs were determined by competition ELISA using $PspA^{3-286}$ as soluble competitor. For the purpose of this analysis, mAbs with a relative avidity $\leq 1 \times 10^{11}$ M^{-1} were considered low avidity binders. By this criterion, all 13 anti-PspA IgM mAbs are low avidity binders. Three of these mAbs lacked D_H gene-derived amino acids (I4D3, D2F3 and A7A1). There was no significant difference in the average relative avidities of the 3 IgM mAbs that lacked D_H gene-derived amino acids ($7.3 \pm 4.6 \times 10^9$ M^{-1}) and 10 IgM mAbs with D_H gene-derived amino acids ($11.1 \pm 6.2 \times 10^9$ M^{-1}). Of the 23 anti-$PspA^{3-286}$ IgG mAbs, 9 had a relative avidity in the range of 1×10^{11} M^{-1} to 5×10^{11} M^{-1}; the remaining 14 were low avidity binders. The 4 anti-$PspA^{3-286}$ IgG mAbs (L5C8, M6B2, P2G11 and B4G5) devoid of D_H gene-derived amino acids had low relative avidities. The average

relative avidities of the 4 anti-PspA IgG mAbs that lacked D_H gene-derived amino acids ($12.7 \pm 2.1 \times 10^9$ M^{-1}) and 10 low avidity anti-$PspA^{3-286}$ IgG mAbs that possess D_H gene-derived amino acids ($19.7 \pm 5.0 \times 10^9$ M^{-1}) were comparable. None of the 9 high avidity anti-$PspA^{3-286}$ IgG mAbs lacked D_H gene-derived amino acids. There was no correlation between relative avidity and somatic hypermutation pattern of the anti-$PspA^{3-286}$ mAbs. Based on these data, it can be inferred that the absence of D_H gene-derived amino acids does not prevent anti-$PspA^{3-286}$ mAbs from attaining a meaningful or average relative avidity.

IgG subclass-associated affinity differences of Ag-specific Abs have been documented in humans. In order to explore whether IgG subclasses differ with respect to their relative avidities for $PspA^{3-286}$, we analyzed the relative avidities of the 23 anti-$PspA^{3-286}$ mAbs belonging to different IgG subclasses. We focused our attention on the 21 tertiary anti-$PspA^{3-286}$ mAbs that were raised from heat-killed R36A immunized mice. These 21 mAbs belonged to IgG_1 (n = 12), IgG_{2a} (n = 5), IgG_{2b} (n = 3) and IgG_3 (n = 1) IgG subclasses. The average relative avidity (± SE) for the IgG_1, IgG_{2a} and IgG_{2b} mAbs was found to be $167.60 \pm 52.32 \times 10^9$ M^{-1}, $39.86 \pm 23.17 \times 10^9$ M^{-1} and $58.46 \pm 32.41 \times 10^9$ M^{-1}, respectively. The average relative avidity of IgG_{2a} and IgG_{2b} mAbs were found to be comparable but appear to be significantly different from the average relative avidity of IgG_1 mAbs. Whether this is also true *in vivo* was not investigated in our study.

Relative avidity of primary anti-$PspA^{3-286}$ polyclonal IgG Abs induced in response to immunization with heat-killed R36A is higher than that induced in response to $PspA^{3-286}$

The nature of B cell responses induced is likely to be dependent on the form of the Ag delivered. Therefore, it is likely that the anti-$PspA^{3-286}$ Ab responses might differ when PspA is provided as a recombinant protein (given with alum) or in the context of the pneumococcal cell surface (given as heat-killed R36A). The relative avidities of primary anti-$PspA^{3-286}$ polyclonal IgG Abs raised in mice immunized with $PspA^{3-286}$ or heat-killed R36A was determined. The results demonstrate that there is avidity maturation during primary IgG anti-$PspA^{3-286}$ polyclonal Ab response in R36A and $PspA^{3-286}$ immunized mice. The relative avidity of the primary IgG anti-$PspA^{3-286}$ polyclonal Abs reached a peak at day 72 beyond which there was no further increase in the relative avidity for $PspA^{3-286}$. The relative avidities of primary anti-$PspA^{3-286}$ polyclonal IgG Abs induced in response to R36A were higher compared to that generated in response to $PspA^{3-286}$ at day 72, 86 and 100 post-immunization.

Avidity maturation could conceivably arise in part through changes in the proportions of different isotypes over time due to differences in isotype-associated structural features such as segmental flexibility. In order to test this possibility we selected two time points - an early time point (day 28) where the relative avidity of the primary anti-$PspA^{3-286}$ polyclonal IgG Abs induced in response to immunization with $PspA^{3-286}$ and R36A were comparable, and a later time point (day 72) where the relative avidities differed the most. We determined the serum $PspA^{3-286}$-specific end point titers of the various IgG subclasses in the $PspA^{3-286}$ and heat-killed R36A immunized mice that were used for determining the relative avidities. Our data suggests that IgG_1 is the predominant IgG subclass and there is no significant difference in the profile of the serum primary $PspA^{3-286}$-specific Abs belonging to various IgG subclasses induced at day 28 and 72 in R36A immunized mice. In the $PspA^{3-286}$ immunized mice, serum primary $PspA^{3-286}$-specific IgG end-point titer was essentially due to IgG_1 subclass; the anti-$PspA^{3-286}$ IgG_{2a}, IgG_{2b}

and IgG_3 subclass titers were below the preimmune cut-off. Thus, the observed relative avidity maturation of the primary $PspA^{3-286}$-specific IgG Abs induced in response to immunization with $PspA^{3-286}$ and R36A does not appear to be due to changes in the proportions of different IgG subclasses over time. This data when viewed in conjunction with the finding that IgG_1 is the predominant serum IgG subclass in the primary $PspA^{3-286}$-specific IgG Abs induced in response to immunization with $PspA^{3-286}$ and R36A provides indirect evidence that the observed relative avidity maturation is most likely due to increase in the intrinsic affinities of the Abs over time. This however requires formal confirmation.

Evidence for Ag-driven selection

The sequence of the H and L chain expressed in the 36 anti-$PspA^{3-286}$ hybridomas was further analyzed for evidence for Ag-driven selection. This was done by analyzing the replacement (R) and silent (S) mutations in the CDR and FR regions of the expressed H and L chain genes. The distribution of somatic mutations in the H and L chain genes expressed in the anti-$PspA^{3-286}$ hybridomas was analyzed using the multinomial distribution method of Lossos et al. The probability that an excess of R mutations in CDRs or scarcity of R mutations in FRs resulted from chance alone was calculated for the expressed H and L chains. In total, 24 H and 7 L chains had 4 or more mutations and these mutated sequences were from 25 anti-$PspA^{3-286}$ hybridomas. Of the 25 anti-$PspA^{3-286}$ hybridomas, 11 (44%) H chain sequences showed evidence for Ag-driven selection, i. e. significant accumulation of R mutations in CDRs or scarcity of R mutations in FRs ($P < 0.05$). Of the 11 anti-$PspA^{3-286}$ hybridomas that showed evidence for Ag-driven selection at the H chain, only 2 (A1D9 and L5C8) exhibited evidence for Ag-driven selection in their L chain partners and 3 showed high avidities for $PspA^{3-286}$. From this data it can be inferred that the H chain is the major contributor towards PspA recognition. This is consistent with the observation that anti-$PspA^{3-286}$ Ab response utilizes a greater diversity of V_κ families compared to V_H families.

D_H gene segments are an important source of HCDR3 diversity. Each D_H segment gives the developing B cell access up to six functional reading frames (RFs) of distinctly different germline sequence. The D_H RFs utilized in H chain expressed in the anti-$PspA^{3-286}$ hybridomas were analyzed. The 7 anti-$PspA^{3-286}$ mAbs that lacked D_H gene-derived amino acids were excluded from the analysis. The distribution of the RF used in the D_H gene expressed in the remaining anti-$PspA^{3-286}$ mAbs was: RF3 (75.9%), RF1 (13.8%) and RF2 (10.3%). D_H RF3 was preferred over RF1 and RF2. Majority (72.2%) of the anti-$PspA^{3-286}$ mAbs utilized a D_H RF that was rich in tyrosine and glycine codons.

Recognition of the Ag by Ag-specific B cell results in clonal expansion. Analysis of the sequence of the H and L chain expressed in the anti-$PspA^{3-286}$ hybridomas indicated the presence of 2 pairs of clonally related hybridomas. The clones were identified based on identical gene segment usage, and HCDR3 and LCDR3 sequences. Both pairs of clonally related hybridomas were obtained from the same fusion.

There was preferential utilization of V_H1 and V_H14 family usage in the anti-$PspA^{3-286}$ Ab response. Preferential H and L chain pairing was seen in three instances: V_H1 family member paired with $V_\kappa1$ family member (8.33%); V_H2 family member paired with $V_\kappa12$ family member (8.33%) and V_H14 family member paired with $V_\kappa3$ family member (8.33%). The mean CDR3 length at the H and L chain loci was 7.8 ± 0.5 and 8.7 ± 0.2

codons, respectively. This is in contrast to CDR3 length reported for the mouse preimmune repertoire, which ranges from 5 to 20 codons with an average length of ~12.5 codons. These data collectively provide evidence for Ag-driven selection during anti-PspA$^{3-286}$ Ab response.

Localization of B cell epitopes recognized by anti-PspA$^{3-286}$ mAbs

To map the B cell epitopes recognized by the anti-PspA$^{3-286}$ mAbs, a series of overlapping and non-overlapping deletion mutants of PspA$^{3-286}$ were generated. The reactivity pattern of anti-PspA$^{3-286}$ mAbs to PspA$^{3-286}$ and its deletion mutants was analyzed by dot and Western blots. The sub-domain specificity and the location of the 'main' B cell epitope of anti-PspA$^{3-286}$ mAbs were determined. All the 36 PspA$^{3-286}$ mAbs reacted with recombinant PspA$^{3-286}$ and R36A lysate on Western blots. Based on the reactivity pattern with PspA$^{3-286}$ and its deletion mutants, the anti-PspA$^{3-286}$ mAbs were classified into 12 independent groups. Groups 1 and 5 had a lone member. Some mAbs exhibited some degree of cross-reactivity between N- and C-terminal halves of PspA$^{3-286}$. The epitopes recognized by the mAbs that lack D_H gene gene-derived amino acids fell in 6 of the 12 groups.

The topographic relationship between epitopes recognized by 36 mAbs was analyzed by ELISA additivity assay. This assay was used to determine whether members within any given group recognized the same/overlapping or different B cell epitopes. Analysis of the anti-PspA$^{3-286}$ mAbs indicated that members within a group recognized the same or overlapping epitope with the exception of group 7 and 8. Anti-PspA$^{3-286}$ mAbs P1C7 and E3D1 recognized topographically unrelated epitopes located within PspA$^{3-192}$ (group 7). P1C7 and E3D1 were found to recognize same or overlapping B cell epitope when tested in combination with other mAbs within the group (i. e. B4G5, C3D5, F4B1, G3B5 and B5E11). It can be speculated that mAbs P1C7 and E3D1 recognize non-overlapping B cell epitopes, but the B cell epitopes they recognize overlap with the epitopes recognized by B4G5, C3D5, F4B1, G3B5 and B5E11. In the second case, anti-PspA$^{3-286}$ mAbs D2F3 and C6H7 recognized two different B cell epitopes within PspA$^{3-192}$ (group 8). These 2 mAbs when tested in combination with the remaining members of the group (i. e. B3D12 and L5C8) were found to recognize same or overlapping B cell epitope. As in the first case, the mAbs D2F3 and C6H7 recognize non-overlapping regions of PspA$^{3-192}$, but recognize B cell epitopes that overlap with the epitopes recognized by B3D12 and L5C8.

Publications

Original peer-reviewed articles

1. Rohatgi S, Ganju P and Sehgal D (2008) Systematic design and testing of nested (RT-)PCR primers for specific amplification of mouse rearranged/expressed immunoglobulin variable region genes from small number of B cells. *J Immunol Methods* **339**:205-219.

Review/Proceedings

1. Kaushik DK and Sehgal D (2008) Developing antibacterial vaccines in genomics and proteomics era. *Scand J Immunol* **67**:544-552.

Patents

1. Sehgal D and Rohatgi S (2009) Immunoglobulin gene specific oligonucleotides and uses thereof. *Indian patent application # 634/DEL/2008*.

2. Sehgal D and Rohatgi S (2009) Immunoglobulin gene specific oligonucleotides and uses thereof. *Eurpoean patent application filed on 13.3.09*.

3. Sehgal D and Rohatgi S (2009) Immunoglobulin gene specific oligonucleotides and uses thereof. *United States of America patent application filed on 13.3.09*.

Study of genetic factors associated with diabetes at young age

Principal Investigator: Rajni Rani

Project Associates/Fellows: Nachiketa Patnaik (till Feb 2009)
Lakshman Singh
Neetu Israni (till Dec 2008)
Bharati Agarwal
Sarang Tartey (till Dec 2008)
Alok Kumar Singh
Jaya Singh

PhD Students: Archana Singh
Avinash Kumar
T Rajarathna

Collaborators: Ravinder Goswami, *AIIMS, New Delhi*
Nandita Gupta, *AIIMS, New Delhi*
HB Bohidar, *JNU, New Delhi*
Anita Kamra Verma, *DU, New Delhi*
SK Sharma, *AIIMS, New Delhi*
SK Sarin, *GB Pant Hospital, New Delhi*
HK Kar, *RML Hospital, New Delhi*
S Vijaya, *IISc, Bangalore*
Peter Stastny, *SW Med Ctr, Dallas, USA*

The project aims to study the genetic factors associated with diabetes of the young, which include Insulin Dependent Diabetes Mellitus (IDDM) and Ketosis Resistant Diabetes of the young (KRDY). The ultimate aim of the project is to decipher ways that can be used for the diagnosis of the prediabetics in the high risk groups and devise approaches to inhibit autoimmunity. The basic problem with the IDDM patients is that by the time they report to the clinic, the insulin producing beta cells of the pancreases have been damaged to a considerable extent. So, the only treatment left is to give insulin which takes care of the daily insulin requirement but does not stop autoimmunity. Hence, there is a need to identify these patients earlier in life for better monitoring and some kind of immune intervention to inhibit autoimmunity. Altered peptide ligands have been designed to be used *in vitro* to inhibit autoimmune T-cell responses. Peptides inhibiting autoimmune Th1 responses *in vitro* are being encapsulated in nano-sized carriers for slow and targeted release to avoid multiple injections if they have to be used in patients.

Since the disease has been shown to have genetic predisposition, to be able to identify pre-diabetics, the project aims to (i) study the HLA polymorphism in IDDM and KRDY patients from North India and ethnically matched controls, (ii) study the polymorphism of 5'-INS gene (IDDM2) or insulin linked polymorphic region (ILPR) in IDDM and KRDY patients and controls, (iii) nvestigate the autoantibody profile to insulin and islet cells and C-peptide levels in IDDM and KRDY patients and controls, (iv) study other Immune function associated genes which may have a role in manifestation of IDDM, (v) study the association of HLA with the type of autoantibodies found in the patients, (vi) design and use peptides *in vitro* to inhibit autoimmune T-cell responses, (vii) encapsulate the peptides that inhibit Th1 immune responses in-vitro, in nano-sized carriers for slow and targeted

release and (viii) study delivery of peptide/vector complexes in BALB/c and C57BL/6 mice followed by NOD mice.

Other immune-response related genes studied

We had shown earlier that MHC alleles HLA-DRB1*0301 was predisposing and HLA-DRB1*0701 was protective. In the vicinity of the MHC class-II on chromosome 6 two very important genes are localized which code for multifunctional proteosomes, LMP-2 and LMP-7. These are the subunits of large cytosolic proteasomes complex, which are believed to be involved in generation of endogenous immunogenic peptides by proteolysis. LMP-2 and 7 have been found associated with several autoimmune diseases. Three known SNPs in LMP2 and LMP7 genes have been studied in 100 type 1 diabetes patients and 150 healthy controls. More samples are being studied and the data will be analysed after completion of all the samples.

Studies on peptides encapsulated in microparticles

The *in vitro* and *ex vivo* sensitivity of the designed carriers with/without peptides on blood, cell lines and animal based study on BALB/c and C57BL/6 was studied after the Animal Ethics Clearance had been obtained.

Biodistribution of radiolabeled gelatin microparticles: Gamma scintigraphy

Biodistribution (BD) of ^{99m}Tc- gelatin microparticles was done in inbred C57BL/6 mice. 100µl of sterile radiolabeled microparticle suspension (1mg/ml) was administered through the tail vein of each mice, (injected dose: 100µCi/100µl) weighing 25-30g. The animals were sacrificed by cervical dislocation at different time intervals and different organs were removed, washed with normal saline, and dried in paper folds. The radioactivity in each organ was counted using well-type gamma spectrometer, and expressed as percent injected dose per organ. The data is shown in Figure-1.

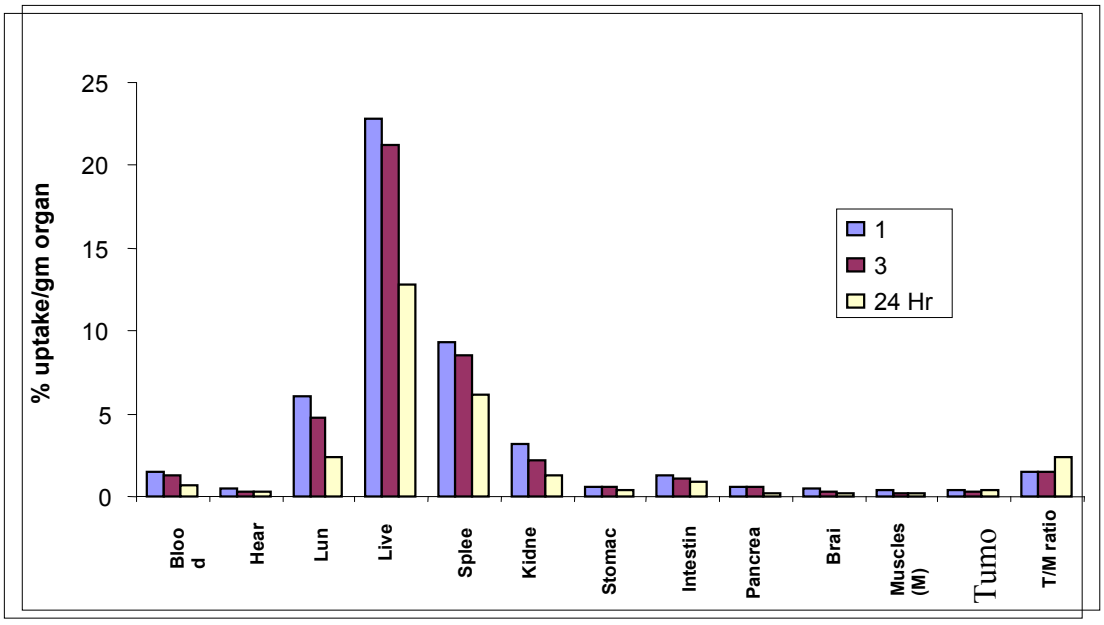

***Figure- 1**: Biodistribution of microparticles in C57BL/6 mice at 1, 3 & 24 hr (% uptake / gm tissue).*

Target moiety binding & binding efficiency (BE%)

A known amount of microparticles were targeted using a target moiety specific for pancreas. The target moiety attached microparticles were separated from unbound moiety after passing the solution through a Millipore filter UFP2THK24 [100KDa cut off] and absorbance of free moiety was noted using the UV-1601, UV visible spectrophotometer (Shimatzu) at 228nm. Accordingly the Binding Efficiency (BE%) was calculated.

Stability of target moiety-microparticle complex

The stability of the complex (target moiety added peptide loaded MP) was studied with respect to time (Table-1).

Table-1: Stability of peptide-microparticle-target moiety complex

Time (Hr)	% Entrapment Efficiency	% Binding Efficiency
0 hr	20	36.25
1 hr	19.1	30.37
2 hr	11	14.7
4 hr	8.6	6.7
24 hr	3.3	4.7

Targeting: Uptake of peptide-microparticle-target moiety complex by pancreatic cells

In vitro:

The experiment was done on the MiaPaCa cell line maintained in 10%FCS supplemented RPMI in CO_2 incubator.

Ex vivo:

6-8 weeks old mice were sacrificed by cervical dislocation and pancreas were aseptically removed. The pancreas were sliced and further subjected to enzymatic degradation by addition of collagenase for two hours. After that the debris was removed & Islets were maintained in RPMI with 10% FCS.

$1x10^6$ cells (MiaPaCa/Islets/MNC) were treated for 1hr with peptide-loaded microparticles, and targeting moiety labeled peptide-loaded microparticles. After treatment cells were scraped and lysed by acetonitrile with 0.1% TFA. The peptide was detected by spectrofluorimetry.

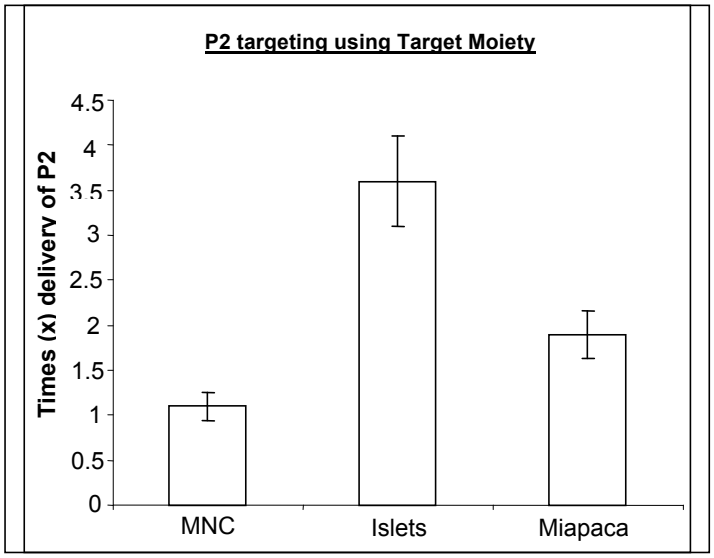

Figure-2*: Uptake of targeting moiety by mononclear cells (MNC), Pancreas (Islets) and by Mia-Paca cell line. [Ex vivo]*

As shown in Figure-2, uptake of the targeting moiety by pancreatic cells and Mia-paca cell line was done *in vitro*, *ex vivo* and *in vivo* in BALB/c mice and C57BL/6 mice. There is negligible uptake by MNC but there is significant uptake by pancreatic cells (~ 4 times).

In vivo:

The experiment was done on 6-8 weeks old male BALB/c mice in group of 4. A known amount of P2 loaded MP with & without target moiety was injected (i.v.) through tail vain and after 2hr they were sacrificed and blood was taken without anti-coagulant for pharmacokinetic & organs (heart, lung, kidney, spleen, liver & pancreas) were taken in chilled PBS pH7.4 to study bio-distribution. The homogenized sample of organs and serum from blood were sent for HPLC. The HPLC analysis did show the peptide peaks, however, they could not be confirmed on MALDI as the sample got too diluted to be detected on mass spectrometry.

Therefore to further validate the targeting of MP by attaching the target moiety, the gelatin microparticles were radiolabelled with ^{99m}Tc, then the targeting moiety was attached to it. Biodistribution studies were done after sacrificing the mice at different time intervals. Owing to the size of the microparticles, they tend to accumulate in liver. Spleen and kidney also indicate some accumulation (Figure-3). The graphical representation does not show any significant accumulation in the pancreas mainly because the uptake by liver is overshadowing all the other organs. However, when we compared the uptake of radiolabelled microparticles with and without targeting in pancreas it gave us encouraging results (Figure-4).

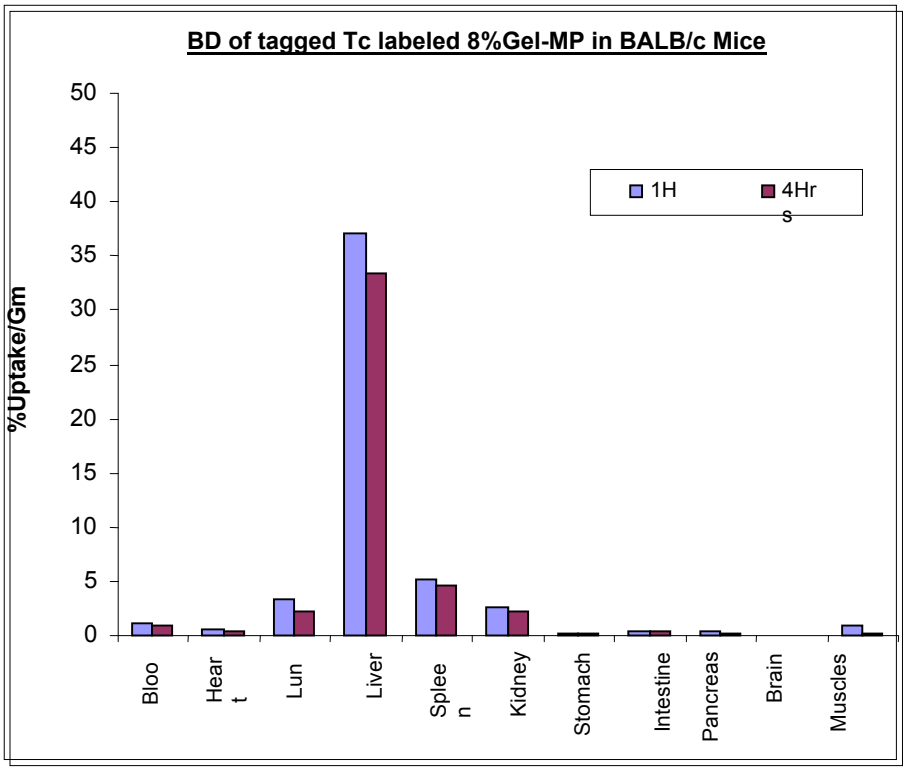

***Figure-3**:Biodistribution of Tc-99 labelled 8% Gelatin icroparticles in different organs in mice at 1hr and 4 hr. (% Uptake/Gm organ [in vivo]*

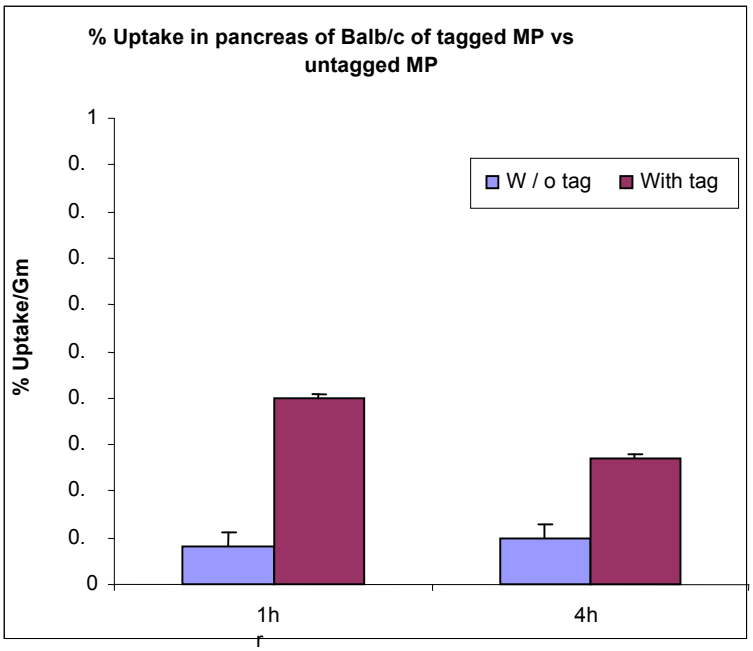

***Figure-4**: Uptake of Tc-99 labelled 8% gelatin microparticles by pancreas in mice at 1hr and 4 hr. (% uptake/Gm organ [in vivo]*

The uptake of the targeted microparticles in pancreas in an hour is ~ 4 times more than that in the control, which substantiate our previous findings in *ex vivo* experiments. Although there is decrease in the accumulation of microparticles in the Pancreas after 4

hours post-injection, the accumulation is still significant, and it warrants further refinement of the experiments.

Publications

Original peer-reviewed articles

1. Bharati K, Rani R and Vrati S (2009) Evaluation of Japanese encephalitis virus DNA vaccine candidates in rhesus monkey (*Macaca mulatta*) *Vaccine* **27**:10-16.

REPRODUCTION and DEVELOPMENT

REPRODUCTION AND DEVELOPMENT

Study on expansion and plasticity in hematopoietic stem cells

Principal Investigator: Asok Mukhopadhyay

Project Associate: Neelam Yadav

PhD Students: Satish Khurana (till Jun 2008)
Sumod K
Mallika R
Amit K Jaiswal (since Jul 2008)

Collaborators: Renu Saxena
Nirja Batala
Lalit Kumar, *AIIMS, New Delhi*
SB Khanna, *Apollo Hospital, New Delhi*

Bone marrow (BM) niche controls self-renewal and differentiation of HSCs. During culture of HSCs, often the stemness and engraftability are compromised. To understand hematopoietic niche, it is important to dissect the adult BM and fetal liver microenvironment during development of mammals. It is hypothesized that artificial BM niche in culture allows *ex vivo* expansion of HSCs without compromising with the engraftability of cells. Expanded cells not only facilitate transplantation for the purpose of hematological reconstitution, they are also expected to contribute in healing of different damaged organs. At present, no suitable system is available for *ex vivo* expansion of stem cells. It is also not clearly understood how HSCs are involved in the regeneration of damaged organs, other than bone marrow. The overall theme of our research are (i) to understand BM niche and expand HSCs, (ii) study on plasticity in adult stem cells and using them as regenerative medicine, and (iii) identifying the origin of ovarian cancer stem cells and molecular characterization.

Thus the aims of our laboratory are molecular analysis of HSCs during expansion, its migration during development and tissue repair, and plasticity. The specific objectives of the work are (i) molecular control of self-renewal and engraftibility of HSCs in adult and fetal mice, (ii) expansion of CB-derived HSCs and SCID repopulation assay, (iii) regeneration of liver and other vital tissues/organs by BM- and fetal liver-derived cells, (iv) molecular mechanism for differentiation of BM cells into hepatocytes and (v) characterization of ovarian cancer stem cells.

A. Hematopoietic stem cells: expansion and marrow niche

We investigated marrow regeneration by donor HSCs in lethally irradiated host. The absolute number of donor-derived HSC ($Lin^-Sca\text{-}1^+c\text{-}kit^+$) was increased between 5^{th} and 15^{th} days of transplantation. After that no further increase in stem cells population was observed. The increase in stem cells population suggested that during marrow regeneration, the donor HSCs might have multiplied by symmetric division. This was possible due to BM niche-directional determination of fate, which causes HSCs to proliferate by symmetric and asymmetric division.

CD133-enriched cord blood cells were cultured for 10 days in the presence of cytokine supplemented medium. A representative dot-plot of expanded cells showed that about

20% cells were $CD34^+$ (Figure 1). Further analysis revealed that among these target population, 40% of them were $CD34^{bright}$. On the basis of five independent experiments, the fold expansion of $CD34^+$ and primitive hematopoietic stem cells ($CD34^+CD38^-$) were 40 ± 4.6 and 6.9 ± 1.1, respectively. The expanded cells were further analyzed for lineage commitment. $CD7^+$ and $CD19^+$ cells were negligibly formed in culture, whereas a considerable number of cells expressed CD14 (46.1 ± 7%). Two-color flow cytometric analysis showed that almost two-third of $CD14^+$ cells also express CD38, indicating that they were not terminally differentiated. A considerable fraction of cells were not lineage committed and expressed only CD38 antigen (37.7 ± 6.5%). In a separate experiment, it was revealed that the expansion of HSCs can be improved, if cultured in the presence of 5% oxygen tension instead of 20%.

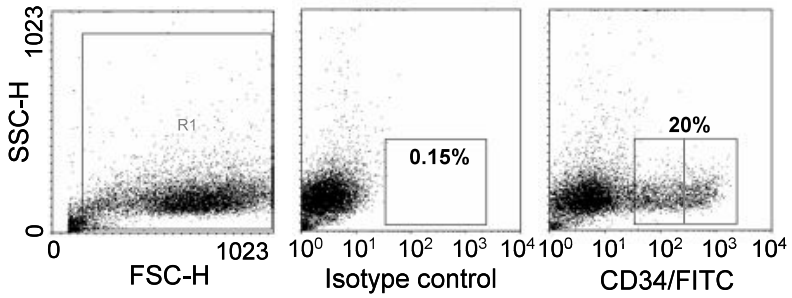

Figure-1: *Flow cytometric analysis of expanded CB cells. Cells were initially gated R1 in forward and side scatter plot (left). The representative dot-plot of cells stained with CD34/FITC showing 20% stem cells population (right).*

B. Plasticity in BM cells

Earlier, we showed that the expression of OSMRβ enhances before BM cells differentiate into albumin expressing cells. The differentiation process is followed by the expression of c-Met and subsequent cellular proliferation. These results perhaps implicated the role of OSM/OSMRβ for differentiation of $Lin^-OSMR\beta^+$ cells into hepatocytes, and HGH/c-Met for providing mitogenic signal. To confirm these events and the involvement of respective signaling molecules, we conducted antibody blocking experiments. The neutralization of OSM in culture medium resulted in significant drop (68.5% to 14.3%) of albumin expressing cells, suggesting that the differentiation process was inhibited (Fig. 2A). The blocking of c-Met showed marginal reduction in albumin expressing cells (68.5% to 64%), as differentiation precedes proliferation of cells (Figure 2A). Differentiation of $Lin^-OSMR\beta^+$ cells to hepatocytes was affected when the functions of both OSM and c-Met were blocked by adding mixture of antibodies (Figure 2A). Overall, these results clearly demonstrated that the interaction between OSM and its receptor (OSMRβ) was critical for transdifferentiation of cells, and blocking c-Met with anti-c-Met antibody suppressed cellular proliferation. The proliferation of cells was confirmed by BrdU incorporation assay, as in control (unblocked) more cells incorporated BrdU than blocked cells (Figure 2B).

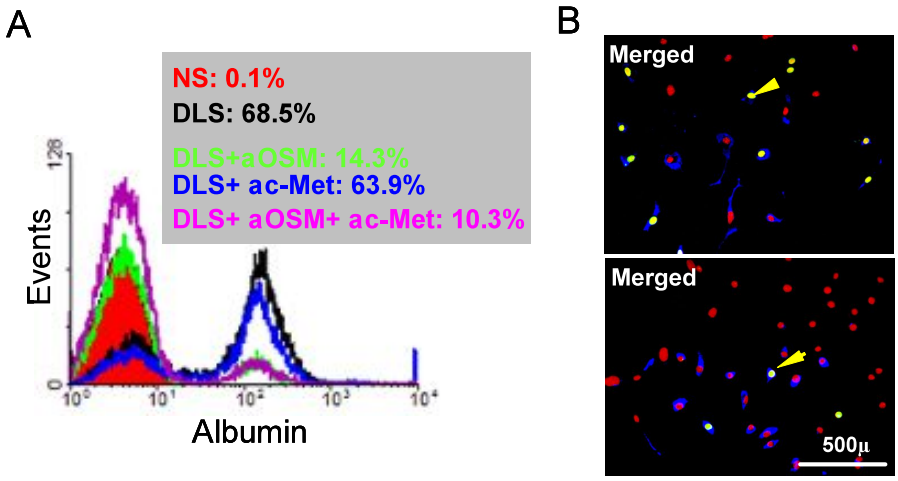

Figure-2: *Effect on cellular response by blocking OSMRβ and c-Met.* ***A****. Flow cytometric analysis of albumin expression. Cells were cultured in normal serum (red); damaged liver serum, DLS (black); DLS, OSM-neutralized (green); DLS, c-Met-neutralized (blue); and DLS, OSM and c-Met neutralized (cyanine).* ***B.*** *Immunocytochemical analysis for the expression of albumin and BrdU incorporation in unblocked (control, top) and c-Met-blocked culture (bottom). Arrows indicated BrdU incorporated cells (yellow nuclei).*

We observed that transcription factors HNF1α, -3β, and -4α were expressed during transdifferentiation of cells. By immunocytochemical analysis, HNF4α first detected in the cytoplasm on day 3 of the culture, but no albumin was found to be expressed by the cells. The synthesis of albumin by the cells on day 5 was associated with increase in HNF4α expression and its nuclear localization. In the later time points, the expression of HNF4α and its nuclear localization augmented albumin synthesis. The expression of HNF4α, its nuclear localization and the synthesis of albumin suggested that these events were interlinked. It was also found that neutralization of OSM resulted in declining the expression and nuclear localization of HNF4α.

To confirm the pivotal role of HNF4α in transdifferentiation process, we over-expressed the same in a myelo-monocytic cell line (32D). Transfected cells with HNF4α showed distinct morphological feature as compare to the untransfected cells. Transfected cells adhered to the culture plate and found to express hepatic markers: albumin (Figure 3A:a), α-fetoprotein (Figure 3A:b), and cytokeratin-18 (CK-18) (Figure 3A:c). Besides expressing hepatic markers, the cells were found to be functionally active as they express metabolic enzyme p450 (Figure 3A:d). In contrast, over-expression of DN-HNF4α in $Lin^{-}OSMR\beta^{+}$ cells causes decline of albumin and TAT gene expression (Figure 3B).

The coagulating protein, factor VIII (FVIII) is produced in liver. We wanted to check the functional recovery of hemophilia A (HA) mice from bleeding phenotype by transplanting BM cells. Various lines of evidence indicated that, within the liver, hepatocytes are major FVIII producing cells. Besides hepatocytes, sinusoidal endothelial cells are also shown as the cellular site for FVIII synthesis in mice. We transplanted Lin^{-} BM cells in acetaminophen-conditioned mice. Mice were analyzed at different times after

transplantation. The survival rate in HAT mice was increased from 23 to 80% in tail-clip challenge experiment (Figure 4A). Twenty five of 31 HAT mice (5 and 12 months post-transplantation) that received BM cells achieved hemostasis between 2-4 h after tail clipping, although most of the HA mice did not survive.

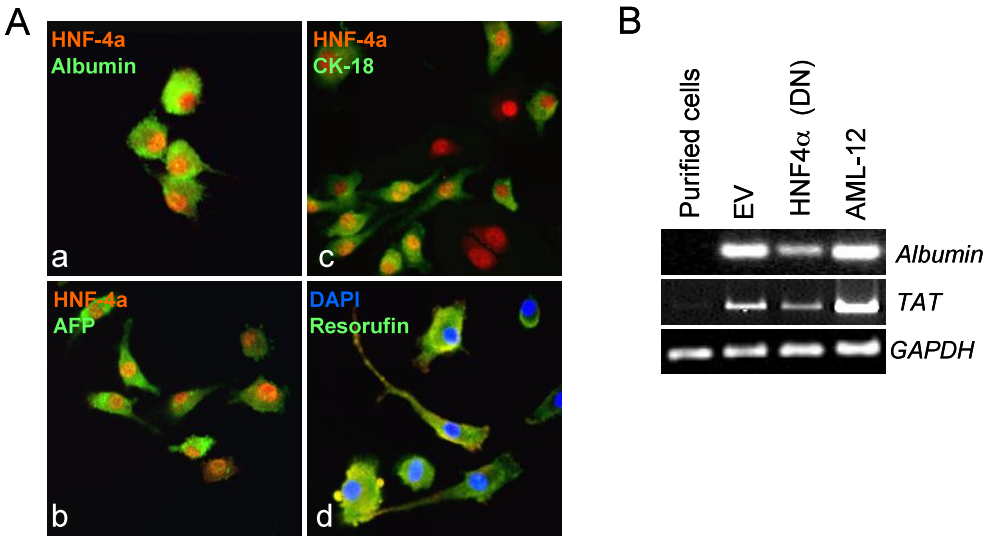

Figure-3: *Over-expression of FL-HNF4α and DN-HNF4α in cultured cells.* ***A.*** *Nuclear localization of HNF4α and expression of hepatic markers by transfecting 32D cell line with FL-HNF4α.* ***B.*** *Inhibition of transdifferentiation by ectopic expression of DN-HNF4α in $Lin^{-}OSMR\beta^{+}$ cells during culture. EV: empty vector; DN: dominant negative; FL: full length.*

The results of these functional assays suggest that BM cells not only produced FVIII protein in liver of HA mice, it was also secreted in the circulation. To confirm phenotypic correction, we conducted gene expression analysis of FVIII light chain by RT-PCR, as intact light chain is missing in HA mice. We designed a primer pair to amplify a specific segment of the light chain A3 domain in which gene disruption was introduced in mutant mice. In PCR amplification, the wild type cDNA provides a 637-bp product. However, due to the presence of *neo* cassette sequence (high G + C content) the same gene segment is not expected to be reverse transcribed and amplified in HA mice. The results of RT-PCR analysis showed that the same gene segment was amplified in wild type (WT) mice, but not in mutant (HA1 and HA2) mice (Figure 4B). Intriguingly, the same gene fragment was amplified in all three HAT mice (Figure 4B). In WT mice, the plasma FVIII:C activity was 96 ± 15% (n = 12) as compare to the normal pooled mice plasma. The FVIII activity in HA mice was 0.7 ± 0.25%, which was increased to 15.7 ± 3.2%, 26.4 ± 9.4% and 19.1 ± 5.1% in

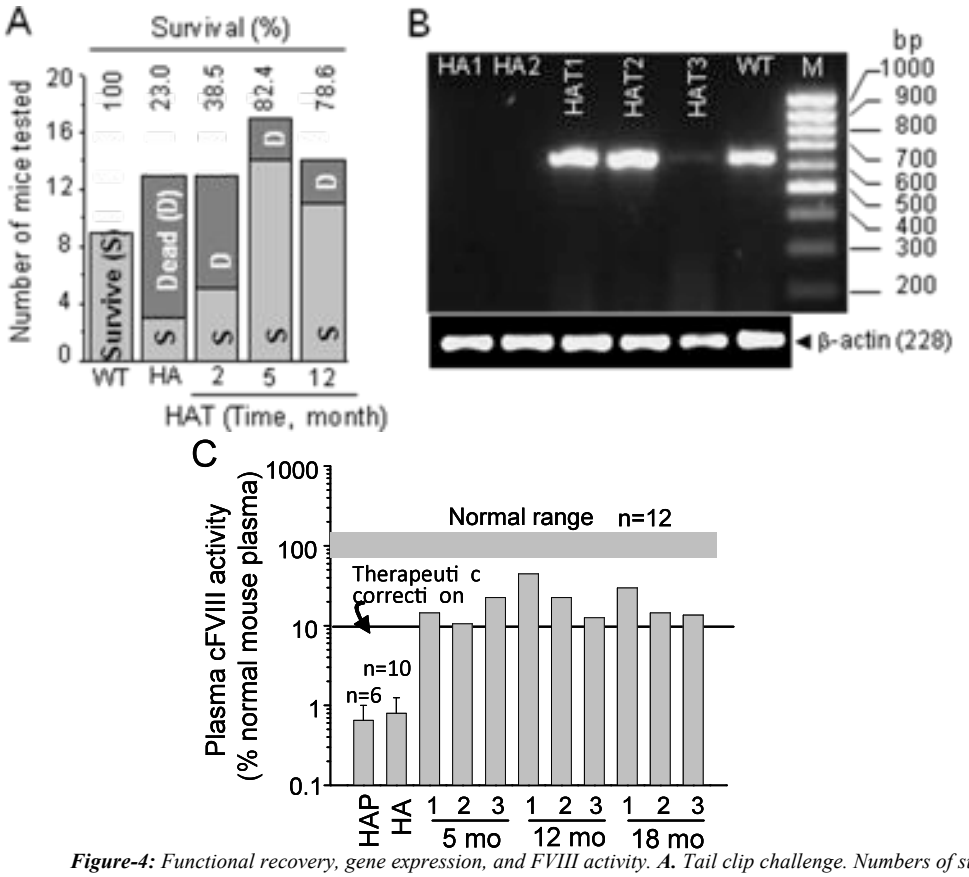

Figure-4: *Functional recovery, gene expression, and FVIII activity.* ***A.*** *Tail clip challenge. Numbers of survived and dead mice are shown after tail clip. In HAT mice, 80% were protected from death due to blood loss.* ***B.*** *RT-PCR analysis for synthesis of target amplicon. HAT1-3 mice show the synthesis of 637 bp amplicon, like WT (wild type) mice. The same product is absent in both the knock-out mice (HA1 & HA2).* ***C.*** *Relative FVIII:C activity. The percentage relative FVIII:C activities in plasma samples of HAT mice were determined by comparing clotting times with the standard curve. The normal range of mouse FVIII activity is indicated by the gray shaded region. HA- hemophilia A (mice); HAT- HA transplanted; WT- wild type mice; HAP- HA patient.*

HAT mice after 5, 12 and 18 months of transplantation, respectively (Figure 4C). Tukey-Kramer multiple comparison analysis suggested that plasma FVIII:C activities in HAT mice were significantly (HA to HAT_{5mo}: $P < 0.05$; HA to HAT_{12mo}: $P < 0.001$; HA to HAT_{18mo}: $P < 0.01$) higher in all three test groups as compare to the HA mice. These results indicated that the average FVIII:C activity during 5 to 18 months of study was stable at 20.4 ± 3.6% (n = 9) (Figure 4C).

Publications

Original peer-reviewed articles

1. Khurana S and Mukhopadhyay A (2008) Hematopoietic progenitors from early murine fetal liver possess hepatic differentiation potential. *Am J Pathol* **173**:1818-1827.

2. Khurana S and Mukhopadhyay A (2008) *In vitro* transdifferentiation of adult hematopoietic stem cells: an alternate source of hepatocytes. *J Hepatol* **49**:998-1007.

3. Gopal PNV, Rentala S, Roy S, Wadhwa R, Sharma S, Roychaudhury PK, Mukhopadhyay A and Ray AR (2008) An artificial niche for expansion of long-term engraftable mouse hematopoietic cells. *J Stem Cells* **3**:245-254.

4. Khaparde SS, Roychoudhury PK, Gomes J and Mukhopadhyay A (2008) External modulation of HT-1080 human fibrosarcoma cells improves urokinase production. *Biotechnol Prog* **24**:1325-1332.

Vaccination against oncofetal antigen human chorionic gonadotropin (hCG): A potential immunotherapy for hormone dependent cancers

Principal Investigator: Om Singh

Co-investigator: Rahul Pal

Project Associates/Fellows: Priyanka Khare
Ruchi Sachdeva
Sandhya Singh (till Sep 2008)
Nitu Bhardwaj (since Jan 2009)

PhD Students: Anjali
Suchismita Sahoo (since Dec 2008)

Human chorionic gonadotropin (hCG), normally produced by the placental trophoblast during pregnancy, is also secreted by a variety of malignant tumors. Its presence has been linked to chemo- and radio-resistance, increased invasiveness and poor prognosis. Neutralization of hormonal activity may be of potential benefit; anti-hCG vaccination is therefore an attractive option for immunotherapy of hormone-dependent cancers.

The objectives of the project are (i) potentiation of immune responses against hCG and (ii) assessment of the effect of anti-hCG responses/antibodies on tumor growth parameters.

hCG-induced proliferation inhibited by anti-hCG antibodies

Experiments were conducted to ascertain whether hCG could act as an autocrine growth factor. Cells were incubated with exogenous hCG at different concentrations. A dose-dependent increase in cell number was observed. While incubation with normal serum had no growth inhibitory effects, incubation with anti-hCG antibodies reversed hormone-induced growth of these cell lines, providing further support for an autocrine role for the hormone.

Effect of hCG on angiogenesis and tumor migration

Transmigration assays were carried out to investigate if, in addition to having growth promoting properties, hCG could also act as a chemotactic agent for endothelial cells. Results showed that hCG induced significant migration, indicating un-appreciated chemotactic properties and a possible role in angiogenesis. Anti-hCG antibodies reduced the hCG-induced transmigration of Colo-205, HTB-168 and Lewis lung carcinoma (LLC, mouse) cells as well as of human brain microvascular endothelial cells.

Effects of hCG on MMP-2, MMP-9, VEGF and IL-8

MMPs have been implicated in the invasion and metastatic processes that characterize aggressive tumorigenesis. The ability of these enzymes to degrade the extracellular matrix is believed to assist tumor cell migration and subsequent colonization at distal sites. MMPs also induce the release of fibroblast growth factor and VEGF, thereby promoting tumor growth. hCG is known to increase the secretion of MMP-2 and MMP-9

from the cytotrophoblast. RT-PCR analysis was employed to assess MMP-2 and MMP-9 mRNA in Colo-205, HTB-168 and LLC cells after culture in serum-free medium or medium containing hCG with or without anti-hCG antiserum. hCG treatment up-modulated mRNA expression of both MMPs. Anti-hCG antiserum inhibited hCG-induced increase of MMP mRNA, whereas normal serum has no effect. Zymograph analysis supported these findings. Gelatinase activity in unstimulated cell supernatants from all three cell lines was detected at 92 kDa (corresponding to the active form of MMP-9) as well as at 72 kDa (corresponding to the active form of MMP-2). hCG up-modulated MMP-2 and MMP-9 activity; in Colo-205 cells, the pro-form of MMP-9 was also observed, particularly in cells stimulated with hCG. Whereas anti-hCG antiserum inhibited the hCG-induced increase in MMP-2 and MMP-9 activity, normal serum had no effect.

RT-PCR analysis revealed that hCG was capable of up-modulating mRNA levels of both VEGF (a molecule known to promote angiogenesis) and IL-8 (a pro-inflammatory CXC cytokine), effects neutralized by the presence of anti-hCG antiserum but not by the presence of normal serum. hCG enhanced IL-8 production by HBMEC, Colo-205, HTB-168 and LLC cells. Anti-hCG antibodies displayed significant inhibitory effects, not observed when normal serum was employed.

hCG-induced invasion

Matrigel-based invasion assays were carried out to ascertain the metastasis inducing potential of hCG and whether anti-hCG antibodies can mediate an inhibitory role. hCG induced a significant increase in the invasion of Colo-205, HTB-168 and LLC tumor cells into the Matrigel substrate. In all instances, invasion was almost completely inhibited when anti-hCG antiserum was employed, an effect not seen when normal serum was used.

Effects of anti-hCG antibodies on tumor growth in nude mice

The *in vivo* anti-tumor activity of anti-hCG antibodies was evaluated in tumor implantation studies in nude mice. The passive administration of anti-hCG antibodies significantly reduced the rate of growth of Colo-205, HTB-168 and LLC cell lines, whereas tumors in animals administered normal serum grew at rates comparable to those in control animals.

Effect of active immunization on tumor growth

The ability of anti-hCG vaccination to inhibit tumor growth was investigated using LLC. Groups of 10-12 mice (C57BL/6, isogenic to LLC) were injected with βhCG-TT with or without *Mycobacterium w*. One group served as tumor control. A total of three injections of alum-adsorbed antigen were given at an interval of 4-weeks. Mice were bled at regular intervals and anti-hCG antibody titres determined in individual sera. Two sets of experiments were employed to assess the effect of immunization on tumor growth. In the first, tumor implantation was initiated along with the hCG immunization. In the second, mice were pre-immunized with the hCG vaccine and tumor implanted at week 9 post-immunization.

Immunization with βhCG-TT prior to tumor implantation resulted in significant decreases in tumor incidence as well as volume. Co-immunization of βhCG-TT and *Mycobacterium w* appeared to provide additional benefits; tumor volumes, as well as the number of animals exhibiting tumors, were further reduced and anti-tumor effects were significantly enhanced when compared with groups receiving βhCG-TT or *Mycobacterium w* alone. These results were further substantiated by survival graphs. Simultaneous immunization and tumor implantation appeared to provide similar tumor inhibitory effects; in these animals too, co-immunization with βhCG-TT and *Mycobacterium w* demonstrated significant advantage over βhCG-TT or *Mycobacterium w* alone, in terms of the number of animals expressing tumors, mean tumor volumes as well as animal survival.

These findings suggest that anti-hCG vaccination has potential as a clinically relevant strategy for the immunotherapy of gonadotropin-secreting tumors.

Immunization studies in transgenic animals

Transgenic mice secreting βhCG were obtained under a collaborative program with the Imperial College of London. This mouse model has provided evidence for the role of gonadotropins as contributing factors to reproductive dysfunction and gonadal tumorogenesis. These animals express ovarian, pituitary and mammary tumors with high penetrance and serve as good model to assess the effects of anti-hCG vaccination. Mouse lines over-expressing βhCG were established by breeding heterozygous males with wild type FVB/N females. Animals were screened for βhCG gene expression by PCR and βhCG levels assessed by RIA. Studies were initiated to evaluate the effects of active anti-hCG immunization. Blood samples were collected at regular intervals and antibody titers determined by RIA. Immunization of transgenic animals prevented the age-dependent increase of body weight (reflective of reduced deposition of fat in the abdominal region) seen in non-immunized animals. Histological analysis of the ovaries and the pituitary glands is on-going.

Characterization of proteins important for cell death regulation

Principal Investigator: Chandrima Shaha

Project Associates/Fellows: Manohar L Chaudhary
Vishnu Agarwal (till Feb 2009)

PhD Students: Rohit Jain
Manikandan Subramanian
Smriti Verma
Rakshamani Tripathi
Abhishek Aich

Collaborators: Chitra Mandal, *IICB, Kolkata*
Avadhesha Surolia
Sarika Gupta

Essentially all animal cells have the ability to kill themselves by activating a gene-encoded cell suicide program. The decision of whether a particular cell will live or die is tightly regulated by many different signals originating both from the intracellular compartment as well as the extracellular environment. The overall goal of our research program is to elucidate the precise mechanisms by which cells die and how these processes are regulated by diverse signaling pathways in various unicellular and multicellular model systems.

Broadly, we aim to explore the underlying mechanisms that induce a cell in a given situation to survive or die and identify the molecular players. One of our experimental model systems is the protozoan parasite *Leishmania* spp. that branched early during eukaryotic evolution and survives in disparate biological environments during its life cycle. It provides an interesting system for studying a broad range of cellular pathways leading to cell death, some of which may be universal features of eukaryotic cells and would help us understand how more complex higher-eukaryotic regulatory systems evolved. Other cellular models that we use to pursue our interests on mechanisms associated with cell death include, mammalian macrophages and the male germ cells. In these culture systems, estrogen is used as a stimulus to create altered situations in the cells and the effects on the signaling pathways are explored with a view to understand the complexities underlying the survival and death response of cells to steroid hormones.

Biology of cell survival and death in protozoan parasites

Under the main theme of our program, the investigations on the unicellular model system of *Leishmania* spp. includes investigation of complex interactions between oxidative stress, defensive enzymes and other molecules related to cell survival or death to understand the processes involved in parasite biology and find targets that could be used for manipulation of parasite survival.

Subsequent to last year's report on the ability of overexpressed cTXNPx to increase cell survival and the establishment of the mechanism of increased viability through manipulation of Ca^{2+}, investigations were undertaken to check if Ca^{2+} had a role in regulation of the enzyme function. Analysis using the calmodulin target database

(Ontario Cancer Institute) revealed the existence of a calmodulin binding site spanning amino acids 26-39 from the N-terminus of cTXNPx. Bioinformatic studies were carried out to see the involvement of calmodulin binding site during interactions with cytosolic tryparedoxin (TxN) which binds to cTXNPx during enzyme activity and calmodulin in conditions that would be favorable within the cell. Cytosolic TXNPx exists as a decamer in the cytoplasm, therefore the *Leishmania donovani* cTXNPx decamer was generated by Swiss Model based on *Trypanosoma cruzi* protein structure (PDB No. 1UUL) and visualized using PyMol. Residues predicted to constitute the calmodulin binding site were on the surface of the decamer indicating the availability of these residues to interact with other proteins. The protein, however, in physiological active conditions is associated with its partner cTXN, hence it was essential to know whether these residues remain free in the cTXN – cTXNPx complex. The protein structure for *L.donovani* cTXN generated by Swiss Model based on crystal structure of native tryparedoxin I from *Crithidia fasciculata* (PDB No. 1EWX) was docked to cTXNPx monomer using ClusPro. The docking results show that the calmodulin binding site remains free even when cTXN binds to cTXNPx (Figure-1A). Further, it was important to see whether calmodulin binds to cTXNPx using these predicted residues. The protein structure for *L.donovani* calmodulin, generated by Swiss Model based on crystal structure of calmodulin from *Bos taurus* protein structure (PDB No. 2F2P) was docked to cTXNPx monomer (the decamer could not be used for docking as it was large for the computational limits of the web-based program). The model obtained as a result, visualized using PyMol, shows that calmodulin binds to cTXNPx using these predicted residues (Figure-1B). Cytosolic TXNPx with mutations at the calmodulin binding site show compromised binding to calmodulin *in vitro*, thus verifying the authenticity of the calmodulin binding site.

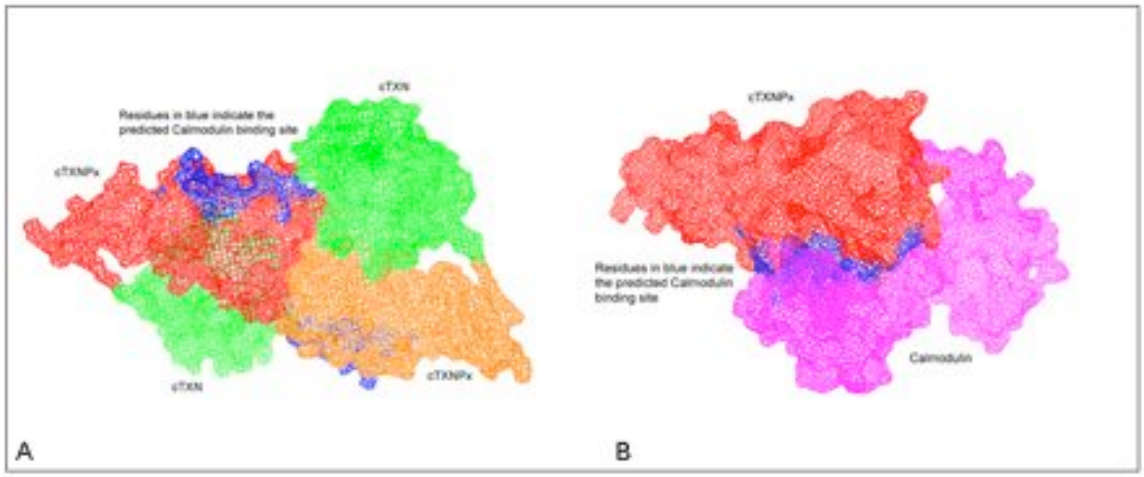

Figure 1: *A. Structure of cTXNPx in combination with cTXN showing the calmodulin binding site indicated in blue even after binding of cTXN. B. Shows binding of calmodulin to the calmodulin binding site on cTXNPx.*

In the current year, we report further characterization of *Leishmania* prohibitin. Our work during the current reporting period show that overexpression of prohibitin with a mutation at the GPI anchor site (by replacing asparagine 252 to aspartic acid at the N-glycosylation site of the prohibitin gene) in *Leishmania* promastigotes show reduced binding to macrophages as compared to parasites overexpressing a wild-type form of the protein. To determine the binding partner for surface prohibitin, macrophage membrane preparation was incubated with recombinant prohibitin and immunoprecipitated with anti-prohibitin antibody. MALDI-TOF analysis of tryptic digests of a 70kDa protein pulled down by a prohibitin antibody gave signature of HSP70. The experiments

presented in this section clearly demonstrate that HSP70 present on the macrophage membrane was able to bind to *Leishmania* prohibitin. Prohibitin being a cell surface molecule, we have also checked if patients of Kala-Azar show antibodies to this protein and all the 34 patients investigated, showed presence of anti-prohibitin antibody titer which correlated with the severity of the disease.

We have earlier reported the cloning and sequencing of 3 cytochrome P450s from *Leishmania donovani.* The CYPs in kinetoplastid parasites have not been explored at all. Further studies were carried out to assess their function through the generation of half knockouts by homologous recombination. CYP5122A1 and CYP710C half knockouts were characterized and functional studies were initiated. In both cases, the transfectants were susceptible to oxidative stress and two currently used anti-leishmanial drugs, miltefosine and potassium antimony tartrate. The CYP5122A1 half knockouts caused poor infection when tested in an *in vitro* macrophage-*Leishmania* binding system which could be a result of faster elimination of the parasite due to a compromised drug elimination system.

Hormonal modulation of cellular apoptosis in mammalian macrophages

This part of our report describes the progress achieved on estrogen induced cell death pathways in mammalian macrophages. Treatment with estrogen simultaneously activated the death and the survival pathway and when the survival pathway was downregulated, cell death ensued. In the current reporting year we describe our efforts to understand how this dichotomous effect of estrogen occurs. Our studies show that plasma membrane associated estrogen receptor (ER)-α participate in E2 induced Bcl-2 increase through activation of the MAP-kinase pathway while cytosolic ER-β transmits signals for the pro-apoptotic event of Bax translocation. ER-α and ER-β receptor mRNA and proteins were selectively downregulated with siRNA for ER-α and ER-β to test the effect of this downregulation on Bcl-2 and Bax and eventually cell death. While Bcl-2 increase was achieved through activation of a signaling pathway via membrane located ER-α receptors, the mechanistic basis of Bax translocation comprised of ER-β mediated increase in intracellular pH facilitated by activation of the Na^+-H^+ exchanger. ER-β mediated intracellular alkalinization leading to Bax migration and ERK mediated concomitant Bcl-2 upregulation did not cause cellular apoptosis, however, siRNA mediated downregulation of ER-α during estrogen exposure led to inhibition of Bcl-2 increase and consequently apoptosis due to the unopposed action of mitochondrial Bax enabling us to propose a model for involvement of the Bcl-2 family member in macrophage survival during estrogen exposure (Figure 2). In summary, this study underscores the importance of integrative signaling modality from multiple estrogen receptor pools in modulating estrogen effects on human monocyte derived macrophage apoptotic signaling pathway which opens new vistas to explore the use of selective estrogen receptor modulators in apoptosis-based therapies. This study also in part explains the previous observations suggesting estrogen mediated survival or death in macrophages. The presence of differential levels of estrogen receptors α and β in these cells could be one of the driving forces in determining cell fate.

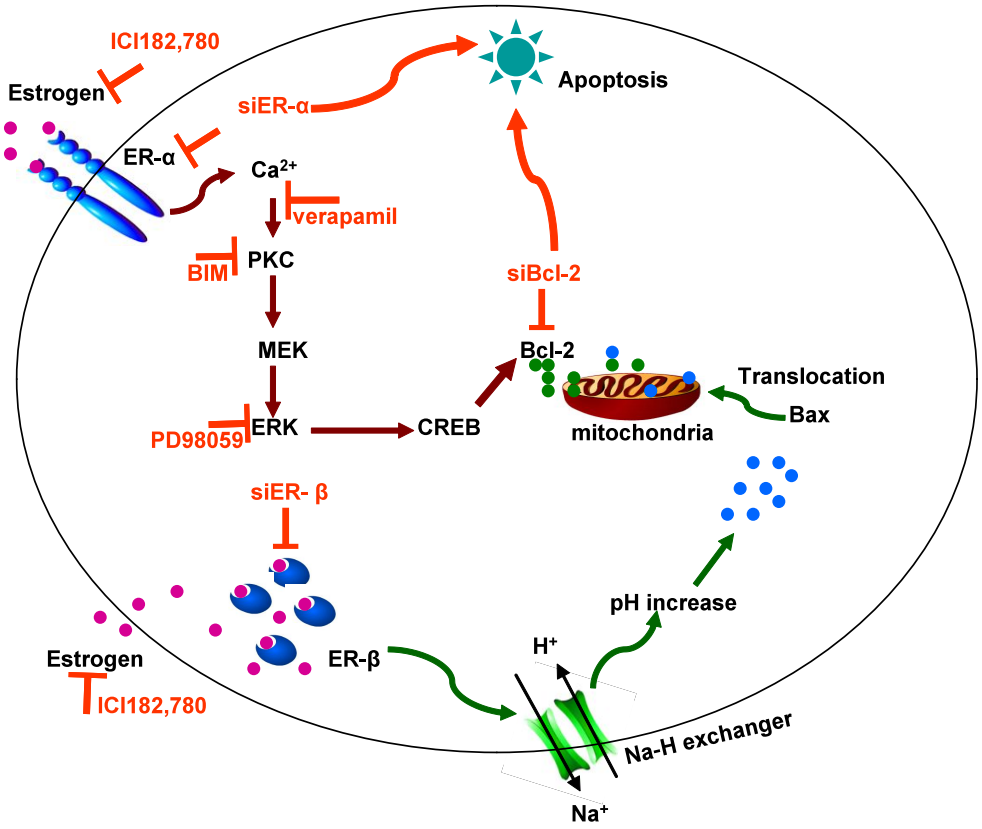

Figure-2. *Schematic representation of the findings detailed in the text showing the dichotomous effect of estrogen on the mitochondrial apoptotic pathway being mediated by two sets of estrogen receptors located at two distinct subcellular locations. Bars in red show inhibition points.*

Publications

Original peer-reviewed articles

1. Iyer J, Kaprakkaden A, Chaudhary M and Shaha C (2008) Crucial role of cytosolic tryparedoxin peroxidase in *Leishmania donovani* survival, drug response and virulence. *Mol Microbiol* **68**:372-391.

Reviews/Proceedings

1. Shaha C (2008) Estrogens and spermatogenesis. **In**: Molecular mechanisms of spermatogenesis (Ed: Cheng CY), Landes Bioscience, Austin, Texas. 42-56.

Patents

1. Shaha C, Jain R and Mandal C (2009) Detection of pathogen using antigenic prohibitin peptide. *Indian patent application # 474/DEL/2009.*

Cellular and molecular biology of human cancer

Principal Investigator: Anil K Suri

Project Associates/Fellows: Manoj Garg
Aashima Khosla
Mohit Vashistha

PhD Students: Deepika Kanojia
Shikha Saini

Collaborators: Rajive Kumar, *AIIMS, New Delhi*
Amlesh Seth, *AIIMS, New Delhi*
Sudha Salhan, *Safdarjung Hospital, New Delhi*
Amar Bhatnagar, *Safdarjung Hospital, New Delhi*
Sushma Suri, *Safdarjung Hospital, New Delhi*
Anju Gupta, *Moolchand Hospital, New Delhi*
Samir Gupta, *RRAH, New Delhi*

Over the last three decades, knowledge on the molecular biology of human cancers has vastly expanded. A host of genes and proteins involved in cancer development and progression have been identified and many mechanisms at the molecular, cellular and even tissue level have been, at least partly, elucidated. In fact, cancer research has now reached a critical stage, in which the accumulated knowledge on molecular mechanisms needs to be translated into improved prevention, diagnosis, and treatment. Understanding the mechanisms involved in tumorigenesis has wide ranging implications for targeting the treatment of cancer. Cancer testis (CT) antigens represent a unique class of tumor antigens, which are expressed in a variety of cancerous tissues and are silent in normal tissues, except for the testis. A characteristic commonly shared by cancer testis antigens is, aside from the highly tissue-restricted expression profile, their likely correlation with tumor progression and immunogenicity in cancer patients. Also the differential expression of germ cell specific genes in various cancer tissues reveals the important link between the two complementary disciplines of cell survival i.e. developmental and cancer biology.

Numerous candidate cancer associated genes have been identified to date by ‘‘ome’’-based technologies, cDNA microarrays, and tissue microarrays. However, for the vast majority of these genes, neither the expression pattern of the protein product, nor its localization and function in the tumor tissues, has been investigated. An important issue in tumorigenesis is the early spread and development of distant metastasis. In this regard, identification of specific genetic markers that are associated with tumor progression and aggressiveness may prove to be useful to assess the progression of disease. We are focusing on tumor associated proteins for the assessment of disease risk, early detection of disease, therapeutic prognosis, and response to treatment as well as disease recurrence. The application of such gene products (biomarkers) to cancer will lead the way because of the unique association of genomic changes in cancer cells with the disease process. Most importantly, cancer biomarkers for prognostic, prediction and pharmacodynamics may aid in the rational development of anti-cancer drugs. Cancer/Testis (CT) antigens are a group of tumour antigens with gene expression restricted in male germ cells and in various malignancies. Therefore, the study sought to determine the functional genomics

of germ cell associated proteins in cancer biology. In addition, our goal is to delineate in greater detail the gene-expression pathways involved in cellular growth, cell migration, and invasion for the treatment of cancer.

Cancer Research Program

Breast cancer is the most common malignancy in women and is the second major cause of cancer-related mortality with a high mortality rate of one in eight women in India. In developing countries, most of the cases arise due to limited awareness and non availability of effective screening systems. To date there have been no tumor biomarkers validated and incorporated into oncological practice for the early diagnosis of breast cancer. Recently, we demonstrated that sperm associated antigen 9 (SPAG9), a member of cancer testis (CT) antigen family, is associated with ovarian and renal cell carcinomas. In the present study, we investigated SPAG9 expression and humoral immune response in breast cancer. We further evaluated the diagnostic potential of autoantibodies to SPAG9 protein in various stages, grades and histotypes of breast cancer. We analyzed the association of SPAG9 immunoreactivity score (IRS) with predicted risk of breast cancer recurrence over 10 years. Our reverse transcription-PCR and immunohistochemical analyses revealed SPAG9 expression in 88% breast cancer specimens independent of tumor stages and grades. Further, the humoral immune response against SPAG9 was detected in 80% breast cancer patients with SPAG9 expressing tumors. The linear regression modelling predicted a direct relationship between presence of lymphovascular invasion and high SPAG9 IRSs. While the univariate and multivariate logistic regression models predicted a strong association of SPAG9 IRS with tumor grade. Further, our data indicated a significant higher trend of SPAG9 IRSs with the predicted high risk of breast cancer recurrence. The present investigation reports for the first time SPAG9 expression and humoral immune response in early stages and low grade breast cancer. Although, our data indicated that autoantibodies against SPAG9 represent a promising approach for the development of biomarker, further large scale validation studies are required to establish its potential use in early diagnosis and monitoring of breast cancer recurrence.[*Cancer Epidemiol Biomarker Prev* 2009;**18**:630–639]

Expression of SPAG9 mRNA in breast cancer tissues

We first investigated the *SPAG9* expression by RT-PCR in breast cancer tissues. mRNA expression of *SPAG9* was found in 87% (82/94) in infiltrating ductal carcinoma (IDC), 100% (2/2) in ductal carcinoma *in situ* (DCIS), 100% in invasive lobular carcinoma (ILC) (4/4) and in testis. 100% (1/1) of stage I, 88% (38/42) of stage II, 83% (40/48) of stage III and 100% (3/3) of stage IV breast cancer patients were positive for the presence of *SPAG9* mRNA. Further, 88 matched adjacent non-cancerous tissue (ANCT) of IDC, 2 matched ANCT of DCIS and 2 matched ANCT of ILC did not show *SPAG9* expression. The amplicon size in tumor was same as in testis. The PCR product was confirmed as SPAG9 by automated sequencing. *SPAG9* expression was found in 90% early stages (I and II) and in 84% late stages (III and IV) of breast cancer tissues. In addition, *SPAG9* expression was detected in 97% (35/36) grade 1, 90% (40/44) grade 2 and 50% (7/14) grade 3 breast cancer tissues. The statistical analysis revealed that *SPAG9* expression was independent of tumor stages indicating no correlation between tumor stages and SPAG9 expression ($P = 0.272$) using Pearson's Chi-Square test. However, SPAG9 expression was significantly associated among the grades using Pearson's Chi-Square test ($P < 0.0001$).

Immunohistochemical staining of breast cancer

A panel of 100 breast cancer tissues and ANCT specimens were studied for the presence of SPAG9 protein expression by immunohistochemistry. A distinct positive immunoreactivity (>10% of cancer cells were stained) for SPAG9 protein was seen in 88% patient tissues studied based on IRS. The immunohistochemical staining results indicated that SPAG9 expression was localized in the cytoplasm of tumor cells in the tissue section of IDC, ILC and DCIS. However, no SPAG9 reactivity was observed with control IgG in serial sections of IDC, ILC and DCIS tumor tissue sections. Furthermore, no positive immunoreactivity was observed in ANCT specimens. The statistical analysis revealed that SPAG9 protein expression was independent of tumor stages indicating no correlation between tumor stages and SPAG9 expression (P = 0.272) using Pearson's Chi-Square test. Further SPAG9 immunoreactivity was investigated in various grades of breast cancer tissues. The SPAG9 reactivity in tumor cells was higher in grade 1 as compared to grade 2 and grade 3 respectively. The statistical analysis revealed that SPAG9 protein expression was significantly associated among the grades using Pearson's Chi-Square test (P < 0.0001). In addition, tumor grades were assessed using cancer cell proliferation marker Ki-67. Our results confirmed high expression of Ki-67 with increasing grades.

SPAG9 Immunoreactivity Score (IRS) and its association with clinicopathologic variables and predicted risk of breast cancer recurrence

SPAG9 IRS was defined as the percentage of SPAG9 stained carcinoma cells in breast cancer tissue. SPAG9 immunoreactivity was observed in 100% (1/1) of stage I, 88% (38/42) of stage II, 83% (40/48) of stage III and 100% (3/3) of stage IV breast cancer patients. SPAG9 IRSs with stages II, III and IV were 61.8% (mean) $\pm$ 2.7 (SE), 67.6% $\pm$ 1.5 and 64.7% $\pm$ 5.0 respectively. However, no significant differences between SPAG9 IRSs in early stages (I & II) and late stages (III & IV) was found by performing student's t test (P = 0.387). 97% (35/36) of grade 1, 90% (40/44) of grade 2 and 50% (7/14) of grade 3 patients showed SPAG9 reactivity by immunohistochemical analysis. SPAG9 IRSs of breast cancer with grades 1, 2 and 3 were 72.60 (mean) $\pm$ 1.6 (SE), 61.95 $\pm$ 2.1, and 45.00 $\pm$ 5.7 respectively. SPAG9 IRS decreased with increasing grades of breast carcinoma. Statistical analysis revealed significant differences between SPAG9 IRS and grades 1 and 2 (P < 0.0001), grades 1 and 3 (P < 0.0001) and grades 2 and 3 (P = 0.002) by Student's t test. Furthermore, there were significant differences of SPAG9 IRSs among grades 1, 2 and 3 by multiple comparisons with Kruskal-Wallis test (P < 0.0001).

Further, association of SPAG9 IRS was examined with the various known risk factors of breast cancer patients such as tumor grade, nodal status and clinical stages. Our data indicated that SPAG9 IRS was significantly associated among various grades of breast cancer using Pearson's Chi-Square test (P < 0.0001). Based on SPAG9 IRS in breast tumors, three groups were formed for statistical analysis [low (20-50% cells), moderate (50-70% cells) and high (> 70% cells)]. Moreover, the 10 year predicted risk of recurrence from breast cancer was calculated for each patient using the Adjuvant! Online programme. There was statistically significant (Pearson's Chi-Square test; P = 0.046) pattern of high SPAG9 IRSs with predicted risk of breast cancer recurrence. Furthermore, when examined using Pearson's Chi-Square test, high SPAG9 IRS (> 70% cells) showed strong correlation with presence of positive lymph nodes (P = 0.041). In addition,

presence of lymphovascular invasion and positive lymph nodes were significant in predicting high SPAG9 IRSs (> 70% cells) in both univariate and multivariate linear regression models. Univariate and multivariate logistic regression models were used to predict the association between SPAG9 expression and testing variables such as histologic grade, tumor size, estrogen receptor status and progesterone receptor status. Only tumor grade was significantly associated with the presence of SPAG9 expression ($P = 0.0001$). Tumor size ($P = 0.656$), estrogen receptor status ($P = 0.553$) and progesterone receptor status ($P = 0.179$) were not found to be statistically significant predictors of SPAG9 expression.

Humoral response against SPAG9

Having established the SPAG9 expression in breast cancer, we did ELISA to detect antibodies against SPAG9 in sera from breast cancer patients and healthy donors. We first established the basal signals in the ELISA system using sera from 50 healthy donors (mean +2SD at $A_{492\ nm}$). Using the mean absorbance value of healthy donors as a cut off value (0.175 + 0.08), positive immunoreaction to SPAG9 were detected in 80% breast cancer patients with SPAG9 expressing tumor, but not in the healthy donors. It is important to note that 88% (38/43) patients belonging to IDC histotypes of early stage breast cancer (I and II) and 70% (36/51) later stage (III and IV) showed humoral response against SPAG9. In different tumor grades, 78% (28/36) of grade 1, 84% (37/44) of grade 2 and 64% (9/14) of grade 3 revealed anti-SPAG9 antibodies. The statistical analysis revealed that anti-SPAG9 antibody response was independent of tumor stages and grades indicating no correlation between tumor stages ($P = 0.203$), grades ($P = 0.118$) and humoral response using Pearson's Chi-Square test. However, the statistical analysis revealed that there was significant difference between anti-SPAG9 antibodies in tumor grade 1 and 3 ($P < 0.0001$), tumor grade 2 and 3 ($P = 0.01$) but not in tumor grade 1 and 2 ($P = 0.191$) using Student's *t* test. Furthermore, there were significant differences of anti-SPAG9 antibodies among grades 1, 2 and 3 by multiple comparison with Kruskal-Wallis test ($P = 0.018$). Furthermore, no significant association was found between SPAG9 antibodies and ER status ($P = 0.428$), and PR status ($P = 0.572$) using Pearson's Chi-Square test.

Our findings reveal that majority of various histotypes of breast cancer tissues expressed SPAG9 at both mRNA and protein level. Our SPAG9 expression analysis suggested a strong relationship between the presence of lymphovascular invasion and high SPAG9 IRS. Furthermore, our data indicates a distinct pattern of high SPAG9 IRSs in low grades which is predicted risk of breast cancer recurrence. Our study further relates SPAG9 *in vivo* immunogenicity with early stages and low grade of breast cancer, suggesting SPAG9 as a candidate target for early diagnosis. Large scale studies are required to determine the potential utility of the SPAG9 in guiding treatment decisions and following disease progression.

Publications

Original peer-reviewed articles

1. Garg M, Kanojia D, Khosla A, Dudha N, Sati S, Chaurasiya D, Jagadish N, Seth A, Kumar R, Gupta S, Gupta A, Lohiya NK and Suri A (2008) Sperm-associated antigen

9 Is associated with tumor growth, migration, and invasion in renal cell carcinoma *Cancer Res* **68**: 8240-8248.

2. Kanojia D, Garg M, Gupta S, Gupta A and Suri A (2009) Sperm associated antigen 9 (SPAG9), a novel biomarker for early detection of breast cancer. *Cancer Epidemiol Biomarker Prev* **18**: 630-639.

3. Suri A (2009) Report on the First International Symposium on Cancer Biology (ISCB), National Institute of Immunology, New Delhi 14–16 Nov 2007, *Cancer Immunology, Immunotherapy* **58**: 311-316.

Patents

1. Suri A (2009) Inhibition of SPAG9 expression with siRNAs. *European patent granted (Application No: 06710485.1).*

Cellular and molecular aspects of reproductive biology and development of microbicides

Principal Investigator: Satish K Gupta

Project Associates/Fellows: Kausiki Chakrabarti (till Feb 2009)
Pankaj Bansal (till Feb 2009)
Manoj Modi
Jaya Prakash Golla
Shweta Malik (since Nov 2008)

PhD Students: Pankaj Bansal (till Jun 2008)
Anasua Ganguly
Beena Bhandari
Pankaj Suman
Nutan
Nachiket Shembekar

Collaborators: Udo RMarkert, *Friedrich Schiller University, Germany*
Antonin Bukovsky, *The University of Tennessee, USA*
Peter Sutovsky, *University of Missouri-Columbia,USA*
William SB Yeung, *University of Hong Kong, China*
Neerja Bhatla, *All India Institute of Medical Sciences, New Delhi*
RK Sharma, *Army Hospital Research & Referral, New Delhi*
Rakesh Tuli, *National Botanical Research Institute, Lucknow*
Raghavan Varadarajan, *Indian Institute of Science, Bangalore*

The major theme of our group is to understand the structural and functional aspects of the zona pellucida (ZP) glycoproteins and to delineate the molecular basis of fertilization in humans. The feasibility to develop an immunocontraceptive vaccine for humane control of street dog population with an industrial partner is being explored. Attempts are also being made to understand the role of cytokines and growth factors in regulating trophoblast cell proliferation, invasion and differentiation. Identification and characterization of novel anti-HIV compounds from medicinal plants as potential microbicide is being pursued.

The objectives of the project are (i) expression of human ZP glycoproteins and its fragments in various expression systems, (ii) mammalian fertilization: delineate the role played by the ZP glycoproteins, (iii) immunocontraceptive vaccine for controlling street dog population, (iv) role of IL-6 group of cytokines and growth factors in regulation of trophoblast cell proliferation, invasion and differentiation and to delineate the downstream signaling events.and (v) discovery of molecules for anti-HIV activity with or without spermicidal activity as potential microbicide.

Delineation of the downstream signaling pathways involved in zona pellucida mediated induction of acrosomal exocytosis

During fertilization, spermatozoa undergo acrosome reaction (AR) subsequent to its binding to ZP matrix of egg. To understand the downstream signaling events associated with ZP mediated induction of AR in humans, human eggs that failed to fertilize in *in vitro*

fertilization protocol were obtained from Assisted Reproduction Technology (ART) Centre, Army Hospital Research and Referral, New Delhi. Eggs were used to obtain heat solubilized isolated ZP (SIZP) at 70°C for 90 min. Incubation of capacitated human sperm (1×10^6) with SIZP (~ 4 zonae per reaction) led to a significant increase in AR. Pre-treatment of sperm with Pertussis toxin (0.1 µg/ml) led to a significant decrease in AR mediated by SIZP suggesting that ZP mediated acrosomal exocytosis involves activation of G_i protein coupled adenylyl cyclase. Inhibition of AR by picrotoxin (100 µM) suggested the involvement of GABA-A receptor associated chloride channels. One of the hallmarks for AR is increase in intracellular Ca^{2+} levels. Inhibition of AR mediated by SIZP in the presence of EGTA (8 mM) suggested that during initial stages this action is dependent on the presence of extra-cellular calcium in the medium. It has been suggested that human sperm has both T- and L-type voltage operated calcium channels (VOCC). To delineate the involvement of either T- or L-type VOCC, further studies were performed in the presence of specific inhibitors. T-type calcium channels play a critical role in the initial surge of calcium as its inhibitors pimozide (20 µM) and mibefradil (5 µM) inhibited SIZP-mediated AR. Activation of L-type calcium channels is not very critical for zona mediated induction of AR as prior treatment of sperm with inhibitors of L-type calcium channels such as nifedipine (10 µM) and verapamil (10 µM) failed to inhibit AR. Both tyrosine kinases and cAMP dependent protein kinases are important for SIZP mediated AR as their inhibitors, herbimycin A (10 µM) and H-89 (20 µM) inhibited AR significantly. Zona mediated AR is not inhibited significantly by treatment with chelerythrine chloride (3 µM), suggesting that activation of PKC is not critical.

Role of ZP1 during fertilization in humans

i) Cloning and expression of human ZP1

In murine model, ZP1 has been postulated to cross-link the filaments formed by ZP2-ZP3 heterodimers and may thus provide stability and structural integrity to the ZP matrix. In order to investigate the role of ZP1 during fertilization in humans, our group has reported last year the expression of human ZP1 in two fragments corresponding to $ZP1_{26\text{-}277aa}$ and $ZP1_{273\text{-}551aa}$ in *E.coli*. This year, employing synthetic gene, human ZP1 devoid of signal peptide and transmembrane-like domain ($ZP1_{26\text{-}551aa}$) was successfully expressed in *E.coli* (Fig. 1). The purified *E.coli*-expressed $ZP1_{26\text{-}551aa}$ resolve as ~70 kDa band in 0.1% SDS-10% PAGE under reducing conditions. The cDNA encoding 'ZP domain' of human ZP1 ($ZP1_{273\text{-}551aa}$) was also expressed in insect cells, using pAcHLT-A transfer vector under a polyhedrin promoter. In addition, human $ZP1_{273\text{-}551aa}$ and $ZP1_{26\text{-}551aa}$ were also expressed in insect cells using the baculovirus transfer vector pAcGP67-A having a polyhedrin promoter and gp67-an insect secretory signal peptide. The purified baculovirus-expressed $ZP1_{273\text{-}551aa}$ revealed a doublet in the range of 35-37 kDa and $ZP1_{26\text{-}551aa}$ resolved as ~85 kDa band. Lectin binding analysis in ELISA as well as lectin blots revealed that baculovirus expressed $ZP1_{273\text{-}551aa}$ has both N- and O-linked glycosylations. *E.coli*-expressed $ZP1_{273\text{-}551aa}$ failed to show any reactivity with any of the above lectins.

ii) Generation of monoclonal antibodies against human ZP1 and their reactivity with native zona

To characterize expression of ZP1 on human eggs and in ovaries, monoclonal antibodies (MAbs) were generated against *E. coli*-expressed recombinant $ZP1_{26\text{-}277aa}$ and $ZP1_{273\text{-}551aa}$. In addition, MAbs were also generated against 40 mer synthetic peptide (P40;

corresponding to aa residues 219-258 of human ZP1). All 5 MAbs generated against $ZP1_{26\text{-}277aa}$ and 4 against P40 reacted with the respective immunogens & human ZP1 and failed to recognize recombinant human ZP2, ZP3 and ZP4 in ELISA as well as immunoblots. One antibody generated against $ZP1_{273\text{-}551aa}$ cross-reacted with recombinant human ZP4 suggesting recognition of common epitope between ZP1 and ZP4. MAbs against recombinant $ZP1_{26\text{-}277aa}$ showed distinct reactivity with zona on human eggs when tested by an indirect immunofluorescence assay. The representative immunofluorescence patten with MA-1766, MAb agaist $ZP1_{26\text{-}277aa}$ is shown in Figure-2.

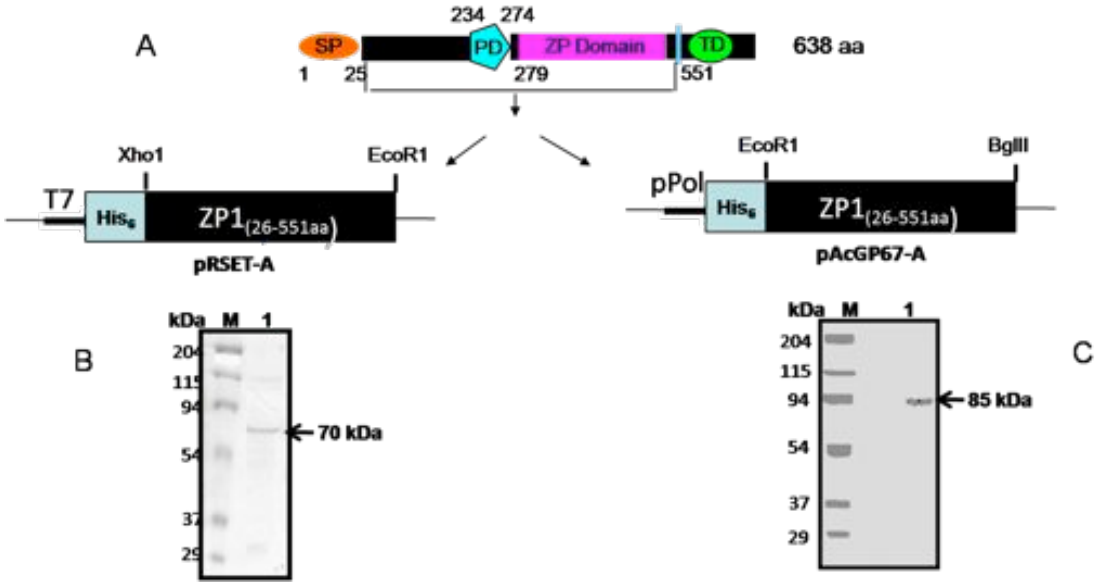

Figure-1: *Expression of human ZP1 in E. coli and insect cells. Panel **A** shows schematic representation of human ZP1 (638 aa). It comprises of a signal peptide (SP) from 1-25 aa followed by a trefoil domain (PD) from 234-274 aa and a 'ZP domain' from 279-548 aa. It also has a consensus furin cleavage site (shown by a vertical bar) followed by a trans membtane-like domain (TD). Panels **B** and **C** represent schematically the constructs that were used to express $ZP1_{26\text{-}551aa}$ in E. coli and insect cells (Sf21) using baculovirus expression system. Western blot revealed E. coli –expressed recombinant $ZP1_{26\text{-}551aa}$ as ~ 70 kDa band while the baculovirus-expressed recombinant $ZP1_{26\text{-}551aa}$ as ~85 kDa band.*

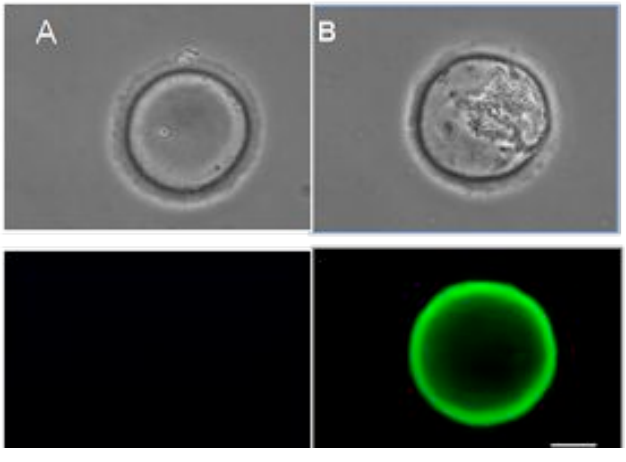

Figure-2: *Reactivity of MAb against E. coli-expressed human $ZP1_{26\text{-}277aa}$ with native human zona. Human oocytes were processed for localization of ZP1 by indirect immunofluorescence assay. Panel **A** represents oocyte treated with culture supernatant of*

*Sp2/O myeloma cells and Panel **B** represents oocyte treated with MA-1766. Top panel shows representative pictures taken under phase contrast. Bottom panel represents immunofluorescence of the same oocyte. The scale bar represents 30 µm.*

iii) Binding of recombinant human ZP1 and its fragments to spermatozoa

The *E.coli*- as well as baculovirus-expressed recombinant human ZP1 fragments were labeled with Fluorescein Isothiocyanate (FITC) and their ability to bind to the capacitated spermatozoa was studied in a direct binding immunofluorescence assay. The status of acrosome was simultaneously assessed using PSA-TRITC staining. Spermatozoa that showed binding of PSA to the acrosomal cap were classified as capacitated acrosome intact sperm. These studies revealed binding of FITC labeled $ZP1_{273\text{-}551aa}$ and $ZP1_{26\text{-}551aa}$ to the anterior head of the capacitated acrosome intact spermatozoa. Few sperm also showed binding only in the equatorial region. Recombinant $ZP1_{26\text{-}277aa}$ failed to show any specific binding to the capacitated acrosome intact spermatozoa suggesting that the 'ZP domain' of human ZP1 plays a role in its binding to spermatozoa. Interestingly, both *E.coli*- and baculovirus-expressed recombinant $ZP1_{273\text{-}551aa}$ showed similar binding profiles suggesting that glycosylation of ZP1 is not critical for its binding to spermatozoa.

iv) Induction of acrosomal exocytosis by recombinant human ZP1

Baculovirus-expressed recombinant $ZP1_{273\text{-}551aa}$ as well as $ZP1_{26\text{-}551aa}$ were able to induce acrosomal exocytosis in capacitated human sperm in a statistically significant manner. Recombinant ZP1 mediated the AR in a dose dependent manner. Induction of acrosome reaction can be seen as early as 10 min after incubation with the recombinant protein. The *E. coli*–expressed recombinant ZP1 and its fragments were unable to induce any significant increase in acrosomal exocytosis suggesting that glycosylation of ZP1 is critical for induction of AR. To check the role of extra cellular calcium (Ca^{2+}) in ZP1-mediated acrosomal exocytosis, capacitated sperm in Bigger's Whitten Whittingham (BWW) medium were incubated with 8 mM EGTA before exposing to recombinant $ZP1_{273\text{-}551aa.}$ This treatment led to a significant decrease in acrosomal exocytosis suggesting that induction of AR mediated by $ZP1_{273\text{-}551aa}$ required extracellular Ca^{2+}. Using different pharmacological inhibitors, the downstream signaling pathway followed by $ZP1_{273\text{-}551aa}$ – induced AR was studied this year. Acrosomal exocytosis mediated by $ZP1_{273\text{-}551aa}$ was inhibited by amiloride (50 µM) and pimozide (10 µM) suggesting the involvement of L-type Ca^{2+} channels while T-type Ca^{2+} channels also seem to play an important role as both verapamil (10 µM) and nifedipine (10 µM) inhibited the $ZP1_{273\text{-}551aa}$ mediated induction of acrosomal exocytosis. This is at variance with respect to induction of AR mediated by ZP3 where L-type VOCC does not play an important role in inducing AR. ZP3 mediated induction of AR is inhibited by Pertussis toxin (0.1 µg/ml) whereas it failed to inhibit recombinant $ZP1_{273\text{-}551aa}$ mediated acrosomal exocytois suggesting thereby that ZP1 acts through a G_i independent pathway. Interestingly, ZP4 which is paralogous to ZP1 also induce AR through a G_i independent pathway. Hence, for the first time these studies suggest that unlike the murine model, ZP1 also plays an important role in sperm binding and induction of acrosome reaction. Further in humans, ZP1, ZP3 and ZP4 collectively participate in binding of sperm to the egg and induction of acrosome reaction by using slightly different downstream signaling pathways.

Role of cytokines on proliferation, invasion and differentiation of trophoblast cells (using choriocarcinoma cell line, JEG-3/BeWo as model)

To study the role of cytokines and growth factors in proliferation, invasion and differentiation of trophoblst cells, this year we have done microarray analysis to see the global gene expression pattern in JEG-3 cells following treatment with IL-11 and LIF for 24 hr. We could find differential expression of certain adhesion molecules like different isoforms of integrins, negative regulators of JAK/STAT signaling pathway, protease and protease activators, transcription factors under the influence of both IL-11 and LIF. Out of these, few genes were getting commonly up or down regulated. We are in the process of validating these observations by Real Time-RT PCR.

Cellular proliferation is governed by coordinated activation of several factors in different cell types including ERK1/2 molecule. Stimulation of JEG-3 cells with IL-11, even at its highest concentration, did not show any increase in p-ERK1/2. On the other hand, treatment with LIF led to activation of both STAT3 (Tyr_{705}) and ERK1/2 in JEG-3 cells. Treatment of JEG-3 cells with LIF lead to an increase in their invasion as well as proliferation. This suggests that the inability of IL-11 to activate ERK1/2 may be attributable to the absence of proliferative responses in JEG-3 cells following IL-11 treatment.

Trophoblast cells of human placenta also differentiate into syncytiotrophoblast in the due course of embryo implantation process. To study the process of syncytialization, we have standardized the protocol to show the BeWo choriocarcinoma cell fusion under the influence of Forskolin (25 μM) by immunolocalizing desmoplakin I+II at the cell surface. Further studies are in progress to delineate the significance of intracellular mediators downstream to Forskolin, EGF and TGFβ mediated cell fusion.

Identification of plant based molecules with anti-HIV activity as potential microbicides

As per the last year report, we had initiated the screening of plant extracts for anti-HIV activity to develop potential microbicides in the newly established BSL-3 Facility. So far, 94 extracts prepared by using different solvents from various parts of 18 different plants have been evaluated for cellular toxicity and anti-HIV activity using reporter based cell assays. Lab adapted X-4 strain of NL4.3 HIV-1 isolate was used to infect the TZM-bl (a recombinant epithelial cell line that expresses CD4, CXCR4 and CCR5 containing reporter cassettes for luciferase as well as β- galactosidase under HIV-1 LTR) and CEM-GFP (a human CD4 and CXCR4 reporter T cell line having GFP reporter gene under HIV-1 LTR) cell lines. Virus was pretreated with varying concentration of plant extracts followed by infection of TZM-bl cells. Alternatively, CEM-GFP cells were infected with HIV followed by treatment with various concentrations of plant extracts. Anti-HIV activity of these extracts was further confirmed by p24 ELISA. These studies revealed that extracts prepared from 5 medicinal plants show anti-HIV activity to varying extent. Out of the 5 plants, anti-HIV activity from 2 plants namely *Argemone mexicana* and *Rhus chinensis* have been reported previously by other groups. This screening program has led to identification of 3 new medicinal plants with promising anti-HIV activity. Activity guided fractionation of extracts from 4 plants, which have shown anti-HIV activity, have been done. Fractions showing promising anti-HIV activity have been selected for dose dependent studies. Production of dual-tropic cytopathic HIV-1 primary isolate 89.6 and R5 tropic HIV-JRCSF to access the broad anti-HIV activity of these fractions have also been initiated. Out of 27 plant extracts evaluated for spermicidal activity, 3 extracts from 2 independent plants showed a significant decrease in sperm motility.

Publications

Original peer-reviewed articles

1. Choudhury S, Ganguly A, Chakrabarti K and Gupta SK (2009) DNA vaccine encoding chimeric protein encompassing epitopes of human ZP3 and ZP4: Immunogenicity and characterization of antibodies. *J Reprod Immunol* **79**:137-147.

2. Chiu PC, Wong BS, Chung MK, Lam KK, Pang RT, Lee KF, Sumitro SB, Gupta SK and Yeung WS (2008) Effect of native human zona pellucida glycoprotein 3 and 4 on acrosome reaction and zona pellucida binding of human spermatozoa. *Biol Reprod* **79**:869-877.

3. Chiu PCN, Wong BST, Lee CL, Pang RTK, Lee K-F, Sumitro SB, Gupta SK and Yeung WSB (2008) Native human zona pellucida glycoproteins: Purification and binding properties. *Human Reprod* **23**:1385-1393.

4. Bukovsky A, Caudle MR, Gupta SK, Svetlikova M, Selleck-White R, Ayala AM and Dominguez R (2008) Mammalian neo-oogenesis and expression of meiosis-specific protein SCP3 in adult human and monkey ovaries. *Cell Cycle* **7**:683-686.

5. Bukovsky A, Gupta SK, Bansal P, Chakravarty S, Chaudhary M, Svetlikova M, White RS, Copas P, Upadhyaya NB and Meter SEV (2008) Production of monoclonal antibodies against recombinant human zona pellucida glycoproteins: utility in immunolocalization of respective zona proteins in ovarian follicles. *J Reprod Immunol* **78**:102-114.

Reviews/Proceedings

1. Bukovsky A, Gupta SK, Virant-Klun I, Upadhyaya NB, Copas P, Van Meter SE, Svetlikova M, Ayala ME and Dominguez R (2008) Study origin of germ cells and formation of new primary follicles in adult human and rat ovaries. *Methods Mol Biol* **450**:233-265.

Studies of Sertoli cells and spermatogonial stem cells of the testis

Principal Investigator: Subeer S Majumdar

Project Associates/Fellows: Hironmoy Sarkar
Manoj Vimal
Suryaprakash R Batta

PhD Students Indrashis Bhattacharya
Sayon Basu
Bhola Shankar Pradhan

Collaborator: Tony M Plant, *University of Pittsburgh, USA*

Spermatogonial stem cells undergo repeated division and differentiation within the testis. One of the themes of the research is to exploit this premise to integrate foreign genes in the testicular stem cells for producing transgenic sperm leading to propagation of the transgene and generation of transgenic animals. Hormone mediated signal transduction by testicular Sertoli cells (Sc) and cell-cell interactions within testis are responsible for inducing germ cell division and differentiation in this organ. The other theme of this work is to understand the mechanism of the governance of germ cell division and differentiation by the Sertoli cells. Although about 200 million sperm are produced everyday by the testes, germ cells are prevented from deviating into a cancerous situation throughout the life of a person. The work of lab is also focused on investigating the important events/factors which govern such a well organized cell division within the testis. Information from such studies may provide an insight into the molecular mechanism(s) underlying endocrine and paracrine control of cell division and differentiation with reference to evaluation and management of idiopathic male infertility.

The objectives of the project are to (i) study paracrine and endocrine modulation of signal transduction in Sertoli cells (Sc) from spermatogenetically inactive (infant) and active (adult-like) monkey and rat testis, (ii) undertake gene expression studies of rat, mice and monkey Sc to identify factors important for spermatogonial stem cell division and differentiation in the testis, (iii) exploit spermatogonial stem cells of testis for insertion and propagation of transgene through several generations in an attempt to make transgenic or knock out animals, (iv) study cell-cell interaction in the testis and to evaluate role of Sc products in preventing germ cell malignancy and (v) use germ cell transplantation technique for restoration of fertility following chemotherapy.

Ontogenic maturation of Sc response to hormonal stimulation: Although neonatal rat Sc are exposed to an adult like hormonal milieu, they fail to induce the division and differentiation of the spermatogonial stem cells. To address this paradox, Sc were cultured from 5, 9, 12, 18 and 40 days (d) old rats to investigate regulation of Sc gene expression by FSH and its ability to bind testosterone (T). On day 4 of culture, Sc were treated with ovine FSH (50ng/ml) or Forskolin (10μM) for 1/2hr and cAMP produced by Sc was measured using RIA. In separate experiment, Sc were treated for 6hr with ovine FSH (50ng/ml) and Sc mRNA was extracted using TRIZOL reagent to evaluate the expression of some important Sc specific genes essential for spermatogonial stem cells differentiation. Androgen binging ability of Sc was evaluated using radioactive T. Infant

(5d and 9d) rat Sc failed to produce sufficient amount of cAMP in response to oFSH as opposed to that by 12d and 18d old Sc. Forskolin induced cAMP production by Sc from all ages including infants suggesting presence of defective FSH-R in them. Transcription of SCF and GDNF were not regulated by FSH treatment before 12 d of age and presumably one of the reasons for lack of robust germ cell division and differentiation. Androgen binding ability of Sc remained similar throughout the development.

It was noteworthy that both cAMP production and *Scf* expression by Sc were modulated by FSH only at or after 12 d of age which coincided with the initiation of robust spermatogonial stem cells differentiation and predominant appearance of spermatogonia B in the testis. Based on our previous findings and the fact that forskolin which acts bypassing FSH receptor can augment cAMP in all age groups, lack of germ cell differentiation in spite of preferable hormonal milieu in the testes of 5 and 9 d old rat is best explained by the presence of a suboptimal FSH receptor in this age group. The developmentally regulated transcriptional events in the phase of unchanging hormonal milieu may reflect graded maturation of Sc with age, causing induction of spermatogonial stem cell differentiation and appearance of advanced germ cells. It strengthened our hypothesis that failure of such an age dependent switch in responsiveness of Sc to FSH, during puberty, may underlie certain forms of idiopathic male infertility.

Differential gene expression by Sc of spermatogenically inactive and active testis: Age specific genes expressed by the Sc from rats and monkeys (infant and pubertal) were determined by DNA Micro array analysis using Agilent rat arrays and human arrays (for monkeys) respectively. About 4700 genes were upregulated and 3500 genes were downregulated in Sc cultured from 12 d old rats as compared to that of those cultured from 5 d old rats. Similarly about 1300 genes were up regulated and more than 1000 genes were down regulated in pubertal monkey Sc as compared to those in infant Sc. Important genes like that of FSH receptor, GDNF, OCT-1, Wnt4 etc. were up regulated in spermatogenically active rat Sc. Genes of interest which show more than 2-3 fold up or down regulation may either be fished out from the genomic DNA or procured commercially (cDNA clones) for the purpose of generating transgenic animals. A gene which is up regulated in pubertal Sc can be tagged to promoter of a gene which is active in infant Sc so that pubertal gene can be over expressed in infants and vice versa to evaluate function of important genes by determining if a gene specifically expressed during puberty can induce spermatogenesis in infants or a gene specifically found during infancy can limit spermatogenesis in the pubertal animals. Although this hypothesis is very attractive, this is possible only when one can efficiently generate several transgenic animals within a short period of time.

Exploiting testicular spermatogonial stem cells for transgenesis: Traditionally, foreign DNA is introduced in the pronucleus of the embryo for making transgenic animals, with the anticipation that this gene would be transmitted through the germ line so that at least some of the future generations carry this recombinant DNA. This technique is cumbersome, expensive and time consuming. This does not allow every scientist to produce their own transgenic animals and hence increase the waiting period for services through centralized facilities available in selected places. Since in our study the number of genes differentially expressed and to be tested is very high, it is impractical to use the current method of male pronuclear micro-injection to achieve this. Hence, there was an urgent need for developing a rapid, repeatable and cost effective technique for producing transgenic animals preferably with minimum or no loss of lives.

The existing transgenic technology is centered around the premise that an enhanced rate of cell division at the time of embryogenesis allows integration of foreign genes easily. Keeping this principal in view, we explored possibility of such gene integration during enhanced germ cell division in the mouse testis after the onset of puberty. To this end, we have developed a reproducible non-terminal technique for inserting genes in testicular spermatogonial cells through *in-vivo* electroporation of the testis. The optimal result was obtained by injecting linearized DNA (10 µg/20µl) into the testis of FVB male mice, followed by electroporation using 8 square 40V electric pulses in alternating direction with a time constant of 0.05 second and an inter-pulse interval of ~1 second. The transgenic animals were primarily identified by PCR analysis of genomic DNA in various generations. This method does not require any assisted reproductive techniques or sophisticated laboratory setup and highly trained personnel. In our hands, electroporated males have sired transgenic pups even after 300 days of electroporation suggesting permanent integration of the gene in the repopulating spermatogonial cells at the time of electroporation. Reproducibility of this protocol has been reported by us using four different constructs and additional methods of screening viz. Southern blot, RT-PCR and immuno-histochemical analysis. The success rate of this method is more than 90% which is better than all existing techniques used for the generation of transgenic mice. Most importantly, spermatogonial cells expressed the transgene (GFP) even after 10 cycles of spermatogenesis (Figure 1) indicating that we could transfect spermatogonial stem cells successfully at the time of electroporation. This ethically superior (deathless) and easily adaptable time saving procedure opens avenues for developing several kinds of transgenic mice within a short span of time and broadens the scope of determining specific functions of genes *in vivo*.

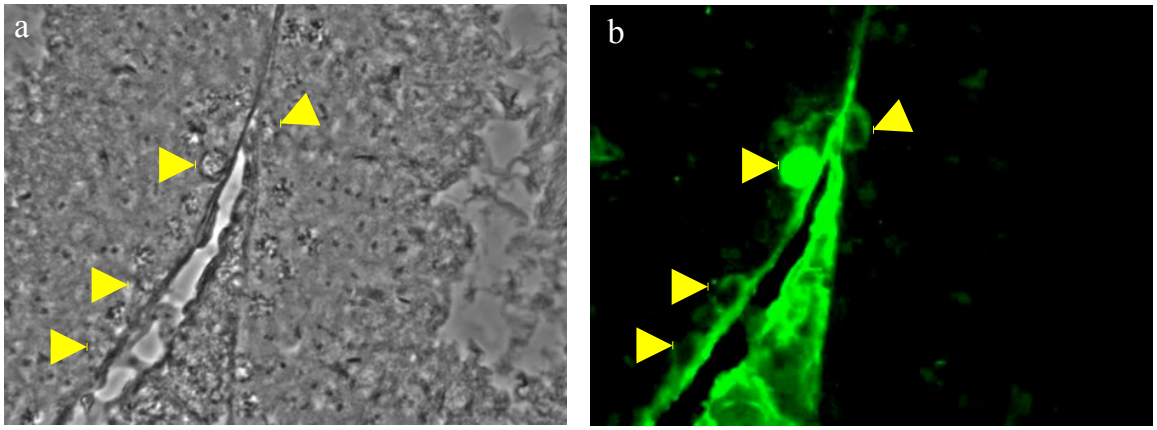

***Figure-1**: Cytoplasm of several germ cells (arrows) displaying expression of GFP after 395 days of electroporation with the DNA containing GFP. a) section of testis showing portion of two adjacent seminiferous tubules under phase contrast. b) GFP expression as seen in the same focal plane of the testicular section.*

Cell-cell interaction in the testis: We have used Sc, peritubular cell (PTc) and Leydig cell (Lc) co-cultures to study cell–cell interaction. PTC failed to augment Sc function but augmented Lc steroidogenesis. Sc had no affect on Lc steroidogenesis.

Publications

Original peer-reviewed articles

1. Dhup S and Majumdar S (2008) Transgenesis via permanent integration of genes in repopulating spermatogonial cells *in vivo. Nature Methods* **5**:601-603.

2. Majumdar S, Dhup S and Usmani A (2008). Deathless transgenesis: A new spermatogonia mediated *in vivo* approach for generation of transgenic mice. *Nature Protocols* DOI: 10.1038/nprot.2008.124.

MOLECULAR DESIGN

MOLECULAR DESIGN

Novel approaches for treating diabetes, multiple sclerosis and osteoporosis

Principal Investigator: Avadhesha Surolia

Co-Investigator: Sarika Gupta

Project Associates/Fellows: Neha Kapoor
Santosh Upadhayay
CM Pathak
Rajesh Gupta
Deepak Sharma
Vineeta Chattree
Varshiesh Raina

PhD Students: Tanushree Banerjee
Rajiv Ranjan Singh
Tandrika Chattopadhyay
Ravi Kant
Shweta Pasi

Collaborators: M Vijayan, *IISc, Bangalore*
K Suguna, *IISc, Bangalore*

The objective of our research is to develop novel methods of treatment for diseases like diabetes, osteoporosis, malaria and multiple sclerosis.

1. Sustained insulin release formulation (SIRF) for a novel and lasting treatment of Type I diabetes mellitus: The etiological heterogeneity of idiopathic diabetes has been recognised for over 30 years, and subdivision into type 1 and type 2 is fundamental to the way we think about the disease. Today, not only are adults being diagnosed with this disease, but it's also affecting the youth. In type 1 diabetes, insulin deficiency accompanied by elevated glucagon secretion results in impaired peripheral glucose utilization and augmented hepatic glucose production, the combined effect of which contributes significantly to elevated blood glucose levels. As a result, type 1 diabetic patients are chronically hyperglycemic and must receive at least twice-daily injections of a mixture of short- and delayed-action insulin before breakfast and the evening meal to prevent blood glucose excursions. However, this conventional insulin therapy is inadequate for blood glucose control between meals and during the night because treated patients still experience fasting hyperglycemia and elevated HbA1c, which are causative for the development of long-term diabetic complications, including nephropathy, neuropathy, retinopathy, and cardiovascular disease. Thus it is important to understand the importance of early, aggressive glucose control in reducing the risk of both microvascular and macrovascular complications in people with diabetes. Therefore, the focus of alternative therapy development has been to achieve better glycemic control by replacing or reducing the frequency of insulin injection.

In an attempt to address the issue of multiple injections and patient compliance, we have developed a novel concept wherein sustained insulin release formulation (SIRF), is used for a lasting treatment of diabetes mellitus I. insulin from two different sources, viz,

recombinant human and bovine was used to generate SIRF. (Data here is presented for rH insulin). To test the hypothesis that insulin released from sustained insulin release formulation (SIRF) achieved better glycemic control for a sustained period of time in animal model of diabetes. SIRF released insulin at an appreciable rate *in vitro* and was further used for the *in vivo* studies. Optimization of insulin dosage was done using 2-8 IU/kg body weight, which has been reported to maintain normoglycemia in diabetic rats. When administered once or twice daily, 4 IU/kg body weight was found to be ideal and did not lead to sudden fasting (pre-prandial) and non-fasting (post-prandial) hypoglycemia. STZ-induced diabetic rats were divided into various treatment groups. SIRF was administered both subcutaneously and intramuscularly to diabetic rats, which led to a significant reduction in the non-fasting blood glucose levels (Figure-1a) without fasting hypoglycemia (Figure-1b).

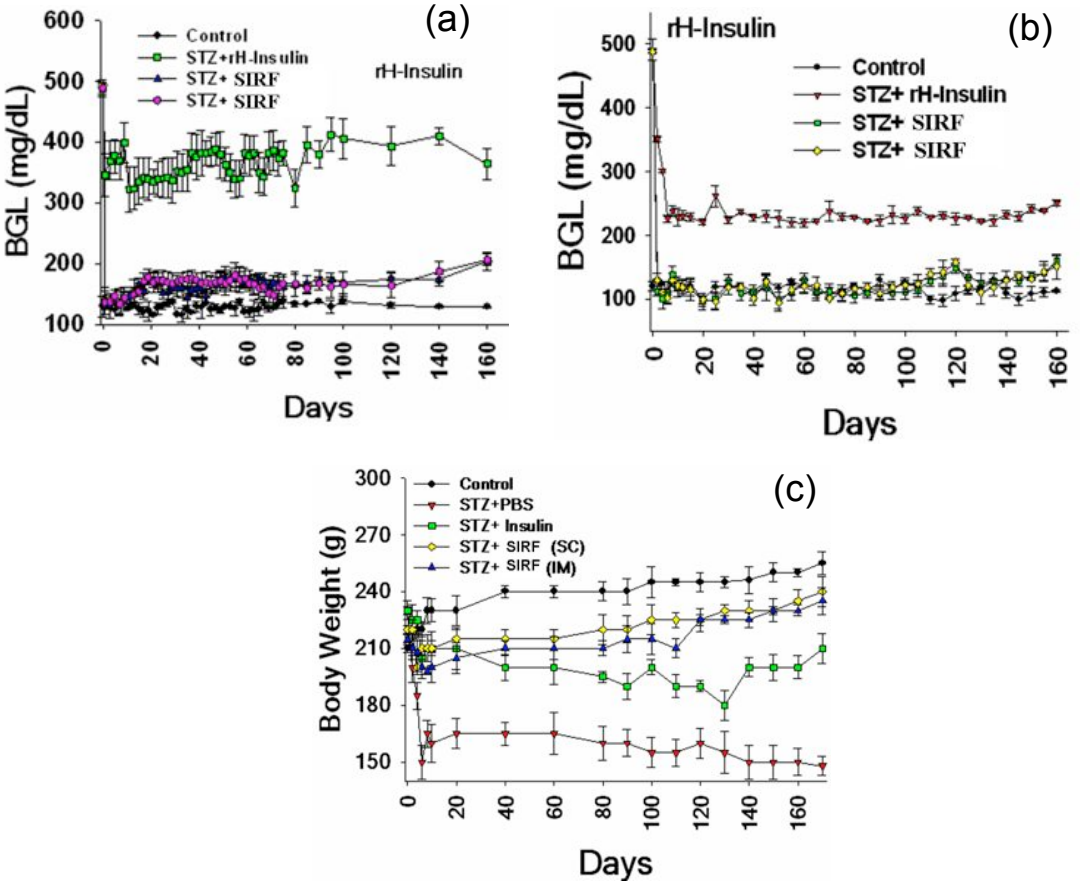

***Figure-1**: In vivo efficacy of SIRF in glucose homeostasis. (a) Post-prandial blood glucose level, **(b)** Pre-prandial blood glucose levels monitored over a period of 135 days for bovine and 160 days for rH SIRF. **(c)** Body weight profile of SIRF treated rats.*

Daily insulin dosage (4 IU/kg) lead to reduced blood glucose levels, non-fasting value of 350-400 mg/dL and fasting value of 240-260 mg/dL for rH insulin. Twice daily injection of 4 IU/kg insulin (bovine and rH insulin) marginally improved the glycemic levels. While daily dose of insulin was able to maintain glucose levels at moderately high values, administration of SIRF resulted in a tight glycemic control with blood glucose levels of 160 ± 13.61 mg/dL (fed state) and 105 ± 15 mg/dL (fasting) for upto 160 days with a single injection (both SC and IM). There was an initial loss of body weight immediately after STZ injection (Figure-1c), but progressive weight gains were achieved in diabetic rats after treatment with SIRF and the weight of SIRF treated animals paralleled that of non-diabetic control.

Insulin ELISA was performed to quantify the serum insulin levels. A sustained release of insulin (0.5-1.2 ng/ml) into the serum was observed (Figure-2), compared to PBS treated diabetic rats (0.08 ng/ml). Thus a basal level of insulin in the blood was maintained throughout the treatment period in diabetic animals administered SIRF.

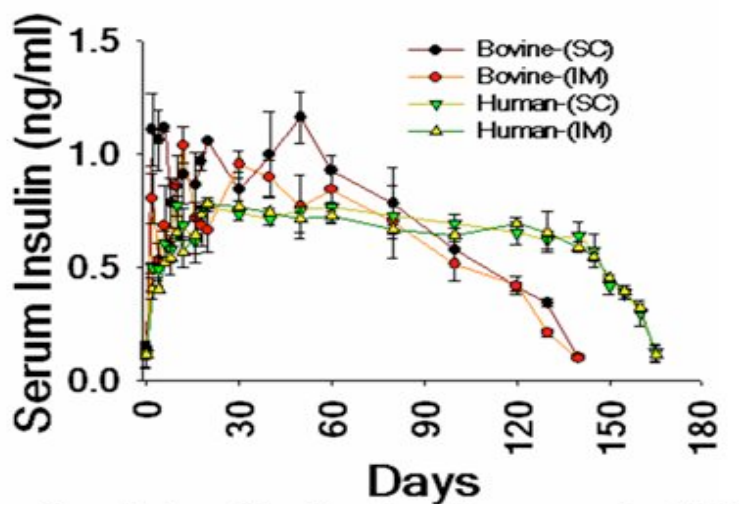

Figure-2: *Quantification of serum (recombinant human) insulin ELISA in STZ treated rats in response to insulin SIRF injected SC or IM*

Intraperitoneal glucose tolerance test (IPGTT) was performed to assess the instantaneous effect of SIRF *in vivo* and its relevance in mitigating acute hyperglycemia. Free Insulin, SIRF and *in vitro* released monomers from SIRF, significantly improved the glucose tolerance in treated animals, with their elevated blood glucose levels due to glucose infusion returning to the pre challenged values within 1.5 h. However, in diabetic controls treated with PBS, blood glucose levels remained hyperglycemic over the period of test (Figure-3a). Thus SIRF was effective in regulating extremely high BGL of upto 600 mg/dL, immediately. Serum bovine insulin levels were also quantified for IPGTT (Figure-3b), which were expectedly negligible for both diabetic and non-diabetic controls (Figure-3c). Whereas, the values for insulin treated animals increased to ~0.9 ng/ml in 30 min, and then decreased in the next 4.5 h, In SIRF treatment, insulin levels in serum reached to 0.8-0.9 ng/ml in 30 min and remained constant over the period of study.

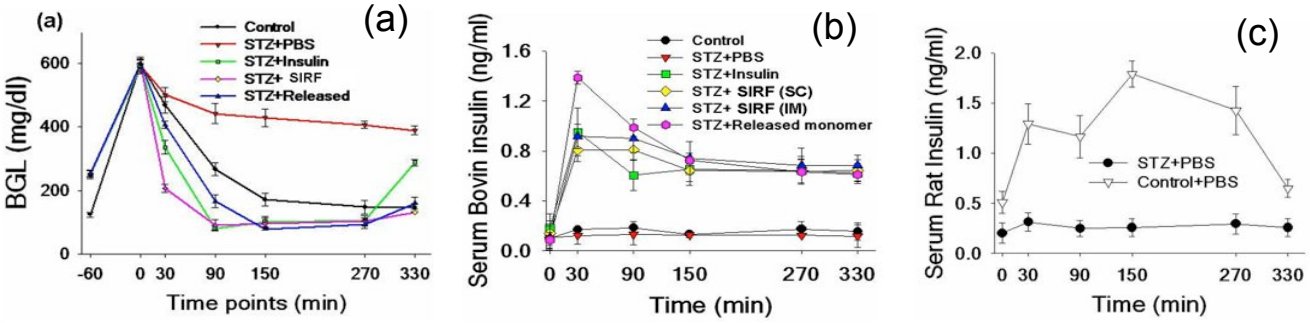

Figure-3*: Intraperitoneal glucose tolerance test (IPGTT). (a) Blood glucose profile of IPGTT after various treatment as indicated, (b) Quantification of serum recombinant human insulin of IPGTT, (c) Serum rat insulin ELISA performed for IPGTT. Results are mean ± s.d. of three different experiments*

The biological activity of insulin released from SIRF was evaluated using signaling studies performed on isolated rat adipocytes. Levels of PI3K, which is the first kinase downstream to insulin signaling via its receptor increased significantly in response to SIRF, native insulin and insulin released *in vitro* (form SIRF) as compared to PBS control (Figure 4a). A significant increase in the phosphorylation of Akt, a threonine/serine kinase important for insulin regulation and various metabolic responses in adipocytes, was observed; similar to the response obtained for insulin. Phosphorylation of GSK3β on Ser-21 increased several fold in adipocytes treated with either free insulin or SIRF compared to control (Figure-4a. A significant activation of ERK1/2 was also observed compared to PBS control in case of treated adipocytes. Similar activation of signaling mediators was observed, when serum from insulin or its SIRF treated animals was added to cultured adipocytes (Figure-4b.

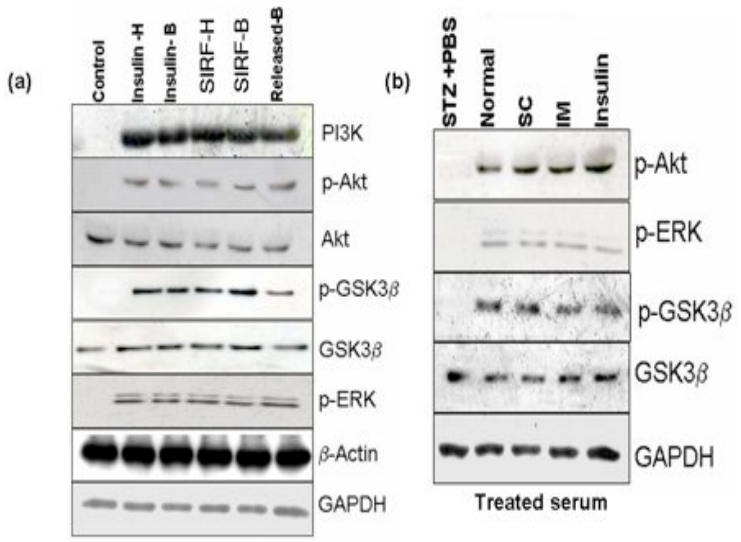

Figure-4: *Western blot (WB) analysis of cultured adipocytes for insulin signaling cascade,* ***(a)*** *treated with PBS (control), Insulin-Human (Insulin-H), Insulin-Bovine (Insulin-B), SIRF-H from rH insulin (SIRF-H), SIRF-B from bovine insulin (SIRF-B) and released monomers from SIRF (Released).* ***(b)*** *Adipocytes treated with serum of treated rats (as indicated in the figure) and analysed for insulin signalling*

Finally heart, liver and kidney sections were analysed for any morphological changes occurring due to the administration of SIRF. Histological sections of the organs were normal without any inflammation or infiltration of immune cells (Figure-5).

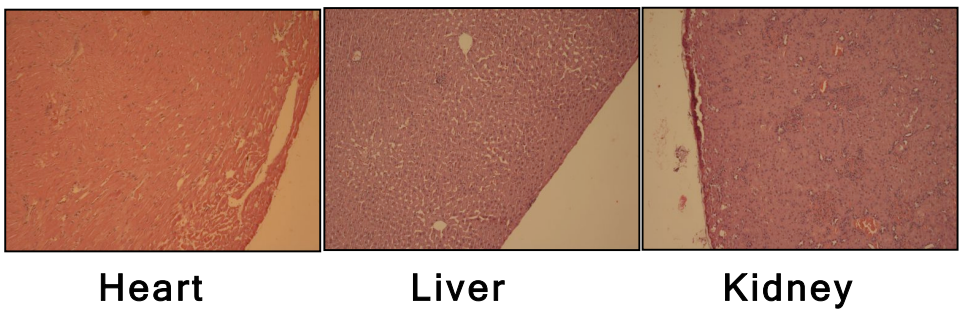

Figure-5: *Heart, kidney and liver tissue sections were examined for the inflammation or toxicity of SIRF injected to diabetic rats after 16 weeks by H&E staining*

The report presented here shows that insulin released from SIRF is equivalent to native soluble insulin as far as its biological function is concerned. A significant difference lies in

the duration of action. While for the standard insulin injection, it is only 6-10 h, for SIRF the duration of action is markedly enhanced upto 160 days. Unlike intensive insulin therapy, by which blood glucose levels is controlled by an increased frequency of insulin injection with concomitant risk of hypoglycemia, the significantly improved glycemic control using insulin SIRF therapy is accomplished without the need for multiple insulin injections and without adverse side effects. SIRF is equally efficacious in treating Type II diabetic animal models.

2. Effect of MBP analogs on progression of EAE: Multiple sclerosis is a slow progressive, autoimmune disease of central nervous system characterized by inflammation and demyelination in brain and spinal cord. MS though less prevalent in Asia, is a commonest progressive neurological disorder in the temperate climates with one million people affected worldwide. Disease is more common in people between 20- 50 years of age with women being twice more susceptible to the disease as compared to men. Certain genetic, environmental and nutritional factors predispose an individual to the disease. Sometimes viral or bacterial infections are known to be associated with MS, which could be a trigger for multiple sclerosis. Currently approved treatments for MS have either limited efficacy (glatiramer acetate and interferon-beta formulations) or sometimes have serious toxicities (mitoxanthrone and cyclophosphamide). Thus, more effective and better-tolerated treatments for MS are required.

Since, a multiple sclerosis patient can manifest broad range of symptoms with varied severity i.e. MS patients exhibit pathophysiologically distinct subtypes at different time during disease progression, therefore, it is important to have disease subtype specific therapy or combinatorial therapeutic approach. We have designed a molecule that we have found to be more effective than existing drugs in an animal model of multiple sclerosis i.e. experimental autoimmune encephalomyelitis (EAE). This molecule, ASC is far superior to the existing therapeutics for both the treatment (Figure-6) and prophylaxis groups (Figure-7).

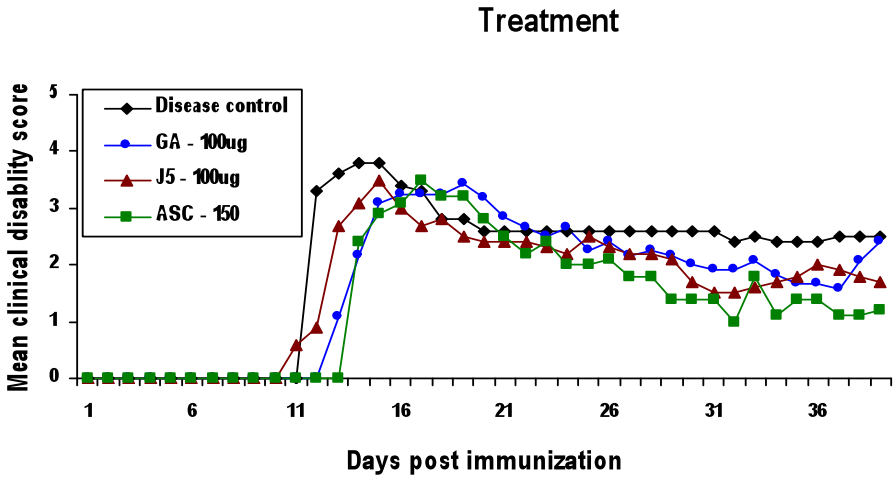

Figure 6: *Treatment: EAE was induced in female SJL/J with PLP (151-151). Symptoms of the disease appeared 12-14 days post immunization. Diseased animals were divided into four groups viz. disease control and treatment groups namely GA 100µg, J5 100µg and ASC 150µg with six animals per group. In the treatment groups animals were treated with various compounds daily for one week*

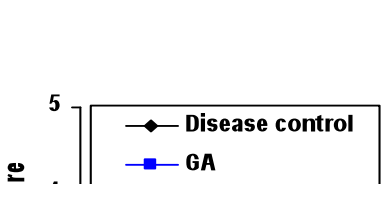

Figure-7: *Prevention: female SJL/J mice were divided into four groups - disease control, GA, J5 and ASC and were pretreated with PBS, GA, J5 and ASC. After two weeks all the animals were challenged for disease with PLP (131-151) and clinical disability score was monitored daily for 40 days*

3. Partial molar volumes of acyl carrier proteins are related to their states of acylation: ACP is a highly dynamic protein. Conformational flexibility of apo, holo and the various acylated forms of ACP which is essential for mediating its interactions with a multitude of enzymes still remains mostly unexplained. We addressed the issue of structural changes in *E.coli* and *P.falciparum* ACPs that take place on acylation by using a sensitive optical analytical technique, optical evanescent wave Dual Polarization Interferometry (DPI) for study which provides unparalleled resolution (~0.1Å) in real time. Our studies find an explicit correlation between the chain length of aliphatic groups covalently linked till C14 and C12 to *E.coli* and *P. falciparum* ACPs, respectively, and the corresponding partial molar volumes.

Observation of two of adlayers of different thickness on DPI chip suggests that they originate because of the ACPs exist in two different orientations (Figure-8) on the chip surface, as the calculated partial molar volumes was constant for both the layer thickness.

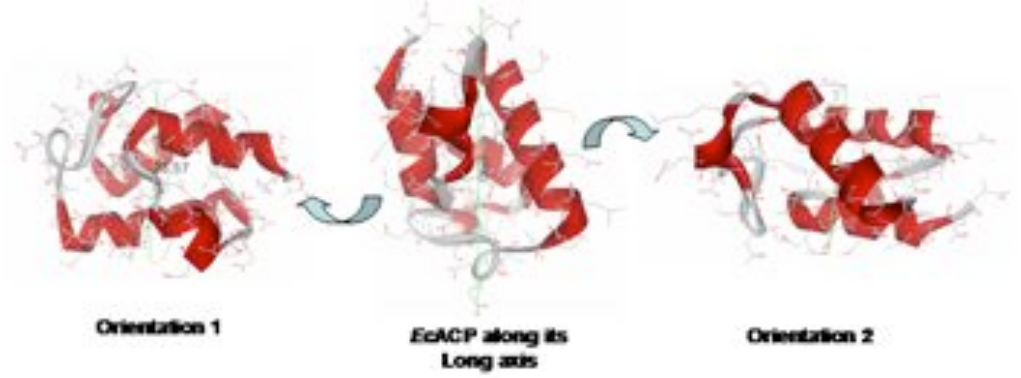

Figure 8: *Two different orientations and not conformations populate the adlayer. Visual presentation of two different orientation of E. coli apoACP molecule with reference to long axis, on chip surface. The long axis passing through the center of mass of the EcACP molecule is shown in center. Orientation1- EcACP (PDB ID 1T8K) is rotated by 116^0 about the z axis (perpendicular to the long axis) in counterclockwise (left). Orientation 2- EcACP in this orientation is rotated by 180^0 about the long axis and 75^0 about the z axis (perpendicular to long axis) in clockwise direction (right). Line (passing*

through the center of mass) shows the thickness (in Å) of the molecule in their respective orientation

Further a comparison of the partial molar volume of different ACP molecules showed increase in partial molar volume from apo to C14-*Ec*ACP. Interestingly, we observe an explicit correlation between the numbers of carbon atoms covalently linked to ACP with an increase in the partial molar volume of the acylated ACP. As can seen from Figure-9 there is a linear increase in partial molar volume of acyl-ACPs of chain lengh C4-C14 and C6-C12 of *E.co*li and *P.falciparum*, respectively. Enhancement in the volume by 65.65 $Å^3$ for *E.coli* acyl-ACPs for every two carbon atom increase in the aliphatic group attached to it are consistently observed till its myrisitoylation. In case of acyl-*Pf* ACPs attachment of every two carbon atom brings about an increment of 63.27 $Å^3$ till the addition of dodecanoyl group only. These observations are in broad agreement with the earlier studies which show that the solvent accessible volume of its internal cavity increases from zero for unligated holo protein to 165 $Å^3$ for decanoyl-ACP from *E.coli*.

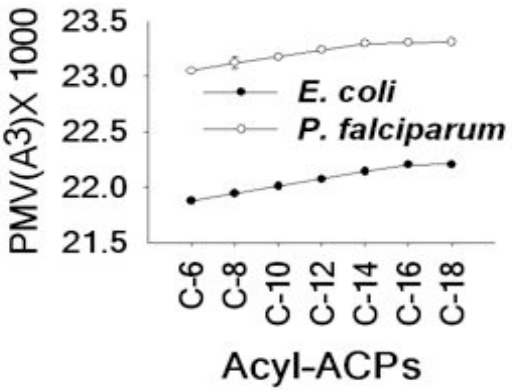

Figure-9: *Plot of partial molar volume ($Å^3$) calculated for different acyl-ACPs of E. coli and P. falciparum against the chain length of acyl group.*

Significantly, these studies are of relevance to the physiologic context in which these ACPs function. For example, several studies have shown that the predominant fatty acids synthesized in *E. coli* are C14 and C16 acids while *P. falciparum* FAS synthesizes shorter acyl chains of which C12 and C14 are the dominant species. Thus it is conceivable that it is not only the specificity pocket of β-ketoacyl-ACP synthase (FabF) that dictates the length of the acyl chains synthesized by a given organism but also the acyl chain hosting pocket of their respective ACPs which modulates the length of the fatty acid synthesized therein. The limitation in the size of the cavity accommodating acyl chains in these organisms is perhaps one of the reasons as to why most elongases utilize acyl-CoAs for the synthesis of fatty acids longer than stearic acid.

Publications

Original peer-reviewed articles

1. Chetnani B, Das S, Kumar P, Surolia A and Vijayan M (2009) *Mycobacterium tuberculosis* pantothenate kinase: possible changes in location of ligands during enzyme action. *Acta Crystallogr D* **65**:312-325.

2. Gupta S, Modak R, Surolia N and Surolia A (2009) Partial molar volumes of acyl

carrier proteins are related to their states of acylation. *Biochem Biophys Res Commun* **380**:763-768.

3. Gupta G, Vishveshwara S and Surolia A (2009) Stability of dimeric interface in banana lectin: Insight from molecular dynamics simulations. *IUBMB Life* **61**:252-260.

4. Banerjee T, Sharma SK, Surolia N and Surolia A (2008) Epigallocatechin gallate is a slow-tight binding inhibitor of enoyl-ACP reductase from *Plasmodium falciparum*. *Biochem Biophys Res Commun* **377**:1238-1242.

5. Kaushik S, Mohanty D and Surolia A (2009) Role of metal ions in substrate recognition and stability of Concanavalin A: A molecular dynamics study. *Biophys J* 96, 21-34.

6. Chopra T, Banerjee S, Gupta S, Yadav G, Anand S, Surolia A, Roy RP, Mohanty D and Gokhale RS (2008) Novel intermolecular iterative mechanism for biosynthesis of mycoketide catalyzed by a bimodular polyketide synthase. *PLoS Biol* **6**:e163.

7. Kulkarni KA, Katiyar S, Surolia A, Vijayan M and Suguna K (2008) Structure and sugar-specificity of basic winged-bean lectin: structures of new disaccharide complexes and a comparative study with other known disaccharide complexes of the lectin. *Acta Crystallogr D* **64**:730-737.

8. Gupta G, Gemma E, Oscarson S and Surolia A (2008) Defining substrate interactions with calreticulin: an isothermal titration calorimetric study. *Glycoconj J* **25**:797-802.

9. Gupta V, Gupta RK, Khare G, Surolia A, Salunke DM and Tyagi AK (2008) Crystallization and preliminary X-ray diffraction analysis of biotin acetyl-CoA carboxylase ligase (BirA) from *Mycobacterium tuberculosis. Acta Crystallogr F* **64**:524-527.

10. Purushothaman S, Gupta G, Srivastava R, Ramu VG and Surolia A (2008) Ligand specificity of group I biotin protein ligase of *Mycobacterium tuberculosis. PLoS ONE* **3**:e2320.

11. Mishra S, Karmodiya K, Parasuraman P, Surolia A and Surolia N (2008) Design, synthesis, and application of novel triclosan prodrugs as potential antimalarial and antibacterial agents. *Bioorg Med Chem* **16**:5536-5546.

12. Gupta G, Sinha S and Surolia A (2008). Unfolding energetics and stability of banana lectin. *Proteins* **72**:754-760.

13. Mishra S, Karmodiya K, Surolia N and Surolia A (2008) Synthesis and exploration of novel curcumin analogues as anti-malarial agents. *Bioorg Med Chem* **16**:2894-2902.

14. Gratraud P, Surolia N, Besra GS, Surolia A and Kremer L (2008) Antimycobacterial activity and mechanism of action of NAS-91 *Antimicrob Agents Chemother* **52**:1162-1166.

15. Kumar R, Srivastava R, Singh RK, Surolia A and Rao DN (2008) Activation and inhibition of DNA methyltransferases by S-adenosyl-L-homocysteine analogues *Bioorg Med Chem* **16**:2276-2285.

16. Damodaran D, Jeyakani J, Chauhan A, Kumar N, Chandra NR and Surolia A (2008) CancerLectinDB: a database of lectins relevant to cancer *Glycoconj J* **25**:191-198.

17. Sharma SK, Kumar G, Kapoor M and Surolia A (2008) Combined effect of epigallocatechin gallate and triclosan on enoyl-ACP reductase of *Mycobacterium tuberculosis*. *Biochem Biophys Res Commun* **368**:12-17.

18. Murthy BN, Sinha S, Surolia A, Indi SS and Jayaraman N (2008) SPR and ITC determination of the kinetics and the thermodynamics of bivalent versus monovalent sugar ligand-lectin interactions. *Glycoconj J* **25**:313-321.

In vitro reconstitution of intracellular transport: Role of GTPases

Principal Investigator: Amitabha Mukhopadhyay

Project Associates/Fellows: Suminder Kaur

PhD Students: Richa Madan
Shruvi Bhal
Sonali Bose
Deepika Gupta

Pathogenesis is related to the survival of pathogens in macrophages. The main goal of this project is to understand the mechanism of survival of pathogens in macrophages. We are also trying to understand the hemoglobin trafficking in *Leishmania* using *in vitro* reconstitution experiments. We have also initiated the studies on cytokine mediated modulation of intracellular trafficking.

Phagocytosis is an important process in host defense and is mediated by complex interactions between defined intracellular compartments. The final fate of the nascent phagosomes usually culminates with the fusion of lysosomes. But some invading microorganisms modulate this central process for their survival in the phagocytic cells. The objectives of the present investigations are (i) modulaton of phagosome maturation by intracellular pathogens, (ii) determination of the role of various cytokines in the modulation of phagosome trafficking and (iii) mechanism of intracellular trafficking of hemoglobin in *Leishmania*.

Evidences from a variety of sources, have established that transport of cargo along the endocytic pathway requires a series of highly coordinated and specific vesicle fusion events regulated by small GTP binding proteins of the Rab family. Not much is known about the regulation of endocytosis and intracellular trafficking in protozoan parasites. The major objective of the project is to understand how *Leishmania* generate heme from the intracellular degradation of endocytosed hemoglobin.

Mechanism of survival of Salmonella in macrophages

In the reporting period, we used SipC knock out *Salmonella* and compared its trafficking with that of WT *Salmonella* in macrophages. Accordingly, we isolated respective *Salmonella*-containing phagosomes at different stages of their maturation and determined the levels of different compartment specific markers present on these phagosomes by western blot analysis and confocal microscopy. Our results showed that levels of early endocytic marker like Rab5, late endocytic marker like LBPA and lysosomal marker like mature cathepsin D are unaltered in both phagosomes at different stages of their maturation demonstrating that SipC knock out *Salmonella* are not transported to the lysosome. Thus, no differences were observed between the trafficking of SipC knock out *Salmonella* and WT:*Salmonella* at least in endocytic pathway.

Previous studies from our group showed that dead *Salmonella* is targeted to the lysosomes and thereby acquire enhanced amount of LAMP1 on their phagosomes. However, live *Salmonella*-containing phagosomes also recruit relatively less amount of LAMP1 on their phagosomes at later stages (90 min) of their maturation in macrophages.

We hypothesized that LAMP1 is possibly recruited by live *Salmonella*-containing phagosomes by fusing with LAMP1 containing vesicles derived from trans-Golgi region in the biosynthetic pathway. Interestingly, results presented in the current investigation showed that LAMP1 recruitment on SipC knock out *Salmonella*-containing phagosomes is further reduced at later stages of their maturation in comparison to control live bacteria-containing phagosomes. These results indicated that SipC knock out *Salmonella* might have defect in recruitment of LAMP1 on their phagosomes. We and others have shown earlier that *Salmonella* resides in a specialized compartment juxtaposed to Golgi as evidenced by the localization of GFP-*Salmonella* with GM130 stained Golgi compartment. Interestingly, we found that SipC knock out *Salmonella* is not targeted near to Golgi compartments. Moreover, our results also showed that SipC knock out *Salmonella* unable to recruit phalloidin labeled actin near their phagosomes suggesting that SipC is require for actin polymerization and might play a role in phagosomes maturation.

Subsequently, studies were carried out to understand the mechanism of recruitment of LAMP1 on *Salmonella*-containing phagosomes. As expected, SipC knock out *Salmonella*-containing phagosomes recruited relatively less amount of syntaxin 6 on their phagosomes in comparison to WT:*Salmonella*-containing phagosomes at later stages of their maturation in macrophages. In addition, SipC knock out *Salmonella*-containing phagosomes also failed to recruit Rab6, a GTPase which shown to regulate the traffic from Golgi. Taken together, these results indicated that SipC mediated recruitment of syntaxin6 and Rab6 possibly promotes the fusion of *Salmonella*-containing phagosomes with the LAMP1 containing Golgi derived vesicle.

Mechanism of hemoglobin trafficking in Leishmania

In the reporting period, we made an attempt to generate hexokinase knoch out mutant *Leishmania* to understand the role of hexokinase in hemoglobin trafficking. Interestingly, it was found that there are two copies of identical hexokinase coding sequences (HK-1 and HK-2) in tandem with an intergenic region of 2627 bp on chromosome 21. Initially, we cloned HbR using the sequence information from HK-1. Thus, studies were carried out to knock out the HK-1 gene from *Leishmania*.

Since *Leishmania* are diploid organisms, the two alleles of the HK-I gene were successively targeted for deletion as detailed in methods using KO-Neo and KO-Hyg constructs. To generate the constructs for this targeted replacement of HK-I, a 450 bp fragment (5'KO) containing a part of the 5'UTR, and a part of the HK-I ORF downstream of the start codon was amplified by PCR using appropriate primers and cloned into the *Eco*RV and *Eco*RI sites of pBluescript to generate the 5'-pBSK-KO construct. Similarly, another 500 bp fragment (3'KO) containing a part of the HK-I ORF upstream of the stop codon and a part of the 3' UTR of HK-I was amplified by PCR using appropriate primers. This fragment was cloned into the *Bam*HI and *Xba*I sites of 5'-pBSK-KO to generate the 3'-5'-pBSK-KO. Subsequently, Neomycin and hygromycin resistance genes were cloned into the *Eco*RI-*Bam*HI and *Bam*HI-*Sma*I sites of 3'-5'-pBSK-KO to generate KO-Neo and KO-Hyg respectively. These constructs were then used for generating the hexokinase knockout *Leishmania* by homologous recombination.

Briefly, in the first round of transfection, one of the two alleles of HK-I was replaced with the KO-Neo construct, and the cells were selected on neomycin (G418) (10μg/ml)

containing medium. Stably expressing cells were further selected on 30μg/ml neomycin. These heterozygous or single knockout cells (LdHK-I (-/+) were then used for another round of transfection with the KO-Hyg construct. Hexokinase being an essential housekeeping gene, the homozygous or double knockout, LdHK-I (-/-) was lethal. Subsequently, attempts were made to supplement the double knockout cells with appropriate metabolic pathway intermediates which could rescue the knockout. Finally, homozygous knock out cells, LdHK-I (-/-), were selected in medium supplemented with appropriate metabolic pathway intermediates along with hemin; and propagated stably.

The knockout was characterized by amplification of various genes using *Leishmania* cDNA as a template. Using HK-I and HK-II specific primers, these genes were amplified from control (UR6) as well as knockout (LdHK (-/-)) cells. Our results demonstrated that HK-I is not expressed in the LdHK (-/-) cells as desired however no change in the expression of HK-II in this cells confirming the specific knock out of HK-I gene from this cells. In addition, no compensatory change in the expression levels of HK-II was observed LdHK (-/-) cells. Moreover, only the LdHK (-/-) cells expressed both neomycin as well as hygromycin resistance genes. The expression of rRNA was used as an internal control and was comparable in both cell types.

Finally, Hexokinase activity was compared from the cell lysates obtained from control UR6 as well as LdHbR:KO(+/-) and LdHbR:KO(-/-) knock out *Leishmania* promastigotes to deter-mine their ability to catalyze enzymatic reaction. Our results demonstrated that there was no significant change in hexokinase activity of single knockout cells (LdHbR:KO(+/-) in comparison to control cells. However, deletion of both strands in the double knockout cells (LdHbR:KO(-/-) cells were devoid of significant hexokinase activity in comparison to control cells indicating the successful knock out of hexokinase gene (HK1) in *Leishmania.* Taken together, our results demonstrated that we could successfully knock out an essential gene like hexokinase from Leishmania using appropriate supplement.

Publications

Original peer-reviewed articles

1. Madan R, Krishnamurthy G and Mukhopadhyay A (2008) SopE-mediated recruitment of host Rab5 on phagosomes inhibits salmonella transport to lysosomes. *Methods Mol Biol* **445**:417-437.

Biophysical and biochemical characterization of *Leishmania* phosphoglycerate kinase: an enzyme in the glycolytic pathway of parasitic protozoa

Principal Investigator: Vidya Raghunathan

It is known that *Leishmania* sp. has only two PGK genes encoding proteins PGKB and PGKC. Both these isoenzymes are simultaneously present in the cytosol and glycosome in a ratio of 80/20, in both promastigotes and amastigote forms. Therefore in *Leishmania* sp. the ratio 80/20 of glycosomal and cytosolic PGK reflects possibly the specific activities of different routes of sugar breakdown; glycolysis, leading to pyruvate and, the formation of malate via PEPCK and MDH respectively. Cytosolic PGK may in addition also be involved in other activities such as gluconeogenesis that has been claimed to be a cytosolic process. It is found that *Leishmania* PGK has some distinct structural features, as PGKB and PGKC differ in a handful of internal residues and in the presence of a long extension at the C-terminus of PGKC. Even though the *Leishmania* sp PGKC extension does not contain the glycosomal targeting tripeptide found in the similar extension of *T.brucei* PGKC it is possible that the former is responsible for the targeting of PGKC to the glycosome by some other unknown mechanism. Alternatively since it contains discontinuous stretches of hydrophobic and charged residues, it may associate with, either soluble or membrane associated glycosomal proteins, or ligands which modulate its enzymatic properties. Using previously published glycolytic reaction-based assays, the activities of PGKB and PGKC form *L.mexicana* can be compared.

Organism of the genus *Leishmania* lead to debilitating diseases in humans. According to current estimates hundred thousand individuals are infected yearly in the third world with a quarter of the world population living under threat of infection. Problems such as drug resistance and toxicity necessitate the development of better more effective drugs. Since glycolysis is very important for the generation of metabolic energy, many research efforts are underway to inhibit the parasite through the inhibition of the glycolytic pathway. One of the unique features of kinetoplastida glycolysis is its partial sequestering in intracellular organelles called glycosomes. Thus drug development efforts can be targeted, either at the glycosome itself or at the enzymes present within them, as has been demonstrated by other workers in the field. In this context it is useful to compare structurally and functionally the glycolytic enzymes present in the glycosome with those present in the cytoplasm.

The objectives of the project are (i) expression, purification and determination of specific activities of PGKB and PGKC, (ii) steady state kinetics by spectroscopic method; determination of the effect of high substrate concentration on enzyme activity, (iii) comparison between PGKB and PGKC of, pH optimum of activity and enzyme inhibition by salt and suramin (iv) ^{31}P NMR studies using substrate/enzyme (PGKB or PGKC) mixtures, with, either no metal, $MgCl_2$, $CaCl_2$, $MnCl_2$ or $CoCl_2$ to determine the change in the dissociation constant of substrate with metal ions. Comparison with data from similar experiments in literature with yeast PGK using Mg-ADP and Mg-ATP .and (v) peptide based studies of, a) the role of the C-terminus of PGKC in, modulating enzyme activity when added to PGKB in solution and b) glycosomal membrane association of PGKC. The peptides used in these studies will be evaluated as useful models to understand the structural basis of the biochemical differences between PGKC and PGKB.

Due to the presence of micelles the spectral overlap in the proton region was worsened by the line-width. It was suggested by RAPSAC members that labeled peptide be used for recording ^{15}N, ^{13}C spectra or else deuterated amino acid be substituted in parts of the peptide. However, making a completely ^{15}N, ^{13}C labeled peptide was prohibitively expensive as the peptide was purchased commercially. Further, partial deuteration would still have left large parts of the spectra unresolved. Fortunately a solution was found by recording the spectra in deuterated MeOH at 500 MHz. This sample gave good resolution and structure although fewer NH-NH connectivities are seen as compared to spectra in deuterated SDS. Sequence specific assignment of the peptide has been completed. Conditions were found for obtaining the proton spectra of peptide in deuterated SDS. High resolution spectra were recorded at 40C for the peptide reconstituted in deuterated SDS using field strength of 700 MHz.

Molecular mechanism of enzymatic reactions and enzyme-ligand interactions

Principal Investigator: Apurba Kumar Sau

Project Associates/Fellows: Pallavi Tripathi (Jun - Oct 2008)
Sadaf Fatima (since Jan 09)
Bharani Srinivasan (til Sep 2008)
Meena Bala Kumari N (till Oct 2008)
Anjana Rani (since Nov 2008)
Nidhi Dubey (since Dec 2008)

PhD Students: Nazish Abdullah
Abhishek Srivastava
Esha Pandita

The aim of this project is to understand molecular mechanism of different classes of GTPases induced by immunomodulatory cytokine interferon-γ (IFN-γ) and to compare the mechanistic similarities and differences with other GTPases within the same as well as different classes. The study has been currently focussed on human guanylate binding protein-1 (hGBP-1) and other proteins in the same family. The mechanism along with the structural data may provide an insight to design drug candidates on novel GTPases and their effectors involved in the disease.

A. IFN-γ induced GTP-binding proteins and their mechansim of GTP hydrolysis

*The o*bjectives *of the project are to (i)* study the molecular mechanism of IFN-γ induced guanylate binding proteins p67 (hGBP-1 and hGBP-2) and (ii) understand their similarities and differences within the same family as well as same and different classes

Circular dichroism measurements on wild type and mutant hGBP-1 proteins

As binding of the substrate to hGBP-1 leads to formation of dimer/oligomer, we wanted to examine whether the substrate binding induces any structural change of the protein that might correspond to dimer formation. Circular dichroism measurements of wild type hGBP-1 were carried out with and without non-hydrolyzable GTP-analogue GppNHp. The protein showed molar ellipticity at around 208 and 222 nm, which is the characteristic of mainly a helical protein. The molar ellipticity at both these wavelengths increased in presence of the analogue, suggesting a structural stabilization of the protein upon binding with the nucleotide, which might be responsible for the formation of dimer/oligomer. To further understand this, we carried out similar experiments with two mutant proteins D108A and R48P. D108A is catalytically important but R48A is known to have no detectable GTP binding or hydrolysis. In presence of the nucleotide, D108A showed similar result to the wild type, but R48P did not show any change, suggesting that the structural change is mainly due to binding of the nucleotide with protein. This result is consistent with the x-ray crystal structure of hGBP-1, where conformational changes were observed in switch I & II, and some unstructured areas became structured upon binding with the GppNHp.

Substrate concentration dependent assay

hGBP-1 is known to catalyze the hydrolysis of GTP to GDP and GMP. Unlike small GTPases Ras, Rho etc, this protein has the ability to hydrolyze GTP with a much higher rate, and the increased activity has been shown to be due to the substrate and enzyme concentrations dependent association and activation of hGBP-1. To obtain further insight into GTP hydrolysis and which particular product formation might be associated with activation of the protein, we carried out steady-state kinetic assay of whGBP-1 with radiolabelled [α-^{32}P] GTP. This protein is known to exist as monomer and dimer/oligomer in the absence and presence of GTP-analogue respectively. With increase in GTP concentration, the formation of GDP and GMP was enhanced, but the concentration of GMP increased more significantly than that of GDP. The experiment was also done at lower concentration of the substrate, where multiple turnover condition was not maintained, in order to see whether self-association and activation of the protein is hampered. But at the low concentration of the substrate (10 nM) GDP was found to be a predominant product. It appears that this activity could be due to monomeric protein. Under the multiple turnover condition, the data for GMP and GDP could be best fitted to Hill equation to obtain the steady-state kinetic parameters k_{cat}, K_m, k_{cat}/K_m and n (Hill co-efficient). The value of n was determined to be ~ 1.4 and 1.05 for GMP and GDP respectively. The value of n ~ 1.4 for GMP formation suggests that at least two molecules of hGBP-1 are involved in catalysis. We reported earlier that pyrophosphate (PP_i) was not found as a reaction product in hGBP-1 catalyzed reaction, suggesting that the hydrolysis of GTP occurs through a successive cleavage. hGBP-1 failed to hydrolyze β-γ resistant GTP-analogues, GppNHp or GTPγS, indicating that the second phosphate cleavage cannot occur without the first. This study shows that the stimulation of activity occurs during the cleavage of second phosphate rather than the first.

Specific activity assay

To examine the mechanism of enzyme concentrations dependent self-association and activation of hGBP-1, we measured the specific GTPase activity at various concentrations of the wild type protein. The data showed an increase in specific activity for GMP formation (~ 4 fold) than that of GDP (~ 1.3 fold) with increasing concentration of protein. Both substrate and enzyme concentrations dependent GTPase assays suggest that the activation of the protein occurs mainly during the cleavage of second phosphate of GTP. This is in fact consistent with our single mutant as well as several truncated proteins data. Thus the steady-state data supports that at the basal level GDP forms from the activity of monomer, whereas in stimulation, GMP and GDP from dimer/oligomer and GDP-bound monomer, which is formed from the dissociation of GDP-bound enzyme dimer respectively.

Pre-steady-state assay

Earlier we reported the pre-steady-state assay of full-length hGBP-1 using radiolabelled [α-^{32}P] GTP. The data showed that at early time scale GDP was found to be the major product but longer time point GMP was found to be predominant. We hypothesized that at early time scale GDP could be resulting from monomeric state of the protein but at longer time scale the formation of GDP and GMP is occurring from the oligomeric state of the protein. To address whether this could be a general trend for GMP formation, we carried out similar experiment with a truncated protein, hGBP1^{317}. As expected, at early

time point only GDP was seen as a major product. In contrast to the wild type, GMP accumulation in hGBP1^{317} was delayed. A ratio of 1:1 GMP to GDP was achieved at about 7 min as compared to 30 s for wild type. This implies that deletion of the helical domain in hGBP1^{317} impairs the ability of the protein to dimerise, which is found by slow accumulation of GMP. This result is consistent with our steady-state assay.

Studies on truncated proteins

We earlier reported preliminary studies on truncated hGBP-1 proteins. We carried out a detailed steady-state kinetic analysis of the wild type and truncated hGBP-1 proteins using radiolabelled [α-^{32}P] GTP. The analysis of our data showed that the catalytic efficiency (k_{cat}/K_m) for GDP formation in hGBP1^{317} increased by about 3-fold than that of the full-length protein, whereas for GMP, it decreased by ~ 2 fold. This suggests that the deletion of the C-terminal helical domain in hGBP-1^{317} destabilizes the enzyme-bound GDP dimer resulting increased amount of GDP formation. To understand the role of intermediate region and whether it can act as an internal GTPase activating protein (GAP) we carried out similar studies on hGBP-1^{311} and hGBP-1^{307}. The catalytic efficiency of both GDP and GMP formation is similar to that for hGBP1^{317}, further suggesting that the deletion of the helical domain destabilizes enzyme-bound GDP dimer, resulting to an increased GDP formation compared to the full-length protein. On the other hand, hGBP-1^{289} produced only GDP and GMP formation is completely abolished. This suggests that globular domain plus one β-sheet and one α-helix of the intermediate region are required for the hydrolysis to GMP. It also demonstrates that α-helix of 19 residues of the intermediate region is primarily responsible for the stimulation of the GTPase activity through allosteric interaction. Thus, this helix may play a role of an internal RGS (regulator of G protein signaling)-type GAP by stabilizing and orienting residues in both switches I & II and ^{103}DxEKGD^{108} motif for efficient catalysis. This helix could also be termed as internal GAP, since its absence greatly reduces the first catalysis and abolishes the second.

Cloning and transfection of mutant and truncated proteins

To understand how the structure of the hGBP-1 is related to the antiviral activity, we cloned several important mutant and truncated proteins into eukaryotic expression vector containing Flag-tag to check the expression of the protein after transfection into HeLaM cells. The genes were verified from sequencing. The recombinant clones were transfected into HeLaM cells using transfection reagent. The cells were allowed to grow for 36 hrs following antibiotic treatment. The western blot analysis showed that 800 μg of antibiotic was optimal for generation of stable cell lines. Subsequently viral assays of these stable cell lines will be carried out.

B. Understanding the function of arginine metabolic enzymes in *Helicobacter pylori*

The aim of the project is to investigate a detailed molecular mechanism of two arginine metabolic enzymes arginase and ADC in *H.pylori*. The mechanism along with structural data from other organisms may provide a novel strategy to develop new antibiotics with greater efficiency against *H.pylori* infection.

Steady-state assays with metal reconstituted arginases

To understand the role of the divalent metal ions on activity, we prepared several metal-reconstituted enzymes and looked their activity. Out of the metal ions investigated, only Co^{2+}, Ni^{2+} and Mn^{2+} showed detectable activity. In contrast to other arginases, *H.pylori* counterpart exhibited highest activity with Co^{2+} ion. We first examined the concentration of metal to enzyme ratio showing maximum activity. The highest activity was obtained when 20 fold of Co^{2+} was used in excess over the protein. The steady-state assay was carried out by taking a fixed concentration of protein with varying concentration of substrate arginine. Interestingly, the data could be fitted best to sigmoidal equation yielding steady-state kinetic parameters and n (Hill co-efficient). The value of n was determined to be 1.8 which suggests a cooperative mechanism of arginine hydrolysis by the enzyme. Similar measurements on Ni^{2+}- and Mn^{2+}-enzymes were carried out. The data could be best fitted to a sigmoidal equation yielding n ~ 1.7 further suggesting that cooperative mechanism of arginine hydrolysis by *H.pylori* arginase is an intrinsic property of the protein. Unlike Co^{2+}-enzyme, Ni^{2+}- and Mn^{2+}-proteins showed highest activity when metals were used approximately 500 fold higher than the protein. Among the metal ions studied, Co^{2+} showed highest activity followed by Ni^{2+} and Mn^{2+}.

pH dependent studies

Mammalian and bacterial arginases are known to exhibit highest activity at around pH 9.0. To understand the role of metal ions and their interaction with the residues that are important for catalysis, we carried out pH dependent experiments of Co^{2+}-reconstituted enzyme within pH range 6.1 to 9.8. The data showed a maximum activity at around 7.2, in contrast to the mammalian counter part. The plot of the second order rate constant k_{cat}/K_m vs pH showed a single ionization with pK_a 9.4. This pK_a is unlikely to be originating from the substrate and protein as these do not have any residues at the active site that might have a pK_a corresponding to this ionization. The crystal structure of the *H. pylori* arginase is not yet reported. However, the structures of the mammalian and other bacterial counterparts are available. Mammalian arginase has a bimetallic Mn^{2+}-cluster at the active site of the enzyme. The two metal ions are bridged by a water molecule which is believed to be important for catalysis. Hence the observed pK_a of 9.4 in *H.pylori* Co^{2+}-arginase may correspond to the metal coordinated water. The pH dependent experiments on the other metal-reconstituted enzymes are currently undergoing in the laboratory.

Publications

Original peer-reviewed articles

1. Abdullah N, Srinivasan B, Modiano N, Cresswell P and Sau AK (2009) Role of individual domains and identification of internal GAP in human guanylate binding protein-1. *J Mol Biol* **386**: 690-703.

2. Li Z and Sau AK (2009) Probing the subunit-subunit interaction of the tetramer of *E.coli* KDO8P synthase by electrospray ionization mass spectrometry. ***Chinese Journal of Chemistry*** **27**:1-10.

Structure, interaction and design studies involving regulatory peptides and proteins

Principal Investigator: Dinakar M Salunke

Project Associates/Fellows: Suman Tapryal
Pankaj Gupta
Anamika (since Aug 2008)
Arpana Vibhuti (since Jan 2009)
Divya Tomar
Shailja Goyal

PhD Students: Suvendu Lomash
Vineet Gaur
Tarique Khan
Arijit Bhowmik
Raghav Sharma
Ashish Kumar

Technical Officer: Sushma Nagpal

Collaborators: Kanwal J Kaur
JK Batra
KVS Rao, *ICGEB, New Delhi)*

The structural aspects of molecular recognition and its applications in analyzing the mechanisms associated with specific regulatory events and in rational molecular design is the theme of research.

*The o*bjectives *of the project are (i)* understanding the protein architecture and the structural biology of various regulatory events, (ii) analysis of the structural principles of immune recognition and molecular mimicry and (iii) rational molecular design studies based on the above.

While attempting to image alternative ways of germline expansion of primary antibody repertoire, we arrived at a mechanism of diversity generation in primary immune repertoire [*Sethi et al, (2006) Immunity 24:429*], which involved differential juxtaposition of independent epitopes within a given paratope conformation of germline antibody. We are further exploring this model using wider range of epitopes and paratopes. We have now co-crystallize Fab fragment of mAb BBE6.12H3 with the corresponding phage-displayed dodecapeptide antigens. We have also co-crystallized the Fab fragment of mAb 36-65, which we have analysed earlier, with the dodecapeptides which were obtained by panning phage-libraries through BBE6.12H3 and mAb 36-65. Thus, using the two antibodies a series of common antigens are being subjected for structural analyses. Of these, crystal structures of BBE6.12.12H3 native, its complex with the peptide PPYPAWHAPGNI (PPY) and the structure of 36-65 complexed with the peptide ATWSHHLSSAGL (ATW) have been determined. Seven residues of the 12mer peptide could be built into the electron density. Most of the interactions of the peptide were with CDRH3 and CDRL3 of the Fab. Residue numbers 1 through 7 were built and out of these first and last residues formed contacts with the CDRs. The C-terminal part of the chain

moves into the solvent and the last five C-terminal residues of the peptide could not be modeled. The peptide binds to the Fab using all the twelve residues. All contacts were formed with the heavy chain, primarily involving CDRH3 and CDRH1. The N-terminal part of the peptide interacts with CDRH1 and C-terminal part interacts with the CDRH3. The middle part of the peptide binds the interface between CDRH1 and CDRH3.

Comparison of PPY peptide and BBE6.12H3 Fab complex with native BBE6.12H3 Fab showed that the two molecules PPY-BBE6.12H3 Fab and unliganded Fab differed in terms of elbow angles; while the elbow angle of PPY-BBE6.12H3 Fab is 176.6º and that of unliganded Fab is 201.8 º. Differences in the V_H-V_L interfaces could be correlated with differences in the elbow angles. The two molecules showed significant changes in the main chain in addition to a number of side chain differences. The most critical differences were seen in the CDRs. Specifically CDR H3 of unliganded Fab was significantly different from the PPY-BBE6.12H3 Fab.

Comparing the mode of binding of the germline antibody 36-65 with three independent previously analysed peptide ligands in the known crystal structures from laboratory [*Sethi et al, (2006) Immunity 24:429*] with the ATW-36-65 Fab complex:. It was evident that, indeed, single paratope conformation recognizes multiple independent epitopes. Surprisingly, CDRs of the three complexes and ATW-36-65 Fab complex exhibited common paratope conformation on peptide binding. CDRs H2 and H3 which were largely responsible for the observed structural diversity in the case of unliganded antibody structures, showed excellent overlap in the all liganded Fab structures, both in terms of the side chain as well as the backbone conformations. The RMSDs and the thermal parameters of the CDRs were consistent with the observed conformational convergence in the liganded state. In other words, the differential justapositions of the antigens, generated for 36-65 is also valid for the antigens generated for BBE6.12H3, while binding to 36-65. The bound peptides showed no structural correlation with any of the previously known peptide-fab complexes. Despite the wide spatial distribution of peptide binding, two interacting residues, Tyr50H and Tyr106H, of the antibody were shared by the three peptides. In case of ATW-36-65 Fab complex none of the twelve residues were making any contact with these two common residues in CDRs, instead it was making altogether different interactions primarily with CDRH3 and CDRH1. In other words, no structural mimicry could be invoked for explaining the conformational convergence on binding to varied peptides, as a wide variety of interactions was involved.

In the on-going structural and physiological studies of carbohydrate-peptide mimicry, involving mannopyranoside and a 12mer peptide (DVFYPYPYASGS), were further extended towards molecular characterization of mimicry. Monoclonal antibodies were generated against α-D mannopyranoside which were then screened for binding mimicking antigen YPY motif containing peptide and mAb 2D10 was isolated and characterized [*Goel et al. (2004) J Immunol 173: 7358*]. The crystal structure of mAb 2D10 in complex with the sugar and peptide ligands would vitally help understand the mechanisms of mimicry. Limitation of the poor secretion of the antibody by 2D10 hibridoma, we have constructed its single chain antibody. The scFv was cloned and expressed using *E.coli* system and refolded with high efficiency. The refolded pVEX-2D10 was subsequently concentrated at 15 °C up to 30 mg/ml to be used further for setting up crystallization screens. The scFv-2D10 and sugar co-crystals were grown in 0.1 M MES, pH 6.5 with 1.6 M magnesium sulphate as precipitant. The co-crystals of scFv-

2D10 and peptide were also obtained under similar conditions. The structures were determined by MR using scFv (1JP5) as a probe model and the refinement is in progress. At the current state of refinement, the sugar moiety model has been built into the corresponding electron density, the peptide which appears to bind in a mode overlapping the sugar. The conformation of the CDRs in scFv bound to sugar and peptide seem to be nearly identical.

In order to understand the molecular mechanisms underlying food allergy, two major classes of seed proteins that are often associated with allergenicity: bicupin and albumin were targeted. Prunin, also known as almond major protein (AMP) or Pru du Amandin, a member of bicupin family (11S Legumin) was purified and crystallized from *Prunus dulcis* (almonds). The crystals diffracted to a resolution of 3.1Å. The protein is exceptionally rich in poly-glutamine stretches. The structure of Prunin was solved by molecular replacement using Glycinin A3B4 subunit (PDB: 1OD5). The structure was refined using six fold strict NCS to an R_{cryst} 25.7% and an R_{free} of 27.9%. Prunin exists as a homohexamer both in solution as well as in crystal structure. The molecular mechanisms involved in stabilizing the quaternary structure of the protein were identified, principal among them are the large hydrophobic interface area involved in stabilising the trimeric structure and deeply positioned salt bridges stabilising the dimer of trimers. The structural stability of the fold was found to manifest in the form of high pH stability of the protein. Known IgE epitopes from the members of 11S Legumin family were mapped onto the surface of the protein demonstrating oligomerisation to be responsible for high allergenicity of these proteins as well.

Structure of LS24, an albumin from *Lathyrus sativus* was solved earlier was further refined and analysed to arrive at the strcture-function correlation. The protein is homodimeric, each monomer exhibiting distinctive hemopexin fold. The structure is folded into a four-bladed propeller with each blade having four β-strands arranged around a central channel through which passes the axis of pseudo 4-fold symmetry. A structure-based sequence alignment of various hemopexin-like domains led to the identification of a conserved sequence motif, highlighting the important aspects of stability and evolutionary history of the hemopexin fold. One of the two independent dimers in the crystallographic asymmetric unit was found to be associated with a molecule of spermine. Heme binds LS24 with physiologically relevant affinity and monomerizes the LS24 dimer. *In silico* heme docking analysis provided insights into the nature of heme-LS24 interaction.

Differential binding of heme and spermine, in different oligomeric states, provided attractive clues for the protein function. While binding of spermine correlates with involvement of LS24 in polyamine biosynthesis pathway that of heme is linked with oxidative stress. The two ligands - spermine and heme - are important players of oxidative stress management in plants. Their differential binding to LS24, in different oligomeric states, prompted a mechanistic model for the involvement of LS24 in the management of oxidative stress in plants requiring fine balancing between the levels of free heme and spermine in the cytoplasm. LS24 may simultaneously be involved in transport of heme to proteins involved in binding reactive oxygen species that require heme as a prosthetic group. Thus, we conclude LS24 to be a moonlighting protein, with multiple functions which are mediated through differential oligomeric states and ligand availability. On the basis of LS24 structure we have proposed a mechanism by which a

plant cell can sense oxidative stress and activate downstream pathways to combat stress, simply by switching from dimeric state to monomeric state.

The structure of CP4, an albumin from *Vigna unguiculata*, showing 48% sequence identity with LS24 was solved in two different crystal forms: C2 and $P2_12_12$ using LS24 as the model by molecular replacement. Although the tertiary structure of CP4 is identical to LS24, but there are apparent differences in surface charge distribution among the two proteins. These differences manifest in the form of quaternary differences between the two proteins. The mode of dimer formation is very different in both the cases. In LS24 dimerization is governed by hydrophobic interactions whereas in CP4 dimer formation is essentially mediated by formation of a continuous β-sheet between the two monomers. The differences seen in quaternary structures indicated the structural divergence of hemopexin fold in plant kingdom.

Publications

Original peer-reviewed articles

1. Gupta P, Gaur V and Salunke DM (2008) Purification, identification and preliminary crystallographic studies of a 2S albumin seed protein from Lens culinaris. *Acta Crystallogr F* **64**:733-736.

2. Gupta V, Gupta RK, Khare G, Surolia A, Salunke DM and Tyagi AK (2008) Crystallization and preliminary x-ray diffraction analysis of biotin acetyl-CoA carboxylase ligase (BirA) from *Mycobacterium tuberculosis*. *Acta Crystallogr F* 64:524-527.

3. Gupta V, Gupta RK, Khare G, Salunke DM and Tyagi AK (2008) Cloning, expression, purification, crystallization and preliminary x-ray crystallographic analysis of bacterioferritin A from *Mycobacterium tuberculosis*. *Acta Crystallogr F* **64**:398-401.

Molecular modelling of peptides and protein-ligand complexes using knowledge-based potentials

Principal Investigator: Debasisa Mohanty

Project Associates/Fellows: Narendra Kumar
MVR Prasad

PhD Students: Sandeep Kaushik
Bhusan N Kate
Swadha Anand
Garima Tiwari
Nikhil P Damle

Collaborators: Rajesh S Gokhale
Avadhesha Surolia

The main theme of the research project is to understand the structural principles that govern binding of various ligands to proteins and folding of peptides/proteins to stable conformations, and use these structural principles for developing computational approaches for structure prediction of peptides/proteins and protein-ligand complexes.

The specific objective of the project is to investigate, whether knowledge-based methods can be used for predicting the (1) substrate specificity of proteins involved in biosynthesis of secondary metabolites, (2) substrate specificity of MHC and kinases, (3) identification of new biosynthetic pathways in various genomes.

A. In Silico analysis of core catalytic domains and tailoring enzymes involved in biosynthesis of secondary metabolites

Prediction of the order of substrate channeling in modular PKS clusters

We have analyzed the docking domain sequences of various modular PKS clusters in detail to investigate if information contained in the docking domain sequences can be used to identify the correct order for channeling of substrates. Using the recently available NMR structure of the docking domains from the erythromycin biosynthetic cluster as template, inter polypeptide contacts were analyzed for various types of cognate and non-cognate pairing of ORFs in various modular PKS clusters. Our investigation revealed that, cognate pairing of ORFs always generated energetically favorable inter polypeptide contacts, while in majority of cases non-cognate pairing resulted in energetically unfavorable contacts. The results of our benchmarking on known modular PKS clusters indicated that, using such inter polypeptide contact analysis, it is possible to narrow down the number of possible choices for the cognate order of substrate channeling. These results have interesting implications for identifying metabolic products of uncharacterized PKS clusters found in newly sequenced genomes.

Molecular dynamics simulations on crystal structures of KS-AT linker and KS-AT di-domain

The crystal structures of multi domain type I PKS as well as type I FAS proteins, showed that the linker connecting the KS and AT domains in PKS as well as FAS proteins adopts a conserved structural fold. This fold is also unique to PKS and FAS proteins. It was of interest to find out whether the linker structure was stable autonomously or it was stabilized by inter-domain contacts with the flanking KS and AT domains. Several explicit solvent MD simulations have been carried out for the KS-AT linker structure from 3rd module of DEBS. The linker structure was found to be stable in isolation and showed RMSD in the range of ~2Å from the crystal structure over several 5ns trajectories. We have also carried out MD simulations on complete KS-AT di-domain to understand the role of inter domain motions if any, in the transfer of acyl group by phosphopantetheine arm of ACP from the active site of AT to KS.

Understanding substrate specificity of antibiotic glycosyltransferases

Biochemical data shows that GtfA is a stringent glycosyltransferse and can transfer only L-*epi*-vancosamine to aglycone desvancosaminyl vancomycin (DVV). In contrast GtfD has relaxed substrate specificity and can transfer both L-vancosamine and L-*epi*-vancosamine. Molecular dynamics and MM/GBSA energy calculations carried out for both GtfA and GtfD in complex with donor and acceptor substrates have provided novel insight to the structural basis of the specificity of donor substrate recognition by these enzymes. In qualitative agreement with experimental studies, stringent GtfA showed overall lower binding free energy for its donor substrates as compared to non-stringent GtfD. Based on the analysis of the contribution of various binding pocket residues to this free energy difference and visual analysis of different snapshots from MD trajectory, specificity-determining residues for vancosamine and *epi*-vancosamine were identified. Most notable of these residues is ASP 333 of GtfD, which is found to make salt bridge with amino group of sugar. Interestingly corresponding ASP 317 residue in GtfA is moved away from active site due to an insertion in the primary sequence. Instead a mutation of GLY to ASP at position 294 in GtfA is probably playing a role of ASP 333 in GtfD. L-vancosamine and L-*epi*-vancosamine differ only in orientation of single hydroxyl group. This hydroxyl group of TDP-L-*epi*-vancosamine is found to make crucial interactions with acceptor molecule and active site ASP 13 and SER 10, which may explain reason for specificity of GtfA for L-*epi*-vancosamine.

B. Protein-peptide interactions

Multi scale modeling of substrate peptides in complex with kinases and MHCs using statistical pair potentials and MM/PBSA

Our earlier work had demonstrated that, using a structure based approach for modeling of kinase-peptide complexes and scoring the binding energy by statistical pair potentials, it is possible to rank the actual substrate peptide within the top 30% of all the other potential Ser/Thr containing peptides. Moreover, because of the scoring by simple statistical pair potential it is not compute intensive and can be used for high throughput analysis of sequences in a genomic scale. However, its utility can be further improved if percentile cut off for bracketing the correct phosphorylation site can be further lowered from 30%. As demonstrated earlier in case of protein structure prediction problems, multi scale modeling strategy can potentially help in improving the rank of the correct substrate. Therefore, scoring by pair potentials can be used as a first level of search, while sites ranked within top 30% can be re-ranked using all atom forcefield. For the ten kinase families for which

MODPROPEP could successfully rank the correct binding site within top 30%, we carried out detailed all atom modeling of all the Ser/Thr containing peptides in the binding site of the respective kinases. In all cases modeled complexes remained close to the template structure. Similar trend was also observed for kinase-peptide complexes belonging to other families. For each kinase-peptide complex, interaction energy between the kinase and the peptide was computed using MM-PBSA approach and all the modeled peptides were re-ranked as per their MM-PBSA binding energy values. It was found that, in case of 7 out of ten kinase families upon re-ranking there is a significant enrichment of true phosphorylation site in top 10% and 20% window. AUC values obtained from ROC analysis for the ranking using pair potential as well as MM-PBSA also confirmed these results. Similar to the modeling of kinase-peptide complexes, the high scoring peptides obtained by the pair-potential were modeled in the binding pocket of their respective MHCs and ranked as per their binding energy using MM/PBSA method. Analysis of MM/PBSA results indicated that, in case of eight out of the 16 alleles, use of MM/PBSA for re-scoring resulted in improvement in the ranks of the experimentally identified substrate peptides. Thus our results demonstrate that, prediction accuracy of MODPROPEP for identifying substrates of various kinases and MHCs can be further improved if a multi-scale modeling approach involving re-ranking of pair potential predictions by MM-PBSA energy values is implemented.

Computational analysis of peptides recognized by PTB domains

Since combination of statistical pair potential and all atom modeling involving MM/PBSA approach could successfully identify substrates for kinases and MHCs, similar computational approach was used to analyze other modular domains involved in peptide recognition. Proteins containing PTB (phosphotyrosine binding) domains are involved in the modulation of a number of physiological processes like neuronal development, immune responses, tissue homeostasis and cell growth. Even though PTB domains are known to recognize peptides containing NPXpY or NXXpY motifs, recent experimental studies based on peptide array have highlighted important role of amino acids flanking the NXXpY motif as determinants of specificity. We have modeled peptides from PTB binding proteins in complex with their cognate PTB domains to investigate whether known PTB binding peptides can be identified based on their binding energy as evaluated by statistical pair potentials. Interaction energies between the PTB domain, 1X11 and a set of peptides have also been calculated using GB/SA approach from conformations sampled during nano second MD simulations. Interestingly, the binding energies obtained by different computational methods show good correlation with the experimental dissociation constants and binding affinities reported in literature.

Publications

Original peer-reviewed articles

1. Ansari MZ, Sharma J, Gokhale RS and Mohanty D (2008) *In silico* analysis of methyltransferase domains involved in biosynthesis of secondary metabolites. BMC Bioinformatics **9**:454.

2. Kaushik S, Mohanty D* and Surolia A* (2008) Role of metal ions in substrate recognition and stability of Concanavalin A: A molecular dynamics study. *Biophys J* **96**:21-34. * corresponding authors

3. Arora P, Goyal A, Natarajan VT, Rajakumara E, Verma P, Gupta R, Yousuf M, Trivedi OA, Mohanty D, Tyagi A, Sankaranarayanan R and Gokhale RS. (2009) Mechanistic and functional insights into fatty acid activation in *Mycobacterium tuberculosis*. *Nat Chem Biol* **5**:166-173.

4. Chopra T, Banerjee S, Gupta S, Yadav G, Anand S, Surolia A, Roy RP, Mohanty D and Gokhale RS (2008) Novel intermolecular iterative mechanism for biosynthesis of mycoketide catalyzed by a bimodular polyketide synthase. PLoS Biology **6**:e163.

Role of carbohydrates in host-parasite interactions

Principal Investigator: Kanwal J Kaur

Project Associates/Fellows: Ratna De
Saroj Kumari

PhD students: Sariya Talat
Deepti Sripad Lele

Collaborator: Dinakar M Salunke

The project is aimed for understanding the differential roles of carbohydrate domains in host-parasite interactions by using synthetic glycoconjugates involving model systems such as antimicrobial glycopeptides of innate immune origin.

The objectives of the project are (i) synthesis and structural characterization of glycoconjugates and structure-function analysis of the synthetic glycoconjugates in the context of host-parasite interactions

The mannosylated threonine (N^{α}-Fmoc-Thr(Ac_4-α-D-Man)-OH) was synthesized at large scale and the final product was characterized by ^{1}H NMR. The proline rich class of antibacterial glycopeptides from insects contain conserved threonine residue which is glycosylated by either a monosaccharide (2-acetamido-2-deoxy-D-galactopyranosyl; GalNAc) or a disaccharide (D-β-galactopyranosyl-GalNAc). The sugar moiety is linked through α-*O*- linkage to the threonine. To understand the significance of α-*O*- glycosidic linkage, an analog of formaecin I containing glycan in β- configuration is designed. The synthesis of β-GalNAc-threonine was standardized. For synthesizing the N^{α}-Fmoc-Thr(Ac_3-β-D-GalNAc)-OH, the trichloroethoxycarbonyl chloride (Teoc-Cl) was added to a vigorously stirred solution of D-galactosamine hydrochloride and sodium bicarbonate in water. The mixture was stirred and neutralized with acid, concentrated, dried and followed by its acetylation with acetic anhydride which resulted the anomeric mixture of tetra-*O*-acetyl-2-deoxy-2-(2,2,2-trichloroethoxycarbonylamino)-galactose. The regio-selective hydrazinolysis of the anomeric *O*-acetyl group was carried out even in the presence of the quite reactive Teoc group. The 1-*O*-unprotected galactosamine derivative was transformed into trichloroacetimidate by treatment with trichloroacetonitrile in the presence of 1,8-diazabicyclo[5.4.0]undec-7-ene(DBU) as base. The reaction of glycosyl donor with Fmoc-Thr-OBzl in the presence of catalytic amounts of trimethysilylmethanesulfonate furnished the β-linked glycosylated amino acid. Subsequent replacement of the *N*-Teoc group by *N*-acetyl group with zinc and acetic anhydride provided N^{α}-Fmoc-Thr(Ac_3-β-D-GalNAc)-OBzl. Finally, the deprotection of benzyl ester by hydrogenolysis yielded the final product, N^{α}-Fmoc-Thr(Ac_3-β-D-GalNAc)-OH for subsequent use. All the intermediate compounds and the final product were characterized by ^{1}H-NMR.

The synthesized N^{α}-Fmoc-Thr(Ac_4-α-D-Man)-OH was utilized for synthesizing glycosylated analogs of formaecin I and drosocin in which the α-D-GalNAc-Thr was substituted with α-D-Man-Thr. The glycosylated peptides were synthesized on HMP resin using N^{α}-Fmoc-protected amino acids and DCC-mediated HOBt ester activation in

NMP. Finally, the peptides were cleaved from the resin and purified by HPLC. The purified peptides were used for the removal of acetyl groups of glycan moiety, followed by their purification again by HPLC. Characterization of the peptides was performed by molecular mass determination. The designed glycosylated peptides were assayed for their comparative spectrum of antibacterial activity against *E. coli* ATCC 25922. The mannosylated formaecin exhibited the lower antibacterial activity in comparison to the native formaecin whereas the level of antibacterial activity was found to be similar for native drosocin and mannosylated-drosocin. The results indicated that the conformation of the peptide is effected by sugars and different sugars alter the conformation of same peptide differently.

During the current reporting year, we continued the studies to explore the mode of action of proline rich class of antibacterial peptides. The comparison of the antibacterial activities of D- and L-enantiomers of designed analog of formaecin I was shown earlier where D-enantiomer was found to be completely inactive. The *in vivo* effect of both the enantiomers on RNA and protein synthesis was studied by monitoring the incorporation of radiolabelled amino acid [^{35}S]methionine and [^{3}H]uridine. The results showed that D-enantiomer of formaecin was unable to inhibit both RNA and protein synthesis whereas L-enantiomer selectively inhibited the protein synthesis. When both the enantiomers were assayed for *in-vitro* transcription/ translation inhibition, it was found that both D- and L-analogs could interfere in the transcription/ translation pathway. To investigate the specific interaction of these enantiomers with the target molecule, the binding kinetics of both the enantiomers with heat shock protein, DnaK were studied by surface plasmon resonance. Both the analogs exhibited comparable binding affinity to DnaK.

Continuing the designing of a glycosylated analog of naturally occurring nonglycosylated antibacterial peptide, apidaecin Hb1b, an analog of apidaecin was designed and synthesized. The designed glycosylated analog exhibited 80% activity to that of native apidaecin.

Ribonucleases and ribosome-inactivating proteins: Role in host defense and development of recombinant toxins

Principal Investigator: Janendra K Batra

PhD Students: Divya Bakshi
Ramteke Anup Karandas
Anu Malik
Deepa Sikriwal (till Jun 2008)
Anubha Singh
Santosh K Yadav

Collaborator: Faizan Ahmad, *Jamia Millia Islamia, Delhi*

The classical functions of ribonucleases are the processing, turnover and degradation of specific RNA. However, some RNase A homologues of the pancreatic ribonuclease family express diverse activities like anti-tumor, immunosuppressive and angiogenic activities. Two human ribonucleases, eosinophil cationic protein (ECP) and eosinophil-derived neurotoxin (EDN) are among the toxic proteins secreted by activated eosinophils, whose role in host defense remains enigmatic. The main theme of the study is to investigate role of human ribonucleases in host defense. Human ribonucleases of the RNase A family, and natural protein toxins targeting RNA or ribosomes are being analyzed for structure-function relationships to understand their molecular mechanism of action. Also, human ribonucleases, and ribosome inactivating proteins are being explored to design knowledge-based recombinant toxins.

The objectives of the project are (i) investigation of molecular mechanism of biological actions of human ribonucleases and their role in host defense, (ii) structure-function analysis of ribosome-inactivating proteins, (iii) construction and evaluation of recombinant toxins as potential therapeutics for cancer and (iv) investigation of involvement of ribonucleases and Clp proteases in pathogenic mechanism of Mycobacterium tuberculosis.

Investigation of molecular mechanism of biological actions of human ribonucleases and their role in host defense

Eosinophils, upon activation, degranulate and secrete an array of cytotoxic granule proteins which include ECP, MBP, and EDN. ECP is cytotoxic to host tissues and inhibits the growth of several cell lines *in vitro*. The mechanism of cytotoxicity of still remains unclear. ECP is a pyrimidine specific ribonuclease of RNase A superfamily. It is a highly basic protein with a large number of basic residues present on its surface. ECP possesses helminthotoxic, neurotoxic, cytotoxic, antibacterial and antiviral activities however only neurotoxic and antiviral activities have been attributed to its RNase activity. We investigated the involvement of basicity in the function of ECP. The unique basic residues of ECP, Arg22, Arg34, Arg61, Arg77, and His64 were mutated to alanine, individually and in various combinations to probe their involvement in various activities of ECP. In most of the mutants the structure of the protein was altered. Generally, there was no change in the RNase activity of ECP upon mutation of these basic residues, indicating that they were not directly involved in the catalytic acitivity of ECP. On J774A.1 cell line, a number of basic residue mutants of ECP were found to have much reduced cytotoxic activity implying that

basicity rather than the RNase activity is a major contributor towards the cytotoxicity of ECP.

ECP possesses antibacterial activity against both Gram positive and negative bacteria. We studied the effect of reducing the basic character of ECP on its antibacterial activity against *E. coli* and *B. subtilis*. The mutation of basic residues decreased the antibacterial activity of ECP against both *E. coli* and *B. subtilis*. Two catalytically inactive mutants of ECP had full antibacterial activity, whereas EDN and RNase A, which are more potent ribonucleases did not show any antibacterial activity. Therefore, basicity, and not the ribonuclease activity of ECP was found to be crucial for its antibacterial activity.

Despite strong *in vivo* an *in vitro* evidences that eosinophils are important effector cells in host defence against parasitic infections, relatively little is known about the eosinophil's potential activity against protozoon pathogens. We checked the effect of ECP on *Leishmania donovani* promastigotes and found it to possess a strong antiparasitic activity against *Leishmania donovani*. The antiparasitic activity was dose and time dependent. The potent ribonucleases EDN and RNase A were not found to be toxic to the promastigotes. The mutation of basic residues decreased the antiparasitic activity of ECP against *Leishmania donovani* promastigotes. Two catalytically inactive mutants of ECP had full antiparasitic activity. Therefore, as for the antibacterial activity, basicity and not the ribonuclease activity was found to be a crucial determinant for the antiparasitic activity of ECP as well.

ECP has been shown to introduce transmembrane non-ion selective channels in the cell membranes thereby destabilizing the lipid matrix. We have studied the effect of reducing the basic character of ECP on its membrane destabilizing activity by investigating hemolysis in human RBCs, and release of ^{15}Cr from labeled J774A.1. ECP was found to be very effective in causing hemolysis in human RBCs and ^{15}Cr release from J774A.1 cells, whereas more potent ribonucleases EDN and RNase A did not show this activity. Mutations of Arg22 and Arg34 individually and in combination with other basic residues abolished the hemolytic and ^{15}Cr release activities of ECP. Two catalytically inactive mutants of ECP had full membrane destabilizing activity. The study demonstrates that the membrane destabilizing activity of ECP depends on its basicity and is independent of the RNase activity. The biological activities of ECP namely cytotoxicity, antibacterial and antiparasitic activities appear to be a consequence of its membrane destabilization ability.

In order to identify the intracellular targets of ECP, proteome analysis of the cells treated with ECP was undertaken. A number of cell lines were screened for their sensitivity towards ECP cytotoxicity, and Jurkat and U373 found to be quite sensitive were chosen as target cells for further studies. These cells were incubated with toxic concentrations of the ECP and total cellular proteins were analyzed by 2D gel electrophoresis. Protein spots that were absent, decreased or increased as a result of treatment with ECP, as compared to the untreated cells, were identified by mass spectrometry. The levels of peptidyl prolyl isomerase, thioredoxin peroxidase, colfilin, actin, lactate dehydrogenase, fructose-bisphosphate aldolase, phoshphoglycerate kinase, α2-HS-glycoprotein precursor, tubulin, aldolase reductase, aminopeptidase B and heat shock 70kDa protein 9B were observed to be modulated after treatment with ECP.

Human pancreatic ribonuclease (HPR) is 500 times more active on dsRNA as compared to RNase A. This activity is retained even under conditions in which dsRNA maintains a stable

secondary structure. It has been proposed that an array of positively charged residues present around the active site enables HPR to destabilize the secondary structure of dsRNA, thereby facilitating dsRNA cleavage. Apart from basic residues, several studies on dsRNA cleavaing pancreatic RNases of primates have reported the importance of non-basic residues, Gln28, Gly38, Pro42, Asp83 and Ala122 for dsRNA cleavage. We have earlier shown Gly38 to be important for dsRNA cleavage activity of HPR. We are now investigating the role of Gln28 and Arg39 in the dsRNA cleavage activity of HPR. Gln28, Gly38 and Arg39 in HPR were mutated to alanine or to the corresponding residue present in RNase A individually and in combination. The activity of mutant proteins was analyzed by measuring steady state rate of cleavage of synthetic double-stranded polymer poly(A).poly(U). Gln28, Gly38 and Arg39 have been shown to be critical for the cleavage of dsRNA by HPR.

Investigation of involvement of ribonucleases and Clp proteases in pathogenic mechanism of M.tuberculosis

The Clp chaperones, ClpA, ClpB, ClpX and ClpY belong to the AAA^+ superfamily of proteins, which are ATPases involved in a variety of cellular activities. In *E.coli* the hexameric ClpA and ClpX ATPases interact with ClpP to form ClpAP and ClpXP proteases respectively. These proteases catalyse the unfolding and further degradation of specific proteins in an ATP-dependent manner. To understand the mechanism of action of *M.tuberculosis* Clp complex, we have cloned, over-expressed, purified and functionally characterized the *M.tuberculosis* ClpX. The recombinant *M.tuberculosis* ClpX showed an inherent ATPase activity. The ATPase activity was modulated by divalent metal ions, Zn^{++} was found to be most preferred metal ion. *M.tuberculosis* ClpX was found to trap unfolded model protein and prevented its refolding, however it did not prevent aggregation of lucifearse.

The mechanism of tRNA maturation is being investigated in *M.tuberculosis*. The protein and RNA components of the RNase P enzyme have been expressed and purified *in vitro* and a functional enzyme has been reconstituted. The RNA component of *M.tuberculosis* RNase P has been shown to process pre-tRNA-ala in the presence of high magnesium, whereas the holoenzyme is functional at low magnesium concentrations. A region in the RNA component has been identified to be crucial for the activity of *M.tuberculosis* RNase P.

Publications

Original peer-reviewed articles

1. Sikriwal D, Ghosh P and Batra JK (2008) Ribosome inactivating protein saporin induces apoptosis through mitochondrial cascade, independent of translation inhibition. *International Journal of Biochemistry and Cell Biology* **40**: 2880-2888.

2. Kar NP, Sikriwal D, Rath P, Choudhary RK and Batra JK (2008) *Mycobacterium tuberculosis* ClpC1: characterization and role of the N-terminal domain in its function. *FEBS Journal* **275**: 6149–6158.

3. Sikriwal D, Seth D and Batra JK (2009) Role of catalytic and non-catalytic subsite residues in ribonuclease activity of human eosinophil-derived neurotoxin. *Biological Chemistry* **390**: 225-234.

To develop strategies for making sensors and actuators for biological processes

Principal Investigator: Pramod K Upadhyay

Co-Investigators: Sangeeta Bhaskar
Amulya K Panda
Asok Mukhopadhyay

Project Associates/Fellows: Anita Mashta
S Tamilzhalagan

PhD Students: Puja Nagpal
Neha Joshai
Jashdeep Bhattacharjee

The theme of research is to develop systems for monitoring biological processes. The objectives are to (i) develop tools for needle free immunization (ii) study the biological processes like hybridization, differentiation etc. and to develop devices and sensors based on such studies.

Local hyperthermia enhanced immunization

Local hyperthermia around the skin is comparatively easy to generate and puts less strain on the recipient animal. Earlier using experimental animals, we have shown that mild local hyperthermia could be used for transdermal immunization. Comparable response was generated when mice were immunized with toxoid antigens by hyperthermia enhanced transdermal route or by conventional intra-muscular (im) injection. Here we analyze how the hyperthermia activate the dendritic cells (DCs) and how this activation affect their migration to transport the antigen from the site of transdermal immunization.

Activation of DCs

Activation of DCs after immunization play an important role in mounting a immunological response. It was of interest to study the effect of short duration mild hyperthermia on DCs. The DCs were generated *in vitro* from bone marrow (BM). These DCs were exposed to 42°C for 30 mins and were analyzed for the expression of MHCII, CD80, CD86 and CD 83 by flow cytometry. In the Table-1 given below, the expression levels of these activation markers is summarized.

Table 1: The expression of DC activation markers after mild hyperthermia.

	Percent Expression of			
	MHCII	CD80	CD86	CD83
Control	80.13	1.43	54.43	6.26
After 30 mins hyperthermia exposure	82.45	10.11	67.24	15.55

These data establish that 30 minutes exposure of mild hyperthermia is sufficient for the activation of BMDCs.

Migration of dendritic cells

The foremost sign of the activation of DCs is their enhanced migration capabilities. It was examined by BMDCs generated from the Fvb-GFP mice. The DCs were exposed to 42 ºC for 30 minutes. After necessary washing, 10^6 DCs were injected into the footpad of age and sex matched FvB/J mice. Draining popliteal as well as inguinal lymph nodes were removed after 24 and 48 hours and cells harvested from them were analyzed to determine the percentage of GFP (+ve) cells. Results are summarized in the Table-2.

Table-2: Percent of GFP+ve cells estimated in the lymph nodes after delivering 10^6 DCs.

	Percent of GFP+ve cells in popliteal and inguinal lymph nodes	
	After 24 hours	After 48 hours
Control (untreated BMDCs injected)	0.3	0.4
BMDCs injected after 30 mins mild hyperthermia exposure	3.7	13.7

The overwhelming migration capabilities of DCs lasting for more than 48 hours, which were exposed to mild hyperthermia for 30 minutes, is established by these data.

Kinetics of appearance of DC markers and antigen in draining lymph node

It is of considerable interest to study the migration of activated DCs after hyperthermia enhanced transdermal immunization. Animals were immunized with TT by local hyperthermia by placing the patch on right thigh. Draining (right) and non-draining (left) inguinal lymph nodes were removed after Day 1, 2 and 3 post immunization. Single cell suspension was prepared and samples were stained for the expression of MHC II, CD 80 and CD 11c and results are given below in Table-3.

Table 3: The kinetics of activation markers in the lymph node after mild hyperthermia

Lymph node	Percent expression of								
	MHCII			CD80			CD11c		
	After 1 day	After 2 days	After 3 days	After 1 day	After 2 days	After 3 days	After 1 day	After 2 days	After 3 days
Draining	38.04	24.05	21.59	77.52	42.02	11.11	77.70	54.92	12.99
Non-draining	27.97	30.73	32.83	11.32	10.45	10.50	16.76	85.78	15.38

These data show that the antigen presentation and DC marker peak around 24 hrs post immunization and reaches the basal level after 72 hrs.

Migration of epidermal dendritic cells out of the skin after local hyperthermia

The epidermal DCs upon encountering the antigen in periphery are known to undergo maturation and migrate out of skin to lymph node, where they present the antigens to T cells. This process usually takes around 48 hrs. Our data indicate that during local hyperthermia the kinetics of this process is accelerated and the DCs reach the lymph node within 24 hrs. To validate it further we compared the epidermis, 24 hrs post immunization, for presence of DCs in mice which received local hyperthermia with control mice. A marked decrease was observed in the expression of CD11c in the epidermal sections from mice which has received mild hyperthermia treatment compared to untreated mice.

These data demonstrate that when the toxoid antigen is delivered through the skin under local hyperthermia the whole process of antigen presentation is accelerated. No adjuvant is required for local hyperthermia enhanced immunization and activation of the immune system is achieved by the local hyperthermia.

Immunization by the aerogenic route

Pulmonary delivery of vaccines being a needle free immunization has an edge over parenteral administration. Pulmonary delivery involves liquid aerosolization, nebulization and dry powder inhalation. We have developed a dry powder formulation of a candidate vaccine, live *Mycobacterium w,* for the aerogenic delivery. The uniformity of particle size suitable to aerogenic delivery was achieved by milling the dry powder with an 'air jet cyclone'. The jet milled dry powder of *M.w* was delivered to the mice by the aerogenic route and the immunological response analyzed.

Two and four weeks after immunization, spleen of immunized mice was removed and T cells isolated. These T cells were stimulated with soluble *M.tb* antigen. After 48 hours, IFN-gamma was analyzed in the culture soup and proliferation of cells was estimated. Uniform and optimal size particles for inhalation are produced by the jet milling. These particles remain viable and generate a desirable immunological response.

DNA detection by q-dots labeled probes

By replacing the gold nano-particles by quantum dots the lower detection limit of the assay was reduced to 500pg of H37Rv DNA. In order to maintain higher specificity, the methodology of DNA capture by latex beads and quantum dots was refined by first melting the DNA test sample and to maintain it with both the probes at annealing temperature for binding. The results obtained by the PCR and Q-dot-latex test establish their parity, however the sensitivity of both the tests is low when compared with the 'gold standard' LJ culture.

A set of Förster Resonance Energy Transfer (FRET) based probes for the detection of *devR* DNA were designed. In these probes the quantum dot donor fluorophore is linked to a 20mer nucleotide. Separated by 10A, which is the Förster distance, the TAMRA acceptor fluorophore is liked to another nucleotide. These FRET probes are very simple to use but have poor sensitivity compared to the Q-dot-latex probes. The quantum dots and the latex beads both are polyvalent and in the presence of the target strand the aggregates of target stand, latex beads and quantum dots are quickly formed which ensure easy detection and enhanced sensitivity.

Publications

Original peer-reviewed articles

1. Gupta A, Geetha N, Mani J, Upadhyay P, Katoch VM, Natrajan M, Gupta UD and Bhaskar S (2009) Immunogenicity and protective efficacy of *Mycobacterium w* against *Mycobacterium tuberculosis* in mice immunized with live versus heat-killed *M.w* by the aerosol or parenteral route. *Infect Immun* **77**: 223-231.

Development of site-specific drug delivery systems

Principal Investigators: Sandip K Basu
Amitabha Mukhopadhyay

PhD Students: Namrata Ojha
Ruchir Rastogi

Collaborator: Chinmoy Mukhopadhyay, *JNU, New Delhi*

The programme aims at developing systems for intracellular delivery of drugs or pharmacologically active agents selectively to specific cell types by exploiting the efficiency of the process of receptor-mediated endocytosis. The objectives include (i) drug targeting for overcoming multidrug resistance in cancer chemotherapy, (ii) modulation of macrophage metabolism through the delivery of biological response modifiers and (iii) therapeutic strategies based on scavenger receptor-mediated delivery of antisense oligonucleotides.

Modulation of macrophage metabolism through the delivery of biological response modifiers

In the reporting year, efforts were made to identify the transcription factor activated IL-6 to upregulate the expression of specific Rab6. Initially, we identified mouse Rab5c (+51 to -999) 5′-flanking regulatory regions containing the promoter sequence from mouse genome database and amplified using appropriate primers. Subsequently, the amplified product of Rab5c was digested with appropriate restriction enzymes and was subsequently cloned into the promoter-less reporter vector (pGL3-basic). The chimeric Rab5 construct was transiently transfected to J774E cells and incubated with different concentrations of IL-6 to determine the expression of the heterologous reporter. Our results showed that transactivation of the Rab5 construct (Rab5 +51 to -999-Luc) was increased about 3.8 folds by treatment with 0.5 μg /ml of IL-6 over the control whereas no significant activation was detected with IL-12 treatment.

In order to identify the transcription factors activated by treatment with IL-6, J774E cells were treated with IL-6 for different time periods (1, 2 or 4 hours) at 37^{o}C. Western Blot analysis after IL-6 treatment resulted in time-dependent increase in the levels of C/EBP-β, with no change in the levels of c-Jun, phospho-c-Jun (ser 63), phospho-c-Jun (ser 73), c-fos, Ets1, Sp1, Stat3, Stat4, phospho-Stat4 or Stat6. These results indicated that IL-6 possible activates the C/EBP-β in macrophage to upregulate the expression of Rab6. To unequivocally prove the role of C/EBP in IL-6 mediated upregulation of Rab5 expression, we performed Electrophoretic Mobility Shift Assay (EMSA). A double stranded 24-nucleotide long region containing this specific C/EBP site was end-labeled with ^{32}P and purified, then radiolabeled probe was incubated with nuclear extracts isolated from IL-6 treated and untreated cells. A strong DNA binding activity was observed from IL-6 treated nuclear extract in compared to untreated cells further confirming this C/EBP site is involved in IL-6 mediated Rab5 expression. The specificity of the binding was tested with competitive EMSA, by adding 30x and 100x excess (in molar ratio) of non-labeled probe before the addition of radiolabeled probe. The result showed complete inhibition of the binding with 100x excess of the cold probe further confirming the role of C/EBP in IL-6 mediated upregulation of Rab5 expression.

However, bioinfomatics analysis of 5′-flanking region of Rab5 revealed the presence of two putative C/EBP sites at –727 and -96 nucleotides. Studies are in progress to determine which C/EBP site is predominantly involved in the regulation of Rab5 expression by IL-6 treatment.

Protease-catalyzed splicing of peptide bond

Principal Investigator: Rajendra P Roy

PhD Students: Sharmishtha Samantray
Uttara Marathe
Sayani Dasgupta
Kanchan Gupta
Tora Biswas

Collaborators: Vinay Nandicoori
Devinder Sehgal

We study the principles underlying peptide ligation reactions catalyzed by proteases and transpeptidases with a view to apply them to the semisynthesis of proteins and bio-conjugates. The amide bond forming specificity of bacterial transpeptidase (referred to as sortases) is being investigated to expand the synthetic ambit of sortases as well as to design inhibitors for this therapeutically important class of enzyme.

A. Peptide ligation reactions catalyzed by protease transpeptidase 'sortase'

The objective of the project is to carry out studies on structure and peptide ligation specificity of sortases.

We synthesized fluorescent Rev peptide and obtained fluorescent Rev-antibiotics conjugate through sortase-mediated reaction. For this, the Rev sequence was assembled on the solid phase resin. The fmoc protection was removed and an fmoc-aminohexanoic acid (AHA) moiety was coupled to the amino terminus using standard procedure. Subsequently, AHA derivatized peptide on the resin, after fmoc deprotection, was reacted with FITC. The fluorescent peptide was cleaved from the resin and purified by reverse-phase HPLC. The electrospray mass of the peptide was in accord with its calculated mass. Conjugates of fluorescent Rev peptide with neomycin were prepared by enzymatic ligation with sortase. Preliminary experiments indicated that both the peptide and conjugates entered the cells and were localized in the nucleus. The bio-efficacy studies are currently in progress.

Peptide dendrimers, linear peptides, cyclic peptides and peptide antibiotics conjugates were prepared comprising certain antibacterial peptides and aminoglycoside antibiotics using sortase catalyzed reaction. The antibacterial activity of these novel molecules were evaluated against E coli and *S. aureus*. Some of these molecules have shown good antibacterial activities. The results offer possibilities of generating enhanced activity through further sequence modifications.

B. Studies on sortases from *Streptococcus pneumoniae*

Detailed studies on S. pneumoniae R6 sortase was carried out as a prelude to assess its utility as a catalyst in synthetic peptide chemistry as well as to develop inhibitors for this enzyme. As reported earlier, the protein was expressed with a His-tag at the C-terminus and purified by Ni-NTA chromatography. The protein eluted from Ni-NTA column was

enzymatically active but yielded two bands on SDS-PAGE. Reverse-phase HPLC, Mass spectrometric analyses and Edman degradation of the protein samples established that the sample eluted from Ni-NTA column contained two species; desired cloned sequence and a truncated version starting from residue Met92. Mutational analyses of the protein involving residues Thr91-Met92 was carried out to see if the generation of truncated protein was a result of proteolytic degradation. Interestingly, a single homogeneous band corresponding to the full-length sequence could be obtained only with mutation of Met92 alone or in combination with Thr91 suggesting less likelihood of a protease-mediated generation of the truncated fragment. The presence of a Met residue at the start of the truncated protein sequence prompted us to examine the gene sequence. Interestingly, the gene sequence revealed the presence of a bonafide Shine-Dalgarno sequence which could have lead to the independent translation of the truncated protein. This interpretation also appears consistent with the mutation data.

R6 sortase was found to be quite different from the prototype sortase A of S. aureus with respect to its substrate specificity, enzyme kinetics and activation by calcium ion. The presence of optimum amount of calcium ions is known to cause about 8-fold enhancement in enzyme activity of S. aureus sortase A. In contrast, the R6 enzyme activity is not affected by the presence of calcium ions. The R6 enzyme prefered Ala as nucleophile in transpeptidation reaction as opposed to Gly residues for S aureus enzyme. Comparative kinetic analyses showed that catalytic efficiency for AAKY for R6 sortase was about 13 fold higher in comparison to GGGKY. This result is consistent with the fact that pneumococcal cell wall has Ala-Ala cross-bridges while Gly-Gly cross-bridges are present in S. aureus. Further, R6 SrtA was found to transfer LPXTG peptides with X=M or N but not E indicating somewhat stringent specificity for LPXTG peptides. The R6 sortase was able to transfer LPXTG peptides to tobramycin but not to 6-amino-6-deoxy mannose.

C. Design and synthesis of sortase inhibitors

Covalent as well as non-covalent inhibitors of sortase were designed and synthesized based on the LPXTG sequence motif recognized by S aureus sortase. Several variations of this pentapeptide sequence with natural, nonstandard and non-peptidic bond functionalities with or without a moiety capable of reacting with active site Cys were generated. The ability of these compounds to inhibit the hydrolysis or transpeptidation was assessed by a FRET-based or HPLC assay.

Publications

Original peer-reviewed articles

1. Chopra T, Banerjee S, Gupta S, Yadav G, Anand S, Surolia A, Roy RP, Mohanty D and Gokhale S (2008) Novel intermolecular iterative mechanism for biosynthesis of mycoketide catalyzed by a bimodular polyketide synthase. *PLoS Biol* **6**: e163.

Structural studies on proteins, dynamics and ligand interactions using NMR

Principal Investigator: Monica Sundd

PhD Students: Arshdeep Sidhu

Proteins are macromolecules that play a central role in nearly every biological process *viz.* enzyme catalysis, bodily movement, defense against foreign antigens etc. Their function is dictated by their 3-dimensional structure. Therefore, the biological function of a protein can be best understood from its atomic resolution structure. A range of biophysical techniques are available, that offer a window into the structure of proteins. Nuclear magnetic resonance (NMR) spectroscopy is one such technique that enables structure determination of macromolecules at atomic resolution, as well as study their interactions with binding partners. We are employing this technique to understand the structure of some important proteins in the cell, for which no structural information is available. B-cell linker protein is one such protein that has been associated with conditions like agammaglobulinemia, malignancy, lymphomas etc. It is an important adaptor protein in B-cell signalling pathway, with very little structural information available and the mechanism by which it orchestrates the formation of a signalosome is still an enigma. The theme of this project is to understand the structural organisation of this adaptor protein and understand the molecular basis of its interaction with other binding partners using NMR as a primary tool. The knowledge gained from this study will allow us to understand how a signalosome is organized in a three dimensional space and relate 'what a signalosome is, to what it does'.

The theme of research is to understand the structure of B cell linker protein (BLNK) and the signalosome it orchestrates with Bruotons tyrosine kinase (Btk), Phospholipase C gamma 2 (PLC-γ2), Spleen tyrosine kinase (Syk) etc. in the B cell, using NMR and other biophysical studies.

The objectives of the project are (i) to clone, express, purify and structurally characterize the domains of BLNK by NMR and (ii) its naturally occurring partners in the B cell and thereby study their interactions. We also plan to study some key interactions *in vivo* as well using DT40 cell lines.

Cloning, purification and chemical shift assignments of the SH2 domain of BLNK

In the past one year, we have been able to express the SH2 domain in minimal media and successfully removed the His tag using immobilized thrombin. Immobilized thrombin is removed by centrifugation. With the His tag, the protein seemed to aggregate over time. Three dimensional NMR experiments that are necessary for chemical shift assignments have been acquired. We are in the process of assigning the chemical shifts of this domain. We have also carried out stability studies on this domain as a function of pH and denaturants using biophysical techniques like circular dichroism and fluorescence. The domain is stable upto 2.5 M urea, 1.25 M GuHCl and pH 4.0. These studies are important from the perspective of the usability of a protein sample inside the NMR tube.

Cloning, purification and biophysical studies on the proline rich region of BLNK

We have expressed the proline rich region of BLNK in minimal media ($^{15}N^{13}C$-rich) and removed His tag using thrombin. The protein is highly soluble at high concentrations. In NMR, the sample did not give a good dispersion as expected. A range of temperatures, and pH were tested to get a better dispersion. We used circular dichroism to further characterize the domain, and it seems to have a poly proline helix structure. Results suggest that the domain belongs to a class of natively unfolded proteins. These proteins are natively unstructured, however they assume a folded structure only in the presence of their binding partners. Given the fact that NMR is an excellent tool to study natively unstructured proteins, we will employ this technique to get structural information on this domain, both with and without binding partners

Cloning and purification of the N-terminal region

The N-terminal region of BLNK has been cloned and expressed, and the domain is soluble. The purification of this domain is being standardized. Once the protein is pure, structure determination of this region using NMR will be carried out. Biochemically, this region has been shown to contain a leucine zipper which is important for the membrane localization of BLNK. However, there is no structural information available. The presence of a leucine zipper will be confirmed by structure determination as well as titration with DMPC micelles.

Chemical Glycobiology: Glycoproteomics and carbohydrate-based drug design

Principal Investigator: Srinivasa-Gopalan Sampathkumar

Project Associates/Fellows: Deepshikha Singh

PhD Students: Kavita Agarwal

The theme of research is to focus, broadly, on the application of powerful chemical tools to study and understand the fundamental roles of glycoconjugates in cellular physiology and disease. Past decade has seen a growing realization of important roles played by spatio-temporal changes in glycosylation in cell signaling, immunity, inflammation, disease, development, and homeostasis. In comparison to advances in genomics and proteomics, progress in the study of glycomics has been challenging owing to its non-template driven nature and lack of sophisticated tools. The objectives of the project are (i) to develop and apply metabolic oligosaccharide engineering (MOE) methods for study of glycoproteomics and glycobiology, (ii) design and synthesis of carbohydrate-based glycopeptidomimetic (GPM) small molecules as anti-metastatic agents and (iii) development of hybrid molecules for delivery of carbohydrate-analogs across the blood brain barrier (BBB) with a goal to develop an integrated program for chemical glycobiology from design and synthesis to biochemical and *in vitro* studies.

A. Design and synthesis of glycopeptidomimetics (GPM) as inhibitors of matrix metalloproteinases (MMP)

Matrix metalloproteinases (MMP) are a family of zinc-dependent endopeptidases that participate in key developmental processes such as tissue remodelling during development and release of signaling and growth factors. However, under pathological conditions the MMPs are over-expressed leading to degradation of extracellular matrix (ECM) resulting in cancer metastasis and arthritis. Of the ~25 MMPs reported, majority of them are secreted as zymogens while six of them are found to be anchored to the plasma membrane. In cancer metastasis it is known that degradation of collagen IV, a major constituent of basement membranes, by MMPs lead to intravasation of primary tumor cells to blood and lymphatic streams.

Inhibitors of MMP (MMPi) have been developed based on the structure of MMP-substrates (collagen) and site-specific cleavage by MMPs using various peptidomimetic approaches. In general peptides or pseudo-peptides, containing a zinc binding group (ZBG) (hydroxamate, thiol and carboxylic acid groups) and incorporating sub-site binding hydrophobic groups complementary to enzyme active site, were found to inhibit MMPs and reduce metastasis *in vitro* and *in vivo*. Intense research efforts over the past three decades by both academia and industry have lead to several promising MMPi candidates at the pre-clinical level. However, the results of recent clinical trials have proven to be disappointing mainly due to non-selective broad-spectrum activity of the MMPi and undesirable side effects. Efforts are underway to rejuvenate development of MMPi, in the post-trial era, as anti-metastatic agents exploiting the differences in active site geometries for differential and selective MMP inhibition. In this context, we intend to utilize glycopeptidomimetic

based ZBG containing small molecules as a new paradigm in the design of MMPi as anti-metastatic agents.

Unlike the peptidomimetics wherein ZBG is usually present on the same axis as the peptide backbone, our design presents the ZBG on the carbohydrate moiety which is perpendicular to the peptide backbone. This unique design we believe would be able to simultaneously achieve efficient chelation to the active site zinc ion as well as selective binding to the subsites / exosites of the enzyme. Towards this end we have designed hydroxamate containing glycopeptidomimetics based on marimastat – one of the most successful candidates in clinical trials – retaining the essential groups based on its structure-activity relationships (SAR). The *tert*-leucine moiety of marimastat has been replaced with L-serine to provide a handle for the attachment of various ZBG-containing glycan moieties.

Based on a convergent retro synthetic analysis the essential peptide and carbohydrate derivatives are currently being synthesized in our laboratory. We have synthesized the glycosyl donor, methyl 2,3,4-tri-*O*-acetyl-1-bromo-1-deoxy-α-D-glucuronate, in three steps starting from D-glucuronolactone. On the peptide counterpart, we have synthesized orthogonally protected serine derivatives as acceptor. Various *N*-protection groups such as Boc-Ser, Fmoc-Ser, and Ethoxycarbonyl-Ser have been synthesized.

B. Study of glycoproteomics using metabolic oligosaccharide engineering (MOE) methodology

Mammalian cells are covered by a dense layer of carbohydrates known as the 'glycocalyx' which actively participate in and regulate biological processes. Glycoconjugates, which express glycans, are commonly found in the form of glycoproteins, glycolipids, glycosaminoglycans, and glycosylphosphatidyl inositol anchors (GPI). Sialic acids, a family of nine-carbon containing acidic monosaccharides, is usually expressed at the non-reducing termini of glycans and is known to play key roles in cell-cell, cell-matrix, and cell-pathogen interactions. Sialic acids, also known as neuraminic acids, are biosynthesized starting from UDP-GlcNAc *via* *N*-acetyl-D-mannosamine (ManNAc), as a committed precursor. The metabolic oligosaccharide engineering (MOE) methodology exploits the promiscuity of sialic acid biosynthetic pathway to engineer non-natural moieties on the cell surface glycans using exogenously supplied non-natural *N*-acyl modified analogs of ManNAc. Using MOE various non-natural groups such as extended hydrocarbon chains, ketone, azide, hydroxyl, and thiol, have been expressed at the *N*-acyl position of cell surface sialic acids.

Particularly incubation of mammalian cells with Ac_5ManNTGc, an efficient precursor for the intracellular generation of ManNTGc, has been shown to result in ~10-fold increase in the expression of global cell surface thiols (CST), as a combination of protein-thiols (PSH) and carbohydrate-thiols (CSH), on glycans in the form of *N*-thioglycolyl-neuraminic acid (NeuTGc) (ref: Sampathkumar, S.-G., *et al*. (2006) *Nat. Chem. Biol.* **2**, 149-152). Whereas, incubation with a corresponding ManNGc precursor, Ac_5ManNGc did not alter CST levels (PSH only). In order to gain further insight into selectivity and efficiency of thiol-engineering of glycoconjugates we have currently undertaken a glycoproteomics study of MOE.

Upon incubation of mammalian cells with Ac_5ManNTGc, although thiol levels increase globally, the efficiency and selectivity of the biosynthetic expression are unclear. It is not

known if there is any selective or preferential expression of NeuTGc among (a) glycoproteins *vs.* glycolipids, (b) *N*-glycans *vs. O*-glycans, (c) aglycon preference, and (d) linkage preference. In order to identify specific candidate glycoproteins that selectively express NeuTGc a glycoproteomics study is undertaken. Herein, Jurkat (human T-cell lymphoma) cells were incubated with either ethanol (delivery vehicle), Ac_5ManNGc (glycolyl control) or Ac_5ManNTGc (thioglycolyl precursor) to allow for biosynthesis and CST expression. After two days, the accessible CSTs were labelled with maleimide-PEO_2-biotin, lysed, and analysed by SDS-PAGE. The global protein bands were detected using silver staining protocol. Biotinylation was detected using far-western blotting using horse radish peroxidise (HRP) – conjugated avidin followed by enhanced chemiluminescence. At equal protein loading the Ac_5ManNTGc treated cell lysates clearly showed a large increase in biotinylation, consistent with flow cytometry results.

C. Design and synthesis of carbohydrate-neurotransmitter (CH-NT) hybrid molecules as tools for crossing blood-brain-barrier (BBB)

The advances in development of tools for study of glycomics in the past decade have greatly enabled elucidation of the role of glycoconjugates in development and growth. Sialoglycoconjugates are critically important in development of central nervous system (CNS) including brain, which is known to be rich in gangliosides and polysialic acids. Aberrant glycoform expression is known to result in neurodegenerative and psychological disorders and cancer. Sialic acid, either in its free form or as secreted glycoconjugates, in cerebrospinal fluid (CSF) is considered as a bio-marker for neurological diseases. The ability to apply MOE methodology described above will open up new possibilities for the diagnosis and treatment of CNS diseases.

Studies by Reutter and Bertozzi have already shown MOE to be effective *in vivo* in animal studies using ManNProp and ManNAz respectively. Efficient incorporation and expression of SiaProp and SiaAz were observed in peripheral organs but not in brain. This could arise due to either a fortified biosynthetic pathway that is restrictive for non-natural intermediates or the inability of non-natural ManNAc analog precursors to efficiently cross the BBB. In this context, we intend to create CH-NT hybrid molecules of non-natural ManNAc analogs coupled with neurotransmitters that are known to cross BBB with ease. Towards this end we have made several selectively protected carbohydrate intermediates that are suitable for conjugation to neurotransmitters *via* bi-functional linkers.

Publications

Original peer-reviewed articles

1. Campbell CT, Aich U, Weier CA, Wang JJ, Choi SS, Wen MM, Maisel K, Sampathkumar SG and Yarema KJ (2008) Targeting pro-invasive oncogenes with short chain fatty acid-hexosamine analogues inhibits the mobility of metastatic MDA-MB-231 breast cancer cells. *J Med Chem* **51**: 8135-8147.

GENE REGULATION

GENE REGULATION

Signaling events in *Mycobacterium tuberculosis* and their host macrophages

Principal Investigator: Vinay K Nandicoori

Project Associates/Fellows: Amit Parikh
Kasturi Goswami
Anshuk Sarkar
Sathya Narayanan

PhD Students: Divya Tiwari
Shazia Khan
Kalpana Rajanala
Sandeep Upadhyay

Collaborators: Balaji Prakash, *IIT, Kanpur*
Rajendra P. Roy
Yogender Singh, *IGIB, Delhi*

Cell-signaling is a process by which environmental signals are transmitted to cells, ultimately resulting in changes in gene expression and activity. One of the major mechanisms by which this takes place is by the reversible phosphorylation of cellular proteins. We are interested in investigating signalling events in the MAP kinase pathways of host macrophages after *M. tuberculosis* infection, as well as signalling by *M. tuberculosis* serine/threonine protein kinases (STPKs) in the host and in the pathogen, and their role in the pathogen's survival in the host. In addition, we are also interested in deciphering the role of phosphorylation in the function of nucleoporins.

Analysis of the *M.tuberculosis* genome sequence suggested presence of 11 putative eukaryotic-like serine/threonine protein kinases. Overexpressing of PknA in *M.tuberculosis* results in a deviation from normal cell morphology with the cells forming an elongated and branched structure, while overexpression of PknB in *M.tuberculosis* results in the formation of widened and bulging cells. Protein kinase G (PknG) has been shown to play a role in the survival of the pathogen in host macrophages by modulating phagosome-lysosome fusion (lysosomal transfer) after macrophages phagocytose mycobacterium, and PknG kinase activity is essential for mediating its effect on lysosomal transfer. We are interested in carrying out extensive biochemical and functional characterization of these STPKs. We propose to identify and characterize direct substrates in *M.tuberculosis* and in the host macrophages. We are also interested in deciphering the role of phosphorylation in the function of nucleoporins Tpr and Nup153.

I. M.tuberculosis serine/threonine protein kinase

Analysis of the *M.tuberculosis* genome sequence suggests the presence of 11 eukaryotic-like serine/threonine protein kinases, two tyrosine protein phosphatases and one serine/threonine protein phosphatase. While much work remains to be done towards understanding the role of the STPKs in *M.tuberculosis* biology, recent reports have established the role of these kinases in modulating cell shape and morphology, glucose transport, glutamine transport, glutamate metabolism and regulation of the expression/activity of transcription factors.

The N-terminal region of protein kinase G from M. tuberculosis plays a regulatory role in modulating kinase activity and survival in the host macrophages.

Protein kinase G (PknG) is closely related to the mammalian protein kinase Cα. This 82 kDa protein has a Trx domain at the N-terminus, a central kinase domain and a carboxy terminal TPR motif. We have used GarA as an *in vitro* substrate of PknG and used GarA phosphorylation as readout of PknG activity to decipher the regulatory roles of various domains of PknG in modulating its activity. We found that the kinase domain of PknG by itself is inactive, signifying the importance of the flanking domains. While the deletion of the N-terminal Trx domain severely impacts the protein's activity, the C- terminal region also appears to contribute in regulating the activity of the kinase. The Trx fold, a structural motif consisting of a four stranded beta sheet and three flanking alpha helices has been implicated in regulating various functions including iron/cadmium binding, maintaining the protein in folded state and in sensing the redox state of the environment. Though the sequence similarity between various proteins that contain this fold is minimal, they are present in most redox proteins. The Trx fold in the PknG was suggested to be a characteristic ruberedoxin domain involved in iron binding. Results suggested that the role of Trx fold in PknG is not that of iron binding. PknG kinase activity is sensitive to the redox environment and mutating conserved cysteines in the to alanines results in abrogation of this response. Furthermore, results revealed T63 to be the major phosphorylation site in the N-terminal region. Though PknG phosphorylates various residues in the N-terminal region *in vitro*, metabolic labelling experiments with *M. smegmatis* expressing various PknG constructs have unambiguously revealed that T63 is the only phosphorylation site *in vivo*. Interestingly, we observed *in vivo* phosphorylation of kinase inactive PknG (PknG-K181M) as well, suggesting phosphorylation of PknG by other serine/threonine kinase(s). The role of an active form of PknG in the persistence of *M. bovis* BCG in macrophages by evasion of lysosomal fusion has been well documented. Our study presents data indicating the importance of the first 73 amino acids in PknG- mediated evasion of the lysosomal transfer of the mycobacteria. Most importantly, our results demonstrated the essential role of threonine 63 residue, the only *in vivo* phosphorylation site of PknG, in modulating the survival of the microbe in its host. Future investigations will be aimed at understanding the PknG signalling cascade and determine the role played by other STPKs in modulating PknG mediated survival of mycobacteria in the host.

The *Mycobacterium tuberculosis* protein kinase K modulates activation of transcription from the promoter of mymA operon through phosphorylation of the transcriptional regulator VirS.

Considering the important functions carried out by the characterized protein kinases, we decided to study the hitherto uninvestigated protein kinase PknK. PknK is a large protein (1100 amino acids). While the N-terminal 290 amino acids are homologous to eukaryotic-like serine/threonine kinase domains, the carboxy-terminal residues show homology with the regulatory region of *Escherichia coli* transcription regulator MalT. The PknK contains an ATP/GTP binding site (P-loop) and a putative PDZ domain between amino acids residues 368-375 and 465-533, respectively. We have cloned, overexpressed and purified protein kinase K (PknK) to near homogeneity and showed that its ability to phosphorylate proteins is dependent on the invariant lysine (K55), and on two conserved threonine residues present in its activation loop. In spite of being

devoid of any apparent trans-membrane domain, PknK is localized to the cell wall fraction, suggesting probable anchoring of the kinase to the cell membrane region. The *pknK* gene is located in the vicinity of the *virS* gene, which is known to regulate the expression of the mycobacterial monooxygenase (*mymA)* operon. The *mymA* operon, located divergently from the *virS* gene, is named after the first gene in the operon, *mym* (**My**cobacterial **m**onooxygenase), that is important for maintaining the integrity of the *M.tuberculosis* cell wall. The *mymA* operon encodes for seven cistrons, that produce proteins proposed to be involved in the biosynthesis of mycolic acids. We report for the first time that VirS is in fact a substrate of PknK. In addition, four of the proteins encoded by *mymA* operon are also found to be substrates of PknK. Results showed that VirS is a *bona fide* substrate of PknK *in vivo* and PknK-mediated phosphorylation of VirS increases its affinity for *mym* promoter DNA. Reporter assays revealed that PknK modulates VirS mediated stimulation of transcription from the *mym* promoter. These findings suggest that the expression of *mymA* operon genes is regulated through PknK mediated phosphorylation of VirS.

PknB mediated Phosphorylation of a novel substrate, N-acetylglucosamine-1-phosphate Uridyltransferase (GlmU), modulates its Acetyltransferase Activity

Previously, we showed that the enzyme N-acetylglucosamine-1-phosphate uridyltransferase (GlmU) of *M.tuberculosis* is a novel substrate of PknB and is phosphorylated on threonine residues. GlmU carries out two important biochemical activities: a C-terminal domain catalyses the transfer of acetyl group from acetyl coenzyme A (acetyl-CoA) to glucosamine-1-phosphate (GlcN-1-P) to produce N-acetylglucosamine-1-phosphate (GlcNAc-1-P), which is converted to UDP-N-acetylglucosamine (UDP-GlcNAc) by the transfer of UMP (from UTP), a reaction catalyzed by the N-terminal domain. GlmU, a bifunctional enzyme, produces UDP-GlcNAc, a crucial precursor for peptidoglycan synthesis. In collaboration with Dr. Prakash's group at IIT, Kanpur, we determined the crystal structures of GlmU in the Apo and UDP-GlcNAc bound form and analyzed them to identify threonine residues that may be accessible to PknB. The structure shows a two-domain architecture, with a N-terminal domain having an α/β like fold and a C-terminal domain that forms a left-handed parallel β-helix structure (LβH). Kinase assays with PknB using the N and C-terminal domains of GlmU as substrates illustrated that PknB phosphorylates GlmU in the C-terminal domain. Furthermore, mutational studies revealed one of the five threonines present in the region 414-439 to be phosphorylated by PknB. Interestingly, the site of phosphorylation resides in the region 414-439 that has 5 threonine residues 414, 418, 425, 432 and 436 and of these, only Thr 425 is exposed to the solvent. The other threonines are buried and make contacts to either stabilize the LβH structure of the C-terminal domain or are involved in trimerization. Structural and biochemical analyses showed the significance of a variable C-terminal tail in regulating acetyltransferase activity. Taken together, this perhaps indicates a relationship between the phosphorylation site(s) and the C-terminal extension. Assuming *in vivo* phosphorylation also occurs between 414-439, this region is in proximity to the C-terminal extension of a neighboring molecule in the biological trimer to favor the aforesaid association. Further experiments are underway to address these possibilities and the affects rendered due to PknB phosphorylation. Notably, we demonstrated that while PknB mediated phosphorylation of GlmU does not affect its uridyltransferase activity, but it modulates the acetyltransferase activity. These findings imply a role for PknB in regulating peptidoglycan synthesis by modulating the acetyltransferase activity of GlmU.

II. Deciphering the role of signaling in modulating the function of nucleoporins

Nucleocytoplasmic transport between the nucleus and the cytoplasm occurs through nuclear pore complexes (NPC), ~ 60 MDa macromolecular structures that span from cytoplasm to nucleus across the lipid bilayers of the nuclear envelope. Though phosphorylation of nuclear transport proteins was shown by various groups, the precise roles of these phosphorylations in the nuclear pore function have not been elucidated. We are interested in addressing the role of phosphorylation in the function of nucleoporins Tpr and Nup153 and their dynamics. Previously, we have identified a nuclear pore complex protein Tpr (translocated promoter region) to be a novel substrates for the MAP Kinase ERK2 (Extracellular signal Regulated Kinase2). Tpr localizes to the nuclear basket of the nuclear pore complex (NPC) and is also found in the nucleus in the form of discrete foci. The functions of Tpr are poorly understood, but several lines of evidence indicate that it is involved in the process of nuclear export. We have shown that Tpr is a direct substrate for ERK2 in cell lysates and *in vitro.* The sites of *in vitro* phosphorylation by MAP Kinase are identical to a sub-set of *in vivo* phosphorylation sites, and these specific phosphorylations disappeared after blockade of the MAP Kinase ERK2 pathway. We also showed that ERK2 binds to Tpr and have identified both the docking domains on Tpr and the complementary domain on ERK2. ERK2 phosphorylation and dimerization are necessary for ERK2-Tpr binding. Surprisingly, the DEF domain and the phosphorylation sites display positive cooperativety to promote ERK2 binding to Tpr, in contrast to substrates where phosphorylation reduces binding. Ectopic expression or depletion of Tpr resulted in decreased movement of activated ERK2 from cytoplasm to nucleus, implicating a role for Tpr in ERK2 translocation. Our data provided direct evidence that a component of the nuclear pore complex is a *bona fide* substrate of ERK2 *in vivo,* and that activated ERK2 stably associates with this substrate after phosphorylation where it could play a continuing role in nuclear pore function.

III. Monofunctional and bifunctional Rel proteins

This project is a collaborative effort with Dr. Balaji Prakash, IIT Kanpur. Prokaryotes have evolved a plethora of cellular regulatory mechanisms to combat the adverse environmental conditions among which stringent response is most well characterized. The hallmark of stringent response is the accumulation of an effector molecule (p)ppGpp. These molecules are responsible for the rapid shut down of stable RNA biosynthesis and up-regulation of specific genes involved in amino acid biosynthesis under stress conditions. Also, the importance of (p)ppGpp arises due to several roles that it plays in pathogenic bacteria like *M. tuberculosis*. Synthesis and hydrolysis of (p)ppGpp are carried out by two distinct domains in the N-terminal region of the Rel family of proteins, that are divided into a bifunctional class (that synthesize and hydrolyse) and a monofunctional class (that can only synthesize. This difference arises due to the absence of a well conserved HDxxED motif required for (p)ppGpp hydrolysis in the monofunctional enzymes. Although the N-terminal (1-395) region of these proteins is sufficient to catalyze synthesis and hydrolysis reactions, the C-terminal domain ensures regulation of these antagonistic activities. Given the critical role that Rel proteins play, it is important to understand the mechanism of (p)ppGpp metabolism. While these proteins require Mg^{2+} for (p)ppGpp synthesis, high Mg^{2+} was shown to inhibit this reaction in bifunctional Rel proteins from *M. tuberculosis* and *S. equisimilis*. Surprisingly, in contrast to bifunctional Rel, we did not find inhibition of pppGpp synthesis at higher

Mg^{2+} in the monofunctional RelA from *E.coli.* Results showed that a charge reversal in a conserved motif in the synthesis domains explains this contrast; an RxKD motif in the bifunctional proteins is reversed to an ExDD motif. The differential response of these proteins to Mg^{2+} could also be noticed in fluorescent nucleotide binding and circular dichroism experiments. In mutants where the motifs were reversed, the differential effect could also be reversed. Based on the results, we inferred that although a catalytic Mg^{2+} is common to both bifunctional and monofunctional proteins, the latter would utilize an additional metal binding site formed by ExDD. In addition, we showed that these motifs also determine substrate specificities (GTP/GDP), co-operativity and regulation of catalytic activities at the N-terminal region through the C-terminal region. Most importantly, a mutant bifunctional Rel, carrying an ExDD, instigates a novel catalytic reaction resulting in the synthesis of pGpp, by an independent hydrolysis of the 5'P_{α}-O-P_{β} bond of GTP/GDP or (p)ppGpp. Further experiments with RelA from E.coli wherein ExDD is naturally present, also revealed the presence of pGpp, albeit at low levels. This work brings out the biological significance of RxKD/ExDD motif conservation in Rel proteins and reveals an additional catalytic activity for the monofunctional proteins, prompting an extensive investigation for the possible existence and role of pGpp in the biological system.

Publications

Original peer-reviewed articles

1. Parikh A, Verma SK, Khan S, *Prakash B and *Nandicoori VK (2009) PknB-mediated phosphorylation of novel substrate, N-acetylglucosamine-1-phosphate uridyltransferase, modulates its acetyltransferase activity. *J Mol Biol* **386**: 451-464. (*corresponding authors)

2. Vomastek T, Iwanicki MP, Burack WR, Tiwari D, Kumar D, Parsons JT, *Weber MJ and *Nandicoori VK (2008) ERK2 phosphorylation sites and docking domain on the nuclear pore complex protein Tpr cooperatively regulates ERK2-Tpr interaction. *Mol Cell Biol* **22**: 6954-6966. (*corresponding authors)

Molecular biology of infectious diseases

Principal Investigator: Lalit C Garg

Project Associates/Fellows: Sindhu KV

Soumya Pati
Sachin Deshmukh
Gagan Chhabra
Himani Kaushik

PhD Students: Avishek Anant
Shweta Chatrath
Vineet Gupta

Theme of research

Infectious diseases rank among the leading causes of death of both humans and animals in global surveys. Vaccination against infectious agents continues to be one of the most effective methods of limiting the cost of management of many infectious diseases. The goal of this study is to clone and express genes of biomedical importance with an emphasis on the development of vaccines against pathogens and to unravel the molecular mechanisms of infectious diseases to explore new drug targets.

A. Development of recombinant ε-toxin and DNA based vaccine against *Clostridium perfringens:*

Gram positive *Clostridium perfringens* is a major cause of human and veterinary enteric disease largely because this bacterium can produce several toxins when present inside the gastrointestinal tract. Epsilon toxin (etx), produced by *C.perfringens* types B and D, is the key antigen implicated in the enterotoxaemia or Pulpy kidney disease of domestic animals. It is the third most lethal of all clostridial toxins and hence is considered a major potential bioterrorism agent. Also, being the most common causes of cattle mortality, it is of great economic importance. The project aims at cloning and expression of ε-toxin from *C.perfringens* type D for the development of recombinant and DNA vaccine against *C.perfringens.* Further, by site directed mutagenesis we aim to study the role of various residues within the gene for its toxicity and immunogenicity.

The recombinant etx mutant proteins were produced in large amounts. Immunization of BALB/C mice with the recombinant etx mutants initiated last year, was completed. The mice were given two booster doses at two week intervals with the same dose of antigen emulsified in 1% alum. Sera collected from immunized mice were analyzed by Western blotting and ELISA for the specificity and titer determination. All the recombinant mutants were found to be highly immunogenic and gave antibody titers comparable with that obtained by immunization with the wild type etx. Subsequently, the anti-serum was tested for their neutralization ability using *in vitro* toxicity assay employing MDCK cells. The anti-serum raised against all the seven mutants was capable of neutralizing the toxic effect of the recombinant wild type etx, as determined by cell viability assay using MDCK cells.

Antiserum raised by immunization with pDisplay vector expressing membrane anchored etx protein was tested for its neutralization ability using MDCK cells. It was noted that the immunization with the DNA vaccine construct of etx in pDisplay vector resulted in the generation of protective immune response as the antisera exhibited good neutralization ability of the toxic effects of the recombinant etx in *in vitro* cytotoxicity assay using MDCK cells. Further, T cell proliferation assay was carried out using splentocytes isolated from the mice immunized with pDisplay.etx DNA construct alone and prime boosted with etx. The results indicated that the DNA immunization was able to generate good T cell response.

Further, DNA constructs were made that targeted the expression of the etx as a cytosolic and secretory protein. Immunization with these constructs was also carried out and the antisera was tested for its ability to recognize recombinant etx by Western blotting. The antisera was able to detect the recombinant etx in immunoblot analysis. An increase in the antibody titer was observed with post-immunization time.

B. Studies on the enzymes of metabolic pathways of *M.tuberculosis*

Recent years have seen an increase in incidence of tuberculosis in both developing and industrialized countries, and there is an immediate need to search for new molecules that can be used as future drug target(s). One of the strategies for developing new drugs to control microbial pathogens is to utilize differences in the metabolism of the pathogenic and host organisms. *In vivo* growth studies of the organism have indicated that up to 70% of glucose metabolizes through the EMP pathway. Thus, glycolysis is central to the organism's survival and targeting the glycolytic enzymes as potential drug targets to control *M.tuberculosis* may be feasible. Enzymes of other metabolic pathways could be equally important for the survival of the organism and hence important drug targets.

The branched-chain amino acid biosynthetic pathway, for the synthesis of leucine, isoleucine and valine, is essential for the growth and virulence of *Mycobacterium tuberculosis,* the causative agent of tuberculosis. The absence of this pathway in humans, and its essentiality in *M.tuberculosis*, make the enzymes of this pathway attractive target for the development of antituberculosis drugs.

The objectives of the project are to clone, express and characterize the enzymes of metabolic pathways of *M.tuberculosis*. Biochemical characterization of the recombinant enzymes will be carried out in order to identify the differences and similarities between *M.tb* and human, which can be exploited for designing new selective inhibitors specific to *M.tuberculosis* enzymes. Further, large amounts of recombinant proteins will be produced in order to carry out structural studies. This will help in defining the 3-dimensional structure of the enzymes ultimately leading to the rational development of new therapeutic interventions. We also plan to study the effect of site-directed mutagenesis of the crucial residues on the enzyme activity.

Large scale purification and refolding of the recombinant PGM of *M. tuberculosis H37Rv* has been carried out for biophysical characterization.

In addition, cloning, expression, purification and biochemical characterization of the genes involved in the branched chain amino acid biosynthetic pathway of *Mycobacterium*

tuberculosis H37Rv, were undertaken. Thirteen genes (Rv1559, Rv3003, Rv3470c, Rv3001c, Rv0189c, Rv2210c, Rv1820, Rv3002c, Rv3509c, Rv3710, Rv2995, Rv2988c and Rv2987c) encoding different enzymes of branched chain amino acid biosynthetic pathway were PCR amplified from the *Mtb* BAC library using gene specific primers. The amplicons were then cloned in frame with the C-terminal His tag in the expression vector pET22 (b) +, under the control of T7 promoter. The positive recombinant clones were transformed into the *E. coli* BL21 (DE3) cells and screened for expression of the recombinant proteins with IPTG induction at 37ºC. Induction conditions were modified to get the proteins in the soluble fraction. All the 13 recombinant proteins were purified to near homogeneity by Ni-NTA chromatography. Soluble recombinant proteins were purified directly while the proteins obtained as inclusion bodies were refolded and then purified. Identity of the recombinant proteins was further established by western blot analysis using Ni-NTA HRP conjugate antibody.

Publications

Original peer-reviewed articles

1. Alone PV and Garg LC (2008) Secretory and GM_1 receptor binding role of N-terminal end of LTB in *Vibrio cholerae.* Biochem Biophys Res Commun **376**:770-774.

Technology transfer

1. Technology for the recombinant epsilon toxin based vaccine against *Clostridium perfringens* D transferred to Indian Immunologicals Limited, Hyderabad.
2. Technology for solubilization of recombinant proteins expressed as inclusion body transferred to Therapus, Chennai.

Molecular analyses of the human and animal genome(s)

Principal Investigator: Sher Ali

Project Associates/Fellows: Sanjay Premi
Jyoti Srivastava
Sudeep Kumar
Ruchi Gupta

DST Fast Track: Saima Wajid
Rana Samad

DST Woman Scientist: Deepali Pathak

PhD Students: Safdar Ali
Masum Saini
Anju Kumari

Collaborators: Lalit Garg

The focus of research in the Lab is on the analyses of human and animal genomes and the present report deals with the genomics of the human Y chromosome. The objectives of the project are (i) analysis of the structural mosaicisms, copy number polymorphisms and possible tandem duplications of the candidate Y-linked genes in patients with Turner Syndrome and other sex chromosome related anomalies (SCRA) and (ii) study of fate of the human Y-chromosome linked genes/loci in males exposed to natural background radiations.

A. Analysis of the human Y-Chromosome in patients with Turner Syndrome

Human Y-chromosome material in the females with Turner Syndrome (TS) enhances the risk of the development of gonadoblastoma besides causing several other phenotypic abnormalities. In the present study, we analyzed clinically diagnosed 15 Turner Syndrome (TS) patients for the Y-chromosome related mosaicism along with samples representing other sex chromosome related anomalies. The Y chromosome mosaicism ranged from 45,XO:46,XY=100:0 in 4; 45,XO:46,XY:46XX=4:94:2 in 8 and 45,XO:46,XY:46XX=50:30:20 % cells in 3 TS patients based on the analysis of ~400 metaphases/interphases.

Unlike earlier reports, no ring, marker or di-centric Y was observed in any of the cases. Of the two TS patients with intact Y chromosome in >95% cells, one was exceptionally tall. Both the patients were positive for *SRY, DAZ, CDY1, DBY, UTY* and *AZFa*, *b* and *c* specific STSs. Real Time PCR and FISH demonstrated tandem duplication/multiplication of the *SRY* and *DAZ* genes (Figure 1, Table 1). At the sequence level, the *SRY* was normal in 8 TS patients while the remaining ones showed either absence of the same or several known and novel mutations within and outside of the HMG box (Figure 2).

The SNV/SFV analysis revealed normal sequences of the *DAZ* genes. All the TS patients showed aplastic uterus with no ovaries and no symptoms of gonadoblastoma. In our

analysis, no two TS patients had identical genotype-phenotype, suggesting that besides several Y linked loci; possibly other autosomal genes may also be affected. This warrants a comprehensive analysis of more number of samples to uncover consensus on the loci affected to eventually use them as potential diagnostic tools. Our work is an attempt on this line broadening the understanding on the genotype/phenotype correlation in such patients.

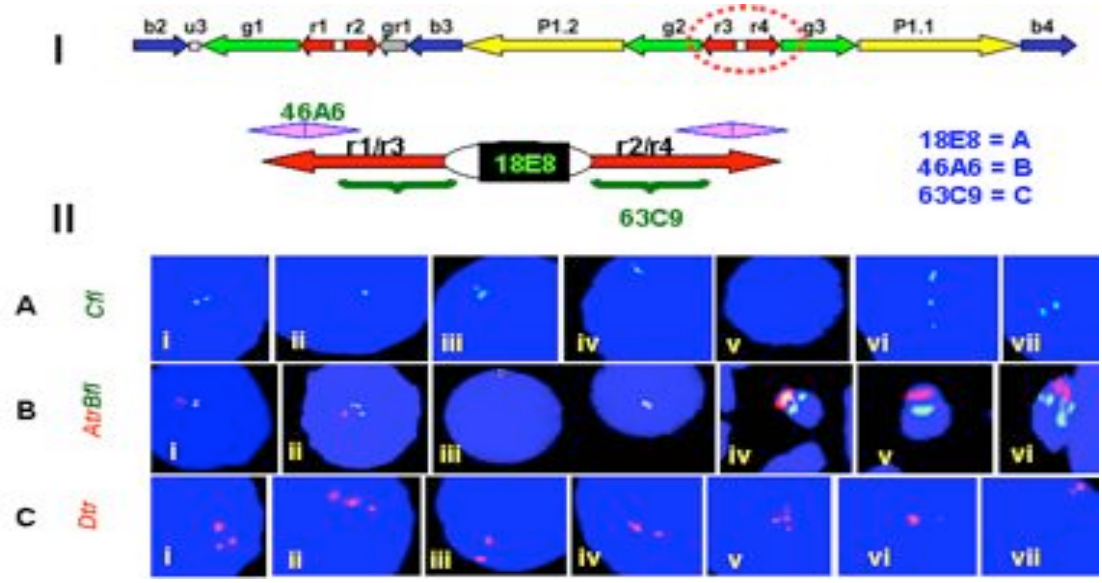

Figure-1: ***(I)*** *Representative map for the AZFc amplicons (above) and detailed structure of r1-r4 amplicons (below) showing the proposed positions of three COSMIDS used as FISH probes for DAZ genes.* ***(II)*** *FISH for DAZ genes in Turner Patient AT1. The A, B, C and D denote DAZ probes (supplementary figure 1) and,* ***tr*** *and* ***fl*** *are for* ***texas red*** *and* ***fluorescein*** *labels, respectively.* ***(A)*** *Note the expected 2 signals or a single one owing to overlap in most of the cells. Some cells lacked the signals* ***(v)*** *and others showed 3 signals in place of 2* ***(vi)****.* ***(B)*** *Dual probe FISH with DAZ probe A in red and B in green. The expected overlap of the probes A and B was not observed in most of the cells except a few* ***(iii).*** *The localized DAZ signals detected by FISH but multiple copies by Real Time PCR highlight the events of tandem duplication.* ***(C)*** *Analysis of the AZFc green amplicons in Turners. Note the presence of all the three green amplicons observed in the form of 3 well separated signals. Few cells even showed 2 signals where 1 was of higher intensity compared to that detected in others* ***(vi, vii).*** *This suggests a possible sequence re-modulation or reorganization of the AZFc in some percentage of cells in TS patients. The conclusions were drawn after analyzing 400 metaphase/interphase cells from each Turner Patient.*

Table-1: Gene duplication/multiplication events detected in the patients with sex chromosome related anomalies (SCRA). Numbers in the parenthesis represents patients analyzed.

Patient	Mosaic		One duplication		Double duplication		Triple duplication	
	SRY	*DAZ*	*SRY*	*DAZ*	*SRY*	*DAZ*	*SRY*	*DAZ*
Turner's Syndrome (20)	95%	80%	1%	5%	1%	10%	3%	5%
Y polysomy (1)	0%	0%	100%	0%	0%	0%	0%	100%
Swyer Syndrome (25)	95%	90%	2%	3%	2%	5%	1%	2%
Oligospermia (50)	10%	5%	30%	85%	40%	5%	20%	5%
Azoospermia (150)	10%	5%	20%	85%	50%	5%	20%	5%

***Figure-2**: Amino acid changes corresponding to the nucleotide sequence of the SRY gene in Turners AT1 and AT15. Note the amino acid changes within, upstream and downstream regions of the HMG box which is underlined. Most of the changes uncovered were novel.*

B Fate of the human Y-chromosome linked genes/loci in males exposed to natural background radiations

Major consequences of ionizing radiation are chromosomal lesions and occurrence of cancers though the entire genome may be affected. Owing to the haploid status and absence of recombination, the human Y-chromosome is an ideal candidate to be assessed for possible genetic alterations caused due to ionizing radiations. We studied human Y chromosome in 390 males from South Indian state, Kerala, where the level of natural background radiation (NBR) is ten fold higher compared to that of worldwide average and that from 790 unexposed males as control. We observed random microdeletions in the Azoospermia factor (*AZF*) *a, b* and *c* regions in >90%, tandem duplication and Copy Number Polymorphism (CNP) of 11 different Y-linked genes in about 80% males exposed to NBR.

The autosomal homologues of Y-linked *CDY* gene largely remained unaffected. Multiple polymorphic copies of the Y-linked genes showing single Y specific signal suggested their tandem duplication (Figure 3).

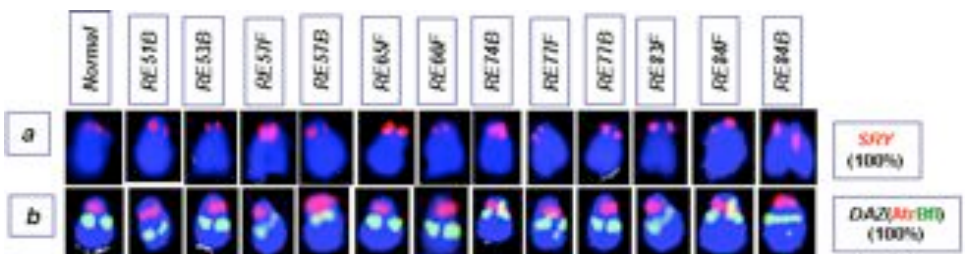

Figure-3: *Structural organization of the human Y chromosome in exposed males. Probes-combinations are described in Premi et al, 2009. The "**fl**" and "**tr**" refer to Fluorescein and Texas red labels, respectively. Probe combination **AtrBfl** corresponds to dual color FISH with 18E8 in red and 63C9 in green. **(a)** SRY-FISH showing a single signal with varying intensities with its multiple copies representing tandem duplication. **(b)** FISH with AtrBfl showing localization of probe 'A' onto the proximal Yp region in all the NBR exposed and normal males. This was substantiated using AtrCfl and AtrDfl probe combinations shown in **(c)** and **(d)**, respectively. FISH with probe 'D' showed exclusive localization of one of the three green amplicons onto the short arm, overlapping with signal for probe 'A' which was substantiated using probe combinations AtrDfl, DtrCfl and Dfl shown in **(d), (e)** and **(f),** respectively. Such localization was detected in 85-90% exposed males. Percentage of cells showing probe D signal on the short arm was higher in the exposed males compared to that in unexposed ones. The ratios show percent of males to percent of cells (eg. Probe D, panel f, 100/40% means only 40% cells of all the males showed alteration with respect to probe "D"). **(g-h)** Variation in length and position of Yq heterochromatin detected using 3.4 kb repeat unit of DYZ1 as FISH probe. This fluctuation was more prominent in the exposed males compared with an almost uniform signal in normal males (NM).*

Some exposed males showed unilocus duplication of *DAZ* genes resulting in six copies. Notably, in the *AZFa* region, approximately 25% exposed males showed deletion of the *DBY* gene, whereas flanking ones USP9Y and *UTY* remained unaffected. All these alterations were detected in blood samples but not in the germline (sperm) samples. Exposure to high level of NBR correlated with several interstitial polymorphisms of the human Y chromosome. CNPs and enhanced transcription of the *SRY* gene after duplication are envisaged to compensate for the loss of Y chromosome in some cells. The aforesaid changes remained confined to peripheral blood lymphocytes, suggesting a possible innate mechanism protecting the germline DNA from the NBR. In addition, the novel configuration of the DAZ genes detected in the exposed as well as normal males (Figure 4) open new vistas of focused research on the structure and genealogy of the human Y chromosome. Genome analysis of larger population focusing on more number of genes may provide new insights into the mechanisms and risks of the resultant genetic damages.

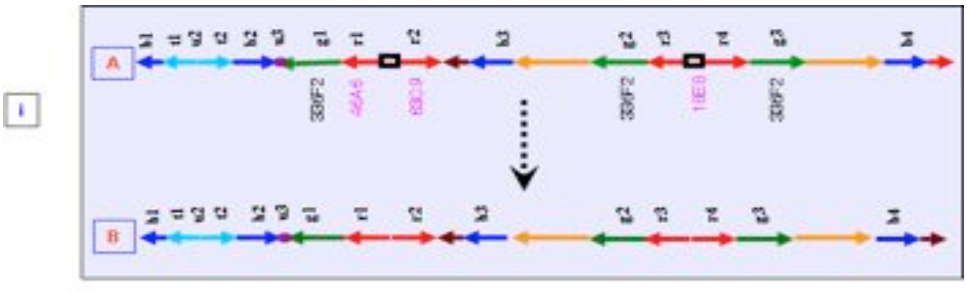

***Figure-4**: (i), Schematic representation of the AZFc region. (A) Arrangement of the AZFc amplicons as reported in the literature. Probes used in this study are given below the corresponding amplicons. Cosmids common to all the DAZ genes are highlighted in pink. (B) Arrangement of the AZFc amplicons in the NBR exposed and control males showing decreased intervening length between the two DAZ genes at each locus. This decrease is hypothesized to be due to translocation of 18E8 sequences onto the Yp. (ii), **(A)** Diagrammatic illustration showing positions of DAZ genes and neighboring AZFc amplicons reported thus far. Red horizontal bars represent two DAZ loci. The amplicons g1, g2 and g3, detected with BAC 336F2 (Probe D) are represented by green horizontal bars. **(B)** Translocation of probe 'A' signal to the Yp shown as red dotted horizontal bar. **(C)** Duplication of either one or all the g1, g2 and g3 amplicons followed by translocation to the short arm with higher frequency in NBR exposed males compared to that in normal ones. **(D)** and **(E)** represent Y chromosomes of Sumatran Orangutan and Pygmy Chimpanzee, respectively where DAZ genes are present on short arm of the Y chromosome. The Yp localization of DAZ genes was not linked with the exposure to NBR since similar arrangement was also detected in the normal males.*

Effects of NBR on gene duplications and sequence polymorphisms seem to be a possible genome strategy to absorb the mutational loads. This is evident from the multiple polymorphic copies of the *SRY* and *CDY1* genes. Moreover, from the enhanced *SRY* expression in blood, it is logical to construe that transcriptional machinery failed to discriminate between normal and altered versions of a duplicated gene. Absence of microdeletions and CNV of genes in germline DNA of exposed males suggested that the same is protected by some innate, still unexplored repair mechanism(s). Present work demonstrates unique signatures of the NBR on the Human Y chromosomes from Kerala.

Analysis of additional samples representing NBR and SCRA along this line would broaden our understanding on the correlation of gene, genome and environment.

Publications

Original peer-reviewed articles

1. Premi S, Srivastava J and Ali S (2009) Unique signatures of the natural background radiation on the human Y chromosome from Kerala (INDIA). *PLoS One* **4**:e4541.

2. Premi S, Srivastava J, Panneer G and Ali S (2008) Startling mosaicism of the Y chromosome and tandem duplication of SRY and DAZ genes in patients with Turner Syndrome *PLoS One* **3**:e3796

3. Srivastava J, Premi S, Kumar S and Ali S (2008) Organization and differential expression of the GACA/GATA tagged somatic and spermatozoal transcriptomes in buffalo *Bubalus bubalis. BMC Genomics* **9**:132.

Determining the signaling and repair pathways that are altered in human cancer using RecQ helicases as the model system

Principal Investigator: Sagar Sengupta

Project Associates/Fellows: Vivek Srivastava
Priyanka Modi

PhD Students: Sarabpreet Kaur
Suruchika Chandra
Siddharth De
Shweta Tickoo
Suhas Kharat

Collaborators: Debasisa Mohanty
K Muniyappa, *IISc, Bangalore*
Chandrasekhar Sagar, *NIMHANS, Bangalore*
Yasuhiro Furuichi, *GeneCare Research Institute, Japan*
Noralane M Lindor, *Mayo Clinic, USA*
Curtis Harris, *NIH, USA*

Our research program evolves around the understanding of the cellular processes that are altered in neoplastic transformation leading to human cancer. Towards this aim, we will focus my research endeavor on the RecQ helicases. *BLM* and *RECQL4* are members of the RecQ family of DNA helicases. Germline mutations in both *BLM* and *RECQL4* helicase result in autosomal-recessive disorders, Bloom syndrome (BS) and Rothmund-Thomson syndrome (RTS) respectively. BS afflicted individuals are predisposed to almost all types of cancers while RTS individuals are predominantly predisposed towards osteosarcomas. Since RecQ helicases are intimately involved in the many vital cellular processes, they are ideal candidates to investigate the reasons for neoplastic transformation. In the current year the work in the lab was aimed to dissect the *in vivo* functions of RecQ helicases. Specifically the objectives are to study the role of (i) BLM in homologous recombination and (ii) RECQL4 in the regulation of cellular functions

A. Role of BLM during homologous recombination (HR)

<u>BLM has a predominant anti-recombinogenic function</u>

We wanted to determine whether the documented anti-recombinogenic function of BLM was dependent on RAD54. For this purpose we carried out spontaneous SCE analysis, which is mediated by HR in vertebrate cells. shRNA against RAD54 stably transfected into isogenic BS (which do not express BLM) and A-15 (BS cells complemented with mini-chromosome 15 encoding BLM) cell lines, resulted in BS shRNA-RAD54 and A-15 shRNA-RAD54 cells, both of which exhibited acute depletion in endogenous RAD54 levels. Compared to normal cells (A-15), loss of RAD54 (A-15 shRNA-RAD54 cells) led to a significant 2.5 fold decrease in the rate of SCEs. The 8-fold increase in the rate of

SCE observed due to loss of BLM, was abrogated in BS shRNA-RAD54 cells, thereby indicating that in human cells *in vivo* BLM has a predominant anti-recombinogenic function. Consistent with this role, we found that the number of foci for RAD54 increased in BS vis a vis A-15 cells, irrespective of the absence or presence of replicative stress.

BLM prevents RAD54-RAD51 complex formation

The N-terminal region of BLM binds to both RAD51 and RAD54. Incidentally the N-terminal region of human RAD54 is involved in its interaction with both RAD51 and BLM. To test the possibility that BLM may prevent RAD51-RAD54 interaction, we carried out *in vitro* pulldown assay with bead-bound purified GFP-RAD54 and soluble His-RAD51 in absence or in presence of increasing amounts of soluble GST-BLM (1-212) or GST. RAD54 and RAD51 formed a readily detectable complex. Increasing amount of BLM (1-212), but not GST, prevented RAD51-RAD54 interaction. Prevention of complex formation was more enhanced for BLM (109-212) fragment. These results were confirmed *in vivo* by carrying out reciprocal IPs in BS and A-15 cells. Interaction between RAD51 and RAD54 decreased in A-15 cells (compared to BS) in both ±HU conditions. At a single cell level RAD51 and RAD54 proteins colocalized extensively in BS cells, whereas in A-15 cells a considerable fraction of RAD51 was present outside the colocalized foci in nucleoplasm. Together the above results indicated that BLM prevented RAD51-RAD54 complex formation in vitro and in vivo.

Based on above results, we hypothesized that the extent of accumulation of RAD51 and RAD54 in the chromatinized foci and the nucleoplasm should be different in absence or presence of BLM. We carried out chromatin fractionation assay in BS/A-15 cells. BLM, present in only the A-15 cells, accumulated predominantly in chromatin enriched fraction (fraction III), especially in +HU condition. RAD54 was predominantly present in fraction I in both BS/A-15 cells, indicating that RAD54 was mostly in soluble form. The small fraction of RAD54 at the sites of spontaneous or damage induced chromatinized foci, was not dependent on BLM. However RAD51 exhibited a BLM-dependent difference in accumulation between fractions I and III. In absence of BLM, RAD51 was more in the chromatin-enriched fraction III and consequently the amount of soluble RAD51 in fraction I was lower.

We hypothesized that BLM might prevent RAD51-RAD54 complex formation by altering the dynamic relocalization of RAD51 between the nucleoplasm and the foci. To test this hypothesis we transfected low levels of GFP-tagged RAD51 into BS/A-15 cells in absence or presence of 2 h of HU-treatment. Fluorescent Recovery After Photobleaching (FRAP) was carried out to determine the dynamics of GFP-RAD51 in BS/A-15 cells. We found that in cells expressing BLM, approximately 75% of RAD51 in the nucleoplasm was mobile. The half maximal recovery time ($t_{1/2}$) for nucleoplasmic RAD51 in A-15 cells was 7.8 s. These values compare well with the reported value for the mobility of GFP-RAD51 in nucleoplasm of cells expressing BLM. By comparison in BS cells, approximately 55% of nucleoplasmic GFP-RAD51 was mobile and it manifested a slower recovery, with a $t_{1/2}$ of 8.4 s. A difference in the dynamic behavior of nucleoplasmic GFP-RAD51 existed even after 2 h of HU treatment. The difference in the mobility was not limited only to the nucleoplasmic GFP-RAD51. As reported earlier a slow RAD51 fluorescence recovery was observed in the foci of wildtype cells (like A-15). However the recovery was completely absent when FRAP was carried out on the

foci of BS cells. Together the above data indicated that RAD51 was more dynamic and exchanged at a faster rate in presence of BLM. Conversely in absence of BLM, RAD51 seems to be more stable both in the foci and in the nucleoplasm.

The above experiments raised the possibility that the mobility of RAD54 may also be altered in presence or absence of BLM. We carried out FRAP after transiently transfecting BS/A-15 cells with GFP-RAD54. As reported earlier, RAD54 foci recovered fully (approximately 100%) and very fast ($t_{1/2}$ of 1 s) indicating that unbleached RAD54 in the nucleoplasm were replacing the bleached RAD54 molecules in the foci in an extremely dynamic manner. Even in the nucleoplasm itself, approximately 60% of RAD54 was mobile. Importantly, the rate the movement of fluorescent RAD54 was not altered in either nucleoplasm or the foci due to the absence or presence of BLM.

BLM undergoes dynamic intra-nuclear exchange

The above biochemical and cell biology experiments hinted at a temporal regulation governing the interaction between RAD54, RAD51 and BLM in the nucleoplasm and foci. BLM maybe regulating the dynamic exchange of RAD51, but not RAD54, between the chromatinized foci and the nucleoplasm. Hence it was possible that BLM also concurrently undergoes exchange at the foci and the nucleoplasm, thereby regulating its own interaction with RAD54 and RAD51. For this purpose we used a stable line expressing GFP-BLM in SV40 immortalized GM08505 cells. The expression levels of BLM, RAD51 and RAD54 between GFP-BLM and A-15 cells were very similar, thereby allowing extrapolation of results between the cell lines. The formation of GFP-BLM foci was observed in only 10-15% of the cells in absence of HU, indicating their formation during spontaneous DNA damage in S-phase. In presence of 2 h of HU treatment, approximately 45-55% of the cells developed detectable GFP-BLM foci.

FRAP experiments indicated that after photobleaching there was 80-85% recovery of BLM present in the foci at a fast rate ($t_{1/2}$ of 7 s), irrespective of the presence or absence of induced stalled forks. Thus BLM resides transiently at the chromatinized foci and dynamically exchanges with its counterpart in the nucleoplasm which itself is present in an extremely mobile form (100% recovery with a $t_{1/2}$ of 1 s). The markedly slower kinetics of recovery for GFP-BLM in the foci, in comparison to the nucleoplasm, indicated that a fraction of the helicase was transiently immobilized at the site of either spontaneous or HU-induced DNA damage. The residence time of BLM in the HU-induced foci (7.2 s) is similar to that of MDC1 and 53BP1 at the double strand breaks. Hence using real-time measurements we have provided evidence to our earlier hypothesis that BLM is an immediate early responder to DNA damage.

BLM stimulates RAD54-mediated ATPase and chromatin remodeling activities in a RAD51 independent manner

The above results indicated that the RAD51-independent binding of BLM to RAD54 may occur in cells. To investigate this possibility, we expressed in NHF a dominant negative form of RAD51, the yeast/mouse chimera SMRAD51, which downregulates HR without affecting cell viability. Expression of SMRAD51 in HU-treated NHF, led to stabilization of both endogenous RAD54 and BLM and decreased the rate of HR as measured by host cell reactivation assay. However BLM and RAD54 colocalized to the same extent irrespective of the presence or absence of functional RAD51. These results demonstrated

that the direct interactions detected between BLM and RAD54 could also occur *in vivo* even in absence of functional RAD51.

Many of the enzymatic functions of RAD54 including the ATPase and the homology driven chromatin remodeling function are upregulated by RAD51. To determine a functional role for BLM-RAD54 interaction, we wanted to elucidate whether the N-terminal 1-212 amino acids of BLM (which interacts with RAD54) could affect RAD54 mediated ATPase assay. Based on our results from pull-down assay, we hypothesized that BLM (1-212), like *Saccharomyces cerevisiae* meiosis-specific gene Hed1, would ablate the enhancement of RAD54 ATPase activity by RAD51. Instead we found that addition of BLM (1-212) fragment led to a further increase in the rate of RAD54-mediated ATP hydrolysis. This result indicated that N-terminal region of BLM might enhance the ATPase function of RAD54. Indeed BLM (1-212), but not GST, could enhance the RAD54 ATPase hydrolysis in a dose dependent manner, to an extent similar to RAD51.

We also wanted to know whether the stimulation by 1-212 fragment of BLM was also observed for the full-length helicase. We did not use wildtype BLM as the helicase has a strong ssDNA dependent and a mild dsDNA dependent ATPase activity. We generated and purified an ATPase dead mutant of the full length BLM, BLM (1-1417) K695A, which did not have any detectable ATPase activity. BLM (1-1417) K695A stimulated RAD54 ATPase activity to an extent almost similar to BLM (1-212) fragment.

Since BLM exchanged with chromatin bound RAD54 more rapidly than RAD51 (7.2 s for BLM vs 7.8 s for RAD51) and could stimulate the ATPase activity of RAD54, it may also stimulate the chromatin remodeling activity of RAD54. It has been reported that RAD51-ssDNA filaments stimulated RAD54 dependent chromatin remodeling in a homology-dependent or independent manner**.** We verified ATP and time dependent RAD54 chromatin remodeling activity by using restriction enzyme accessibility (REA) assay on the G5E4 array, containing 12 nucleosomes with a centrally located HhaI site occluded by one nucleosome. Though BLM (1-212) alone did not have any effect on the REA assay, it enhanced RAD54-dependent chromatin remodeling activity, especially at the early (15 s) time point. The effect was also seen for BLM (1-1417) K695A mutant. At the early time point BLM (1-212) fragment enhanced RAD54 chromatin remodeling activity by 3-fold much more than that observed by RAD54 alone, thereby indicating that stimulation of RAD54 remodeling by BLM is an early event in HR.

B. Role of RECQL4 in the regulation of cellular functions

N-terminal regions of both RECQL4 and p53 interact

Other members of the RecQ helicases, BLM and WRN, bind to p53. To determine whether RECQL4 also physically interacts with p53, we carried out *in vitro* GST pull-down assays with S^{35} labeled RECQL4 and the different deletion fragments of the tumor suppressor. We found that the minimal region of p53 that interacts with RECQL4 encompasses the amino acids 293-362. This region contains the major Nuclear Localization Signal (NLS1) of p53 along with the tetramerization domain (TD). p53-RECQL4 interaction is independent of nucleic acids. Two tumor derived mutants of p53 (175H, 248W), also show interactions with RECQL4, albeit to a reduced level compared to the wild-type tumor suppressor.

To determine the region of RECQL4 which interacts with p53, we initially generated and purified three mutant protein fragments of RECQL4: 1-459, 460-868, 869-1208. We found that the N-terminal 459 amino acids of RECQL4 interacted with p53. Subsequently we generated N- and C-terminal mutants within the first 459 amino acids, purified them and performed GST pull down assays with S^{35}-labeled p53. We found that a stretch of 130 amino acids (270-400) of RECQL4 interacted with p53. Significantly this interacting domain includes the NLS of RECQL4. The interaction with p53 was verified either with a GST-tagged RECQL4 (270-400) fragment *in vitro* or by using a Flag-tagged RECQL4 (1-459) fragment *in vivo*. Further we found that full-length RECQL4 but not the N-terminal 404 amino acid truncated variant interacted with GFP-tagged full-length p53, thereby validating the region of interaction in the context of full-length proteins.

To further characterize the interaction between endogenous RECQL4 and p53, we performed reciprocal coimmunoprecipitation on cellular lysates from hTERT immortalized Normal Human Fibroblasts (NHF). We found that interaction between the two proteins was limited to asynchronous conditions. Exposure of NHF to DNA damage causing agents led to disruption of p53-RECQL4 interaction.

RECQL4 and p53 colocalize in mitochondria

To determine the subcellular distribution of p53 and RECQL4, we stained asynchronously grown NHF with p53 and RECQL4 antibodies and carried out the imaging with confocal microscopy. We found that p53 and RECQL4 colocalized to a high degree in the cytoplasm as punctate staining. It has been demonstrated that p53 is targeted to mitochondria after different types of DNA damages, where it can promote apoptosis by a transcription-independent mechanism. However a small amount of p53 is present in mitochondria even in absence of exogenous stress. A significant portion of endogenous RECQL4 is also present in the cytoplasm. We tested whether cytoplasmic punctate staining was due to the localization of p53 and RECQL4 in the mitochondria. Indeed we found that both p53 and RECQL4 colocalized extensively with mitochondrial marker, cytochrome c and Mitotracker Red and mitochondrial helicase, Twinkle. However the localization was not in mitochondrial fibriller network structure. Instead both p53 and RECQL4 colocalized with mitochondrial nucleoids which are the storehouse of mitochondrial DNA (mtDNA), and Twinkle. The mitochondrial localization of RECQL4 and p53 was further demonstrated by cell fractionation experiment. The integrity of the cell fractionation was tested by specific markers. Substantial amount of both p53 and RECQL4 were found to be present in nucleus and mitochondria.

Since nucleoids contain mtDNA, we performed immuno-colocalization of RECQL4 and p53 with BrdU or Ethidium Bromide (EtBr) according to published protocols. Both p53 and/or RECQL4 colocalized with BrdU or EtBr. Using NHF E6 cells the localization of RECQL4 with mtDNA was found to be independent of p53. Significantly the total amount of RECQL4 was increased in absence of p53. This maybe due to the lack of p53 mediated repression of RECQL4 transcription.

Role of TNF α and IGF-1 in neuronal apoptosis

Principal Investigator: Kakoli Ghosal

Project Associates/Fellows: Kanchan Mishra

PhD Student: Sakshi Gupta

Proinflammatory cytokines especially tumor necrosis factor-alpha (TNFα), is a pleiotropic mediator of diverse array of physiological and neurological functions and has been implicated in the pathogenesis of several disorders and injuries in the central nervous system (CNS). IGF-1 on the other hand exerts anti-apoptotic and neuroprotective effects in primary neuronal cultures and neuronal cell lines. The signal transducers and activators of transcription (STAT) factors function as downstream effectors of cytokine and growth factor receptor signaling. STAT signaling is critical for normal cellular processes such as embryonic development, organ genesis and function, innate and adaptive immune function, regulation of cell differentiation, growth, and apoptosis. Members of the suppressor of cytokine signaling (SOCS) family, function as negative regulators of signaling pathways involved in the cellular actions of cytokines, growth factors and hormones. Cytokine-triggered phosphorylation of STATs induces the transcription of SOCS genes. Since cytokines and growth factors modulate a wide variety of biological responses in the CNS, members of the SOCS family might play crucial roles in regulating intra-cellular signaling in both normal and diseased states. Thus research directed towards understanding of actions and interactions of SOCS with cytokine signaling machinery proteins would help in identification of novel ways of modulating aberrant cytokine signaling. Previously we have shown that IGF-1 mediated neuronal cell signaling upregulated SOCS3 and SOCS6. These proteins were involved in neural cell differentiation. More detailed studies were undertaken this year to confirm the roles of SOCS3 and SOCS6 in differentiation.

The objectives of the project are to (i) explore the role of SOCS3 and SOCS6 in processes of neuronal cell survival and differentiation in response to IGF-1 and (ii) study the mechanism of signaling by these specific SOCS proteins.

In the previous year SOCS6 transient transfections in neural stem cells showed SOCS6 transfected neurospheres enhanced differentiation of neurons substantially as compared to vector only controls. This year the number of primary, secondary and tertiary neurite and the total neurite length was measured. SOCS6 transfected neurons not only had significantly longer primary neuritis but also had greater number of secondary and tertiary branches. EGFP transfected neurons had very few secondary and no tertiary neurite branching. Mean total neurite length per cell was also much higher in SOCS6 transfected cells as compared to the controls. To confirm that the enhanced neurite outgrowth was not only a property of neural stem cells, neurite outgrowth in SOCS6 over expressing PC-12 cells was also checked. When the PC-12 cells were induced to differentiate by treatment with NGF, ~60% of SOCS6 overexpressing cells showed increased neurite outgrowth, as compared to the neurite length of EGFP transfected PC-12 cells. Besides the neurites were longer and more numerous in SOCS6 transfected cells as compared to EGFP alone.

We then wanted to see if SOCS3 also had differentiating properties. Under nondifferentiating conditions (no NGF) neurite formation was observed in approximately 20% of all cells in the SOCS3 stable PC12 cell lines; however, under these

nondifferentiating conditions, there was no detectable neurite extension observed in control cells transfected with EGFP alone. When PC12 cells were transfected with SOCS3in the presence of NGF, the neurites were longer and more numerous as compared to cells transfected with EGFP alone. Furthermore, SOCS3 overexpression also induced expression of GAP43, a neuronal marker associated with neurite outgrowth. Overexpression of SOCS3 therefore appeared to directly promote neurite outgrowth of a neural cell line by itself, as well as markedly potentiating the effects of NGF mediated differentiation. Overexpression of SOCS1 or SOCS4 in PC12 cells had no effect on neurite outgrowth.

In the previous year we had shown that SOCS6 levels increased on inhibiting the PI3kinase pathway. This indicated that PI3 kinase pathway inhibits SOCS6. pERK levels decreased in differentiated cells as compared to the neurospheres. This year we show that inhibiting erk or PI3 kinase pathways donot have any effect on neuronal stem cell differentiation.

Previous bioinformatics studies had revealed putative STAT binding sites on SOCS6 promoter sequences and preliminary luciferase studies implicated STAT3 and STAT5 to be the specific players in SOCS6 activation, this year we transfected PC12 cells with STAT5a, STAT5b and dominant negative STAT5a and dominant negative STAT5b. We observed that STAT5a and 5b stimulated SOCS6 expression which was inhibited by dominant negative STAT5a and 5b thereby showing that STAT5a and 5b are the specific players in SOCS6 activation.

This was again confirmed by the EMSA studies. Nuclear extracts of PC-12 cells, transfected with STAT5a-EGFP and STAT5b-EGFP and stimulated with IGF-1 was used for binding studies in EMSA. We found that extracts from STAT5a and STAT5b stimulated with IGF-1 shows mobility shift with both STAT5a and STAT5b. Cold competition experiments using 100 fold excess of cold oligomer showed that both STAT5a and STAT5b transfected extracts could be specifically competed out**.**

Further we looked for the effect of SOCS6 siRNA in neural cell differentiation. In the presence of SOCS6 siRNA, neural differentiation was inhibited thereby confirming the role of SOCS6 in neural cell differentiation. The number of primary, secondary and tertiary neurite and the total neurite length was measured. As expected the length of the primary neurite in SOCS6 siRNA transfected neuron was significantly decreased and cells showed very less secondary and no tertiary neurite branching. Similarly the mean total neurite length per cell was also much less in SOCS6 siRNA transfected cells as compared to the control.

Epigenetic regulation of the eukaryotic genome

Principal Investigator: Madhulika Srivastava

Project Associates/Fellows: Garima Varma

PhD Students: Vikrant Singh
Sweety Shrimali
Ananya Sadhu
Pratishtha Rawat

Despite the importance of enhancers, promoters, insulators, transcription factors, chromatin remodelling factors etc. in the context of gene regulation, the current understanding with regard to the mechanisms by which they interact with each other to control chromatin based reactions is rather limited. Global analysis has recently predicted the presence of nearly 14,000 sites in the human genome that could potentially act as insulators and restrict the enhancer activity to specific promoters and thus aid in appropriate spatial and temporal regulation of genes. Our current efforts are focussed on understanding different aspects of the mechanisms by which mammalian insulators influence chromatin domain organization and prevent enhancer-promoter interactions.

In view of the diverse mechanisms that might operate to achieve functional abrogation of enhancer-promoter interaction by the insulators, we are investigating the following aspects regarding the murine insulator at *H19-ICR* that controls the monoallelic imprinted *Igf2* expression.

1. Analysing the mechanisms by which *H19-ICR* insulator organizes chromatin structure at the endogenous locus to prevent the enhancer-promoter interaction.
2. Evaluating the ability of the *H19-ICR* insulator to organize chromatin at a heterologous locus and interfere in *cis* interactions

The TCR-ins ES cells were used to generate mutant mice which carried *H19-ICR* inserted at the TCRβ locus. The developmental profile of thymocytes in TCR-ins mutant mice was comparable to the wild type indicating that the TCR-ins allele was able to support VDJ recombination leading to functional T cells. Analysis of transcription from PDβ1 promoter was carried out on thymocytes from mutant mice (TCR-ins) using quantitative realtime RT-PCR. Upon maternal inheritance, the inserted insulator sequence reduced the transcription to less than 15% in the mutants compared to control littermates indicating that the insulator is active despite the new genomic context devoid of DMR1, DMR2 and MAR3 elements of the *Igf2/H19* locus. The *H19-ICR* also continues to be hypomethylated upon maternal inheritance as discerned based on methylation analysis by bisulphite sequencing

Upon paternal inheritance, a loss of insulator activity is predicted if the *H19-ICR* acquires a hypermethylation imprint. In concordance with such a prediction, we observed lack of reduction in PDβ1 initiated transcription in several paternal mutants. However, some paternal mutants did exhibit a reduction suggesting partial loss of paternal imprints. Currently, efforts are directed towards analyzing the methylation status of the *H19-ICR* from from these two kinds of paternal mutants to gain insights into the ability of *H19-ICR* to imprint a new locus.

Since at the endogenous location, the *H19-ICR* does not act as a chromatin barrier preventing the spread of chromatin states, it would be of interest to study this aspect in a scenario where the enhancer is clearly known to lead to domain-wide alteration in the histone modifications. Since Eβ is known to alter the chromatin structure of the entire 25kb region encompassing the DJC clusters of the TCRβ locus, we would like to study the effect of the *H19-ICR* insulator insertion on chromatin structure regulated by the Eβ. Towards this goal, we have initiated experiments to optimize the ChIP against specific histone modifications such that they can be analysed in an allele specific manner at the key regulatory elements and other important regions of TCRβ.

Publications

Original peer-reviewed articles

1. Singh V and Srivastava M (2008) Enhancer blocking activity of the insulator at *H19-ICR* is independent of chromatin barrier establishment. *Mol Cell Biol* **28**:3767-3775.

Role of cell signaling in eukaryotic development

Principal Investigator: Pushkar Sharma

Project Associates/Fellows: Aparna Dixit
Narayana Komaravelli (till Nov 2008)
Anwar Ahmed
Piyush Paliwal (since Jan 2009)
Guru Prasad Sharma (since Dec 2008)

PhD Students: Ravikant Ranjan
Neha Singh
Divya Catherine Thomas
Suran Nambisarn

It is well known that extracellular signals control biological responses in most eukaryotic cells by regulating specific intracellular signaling cascades. We are interested in exploring signaling events in the biology of two diverse cell types; 1) malaria parasite *Plasmodium falciparum,* 2) mammalian neurons.

We have two major areas of interest:

(I) *Dissection of intracellular signaling and trafficking cascades of Plasmodium falciparum:* Characterization of signaling pathways that operate in malaria parasite may help unravel novel mechanisms involved in its development. We are interested in elucidating the role and regulation of phosphoinostides, their effectors and calcium mediated signaling in the life cycle of *Plasmodium falciparum*.

(II) *Role of cyclins and cyclin dependent kinases in neuronal apoptosis:* Apoptosis of neurons is important for proper brain development and can also lead to neuronal loss in neurological disorders. During apoptosis, terminally differentiated neurons attempt to re-enter into the cell cycle, which is reflected by the aberrant modulation of cell cycle proteins like cyclins and cyclin dependent kinases (cdks). Molecular mechanisms underlying this process are not understood clearly. We are investigating how levels of cyclin/cdks are modulated during neuronal apoptosis and via what mechanisms aberrant cdk activity causes neuronal cell death.

I. Dissection of intracellular signaling and trafficking cascades of Plasmodium falciparum

A. Regulation of parasite Glideosome Assembly and Inner Membrane Complex (IMC) by phosphorylation

We reported in the previous year that PfPKB associates with the glideosome assembly, which is known to control the function of actin-myosin motor of the malaria parasite. It phosphorylates Glideosome associated protein 45 (GAP45), which may help explain its involvement in RBC invasion as this motor complex is important for this process. We have further explored the involvement of PfPKB with GAP45 and the motor complex in detail. The phosphorylation site of PfPKB on PfGAP45 was identified using mass spectrometry, which was confirmed by site-directed mutagenesis and phosphopeptide mapping. PfGAP45

also turned out to be a target of another enzyme, Calcium Dependent Protein Kinase 1 (PfCDPK1). Mass spectrometric analyses and phosphopeptide mapping results indicated that this enzyme phosphorylates PfGAP45 at several additional sites, which were identified. Immuno-fluorescence studies suggested that PfGAP45 co-localizes with PfCDPK1 and PfPKB. Since both PfPKB and PfCDK1 phosphorylate PfGAP45, it is important to dissect out the role of phosphorylation in the function of this protein by these kinases. We have identified A443654 as an inhibitor of PfPKB, which blocks the phosphorylation of PfGAP45 *in vitro* and in the parasite. This compound does not cause much change in PfCDPK1 mediated PfGAP45 phosphorylation. Efforts are being made to develop a specific PfCDPK1 inhibitor to be used as a tool to study its function (see below). It is important to investigate the role of phosphorylation of PfGAP45 on Glidesome assembly and other related events.

B. Role and regulation of calcium dependent kinases

Recent studies indicate that Calcium Dependent Protein Kinases (CDPKs) are used by calcium to regulate a variety of biological processes in the malaria parasite *Plasmodium*. CDPK4 plays a key role in gametogenesis and sexual differentiation in *P. berghei* and PfCDPK1 may play a role in invasion of RBCs . Our above-mentioned findings and other reports suggest that PfCDPK1 may participate in invasion by controlling the actin-myosin motor via regulation of the Glidesosome assembly.

It is not understood how malaria PfCDPKs like PfCDPK1/4 are regulated by calcium at the molecular level. We have made efforts to understand how these important parasite enzymes operate. Biochemical studies performed on PfCDPK4 revealed a novel mechanism via which calcium may control its regulation. PfCDPK4 was detected on the gametocyte periphery and its activity in the parasite was dependent on PLC. The J-domain, which connects the kinase and the calmodulin like domain, plays a pivotal role in PfCDPK4 regulation. The regions of the J-domain involved in interaction with both the kinase domain and the CLD and its regulatory autophosphorylation site were mapped. While the N-terminal of the JD interacts with the catalytic domain in a pseudosubstrate-like manner, its C-terminus interacts with the Calmodulin-like domain. Based on these studies, the regulatory elements in other PfCDPKs were predicted. Some of these predictions were tested successfully on PfCDPK1. These findings may aid design of inhibitors against PfCDPK1/4, which may prove useful for exploring their function in events like RBC invasion.

II. Role of cyclin/cyclin dependent kinases in neuronal apoptosis

The role of cell cycle protein cyclin D1 in apoptosis of neuronal PC12 cells and rat cortical neurons was investigated. The role of cell cycle proteins in neuronal apoptosis triggered by $A\beta_{1-42}$, which is neurotoxic and is considered one of the major causes of Alzheimer's disease, was also explored. Camptothecin (Cpt), a DNA topisomerase inhibitor, which is known to cause neuronal cell death, was also used to induce apoptosis. Treatment with Cpt and $A\beta_{1-42}$ resulted in an increase in the levels of cyclin D1 and caused resulted in apoptosis neurons. When recombinant adenoviruses were used to overexpress Cyclin D1, apoptosis was observed. Strikingly, neurons undergoing apoptosis in these experiments exhibited signs of cell cycle re-entry as suggested by increased levels of Proliferating Cell Nuclear Antigen (PCNA) and enhanced Brdu incorporation. Since siRNA mediated Cyclin D1 knock-down prevented both increased levels of cell cycle markers and apoptosis, we

propose that the apoptotic stimuli like Cpt and $A\beta_{1-42}$ leads to an aberrant increase in cyclin D1 levels which forces these cells to enter the cell cycle resulting in their apoptosis. Presently, we are trying to dissect signaling events that are regulated by cyclin D1 during neuronal apoptosis.

Review/Proceedings

1. Doerig C, Billker O, Haystead T, Sharma P, Tobin AB and Waters NC (2008) Protein kinases of malaria parasites: an update *Trends In Parasitology* **24**: 570-577.

Chemical biology of *Mycobacterium tuberculosis*: Deciphering the role of polyketide synthases in *Mycobacteria*

Principal Investigator: Rajesh S Gokhale

Project Associates/Fellows: Archana Vats
Ratna Ghosh
T Vivek
Brahm Prakash
Rajesh Mondal
Priti Saxena
Alzu Manocha
Lavanya Muthukumar
Pooja Rao

PhD Students: Tarun Chopra
Arush Chhabra
Divya Nair
Priyanka Verma
Parul Ganju

Collaborators: Debasisa Mohanty
R. Sankaranarayanan, *CCMB, Hyderabad*

Our laboratory is interested in genome-based approaches to identify and exploit the microbial metabolic pathways that are involved in the biosynthesis of various natural products. The primary focus is to understand the importance of various polyketide synthase gene clusters from *Mycobacterium tuberculosis*. We are now extending these studies to other organisms like *Dictyostelium discoideum* to understand how polyketide synthases generate metabolic diversity.

The genome sequence of *M. tuberculosis* (Mtb) and *Dictyostelium* (Dicty) has revealed a remarkable array of genes that are homologous to polyketide synthases. Polyketide synthases (PKSs) are a class of enzymes that are involved in the biosynthesis of secondary metabolites such as erythromycin, rapamycin, tetracycline, lovastatin, and resveratrol. Our study attempts to understand and exploit the role of polyketide synthases in the biology of Mtb and Dicty. The objectives of the studies are (i) identification and biochemical analyses of enzymes that are involved in the biosynthesis of metabolites, (ii) isolation and characterization of PKS gene products by heterologous expression of these genes in *Streptomyces coelicolor* and *Escherichia col*, (iii) characterization of molecular mechanisms mediating the crosstalk between various polyketide synthases (PKSs) and fatty acid synthases (FASs) in *M. tuberculosis*, (iv) genetic and/or chemical knock-out of PKS genes to synthesize novel polyketides to study the effects of these changes on mycobacterial pathogenecity and Dictyostelium development and (v) delineation of mechanisms that generate metabolic diversity, particularly by using versatility of polyketide biosynthetic machinery.

A. Mechanistic and functional insights into fatty acid activation in Mycobacterium tuberculosis

The recent discovery of FAALs in Mtb has provided a new perspective to fatty acid activation dogma. These proteins by activating fatty acids as acyl-adenylates redirect the metabolic flux towards biosynthesis of complex lipidic metabolites. The free fatty acids could either come from direct uptake mechanisms or by hydrolysis of acyl-CoA or acyl-ACP thioesters. We have now delineated evolutionary relationship between FACL and FAAL proteins. Our studies show that FAAL proteins indeed possess CoASH-binding pocket and their inability to synthesize acyl-CoA manifest from the changes in domain movements. Such alteration is brought about by a novel insertion motif identified during the three-dimensional structure determination of this protein. Remarkably, the interconversion between the catalytic functions can be achieved by mere insertion and deletion of this region. By using this criterion of an insertion motif, we show that FAAL homologues could be identified in genomes of other bacteria. Since many of the *Actinomycetes* produce mycolic acids and are grouped in taxon mycolata and a FAAL homologue is required for biosynthesis of mycolic acids in Mtb, we decided to characterize this homologue from *Rhodococcus*. Sequence analysis also indicated the presence of an insertion sequence. The Rhodococcus FAAL homolog ro_4064 was cloned and expressed in *E.coli*. Cell-free enzymatic assays demonstrated that this enzyme could only synthesize palmitoyl-AMP and formation of palmitoyl-CoA could not be detected even at 1mM concentration of CoASH. It is interesting to note that all these organisms apart from utilizing mycolic acids as part of their cell envelope have also retained the novel mechanistic basis of fatty acid activation.

In most instances FAAL homologues are positioned next to their cognate PKS/NRPS proteins in the genomes. This conserved organization provides a dual advantage, both in terms of co-expression of the two proteins as well as in substrate channelling of the labile acyl-AMP intermediate. FAAL proteins also circumvent the need to sustain metabolic pools of fatty acyl-CoAs to produce diverse lipidic metabolites. The promiscuous substrate specificity of Mtb FAALs can produce spectrum of metabolites, which could be a mechanism to generate phenotypic heterogeneity in intracellular pathogens. A FAAL homologue was recently characterized from *Bacillus subtilis* by Walsh's group and is proposed to be involved in the production of a lipopeptide mycosubtilin. Other lipopeptide-producing organisms also reveal FAAL-like domains in genomes of *Nostoc sp*, *Nodularia spumigena* and *Streptomyces coelicolor*. These observations emphasize that acyl-AMPs could routinely be employed during biosynthesis of lipidic metabolites in diverse organisms.

Systems biology-based approaches in recent years are beginning to reveal new insights into the understanding of metabolic networks, which enables pathogens to overcome unfavourable conditions, including insults imparted by target-specific drugs. It is because of this reason that pharmaceutical industry is thinking beyond the traditional 'one-disease-one-drug-one-target' paradigm and is interested to develop strategies that can simultaneously inhibit more than one target. The pivotal role of several FAAL homologues in biosynthesis of virulent lipids in Mtb prompted us to develop inhibitors that would simultaneously target multiple pathways. Our studies with the bi-substrate acyl-sulfamoyl analogues, which resemble common reaction intermediate of FAAL and FACL proteins, showed dramatic effect on the cell surface architecture of Mtb. *In vitro* analysis indeed showed inhibitions of both FAAL and FACL proteins. Since FACL enzymes in Mtb are being implicated in providing alternate energy sources during dormancy stage of infection, this strategy suggest a possible means to target different stages of Mtb infection.

B. Delineating role of two essential phosphopantetheinyl transferases in Dictyostelium discoideum

Dictyostelium genome has revealed a vast repertoire of secondary metabolite genes, which emphasizes the significant role of small molecules in dictating its life cycle. Our group is interested to dissect out various enzyme systems involved in biosynthesis of these metabolites, which orchestrate the cascade of events leading to multicellular development. The genome of this organism has revealed an astoundingly large number of Type I PKSs, which are known to utilize a thio-template-based mechanism of biosynthesis. In this mechanism both starter and intermediate moieties are covalently acylated as thioesters either on the cysteine residue of ketosynthase (KS) domain or on the phosphopantetheine arm of acyl carrier protein (ACP). Phosphopantetheinyl modification of the ACP domains is a post-translational event and is essential for activity of PKSs. This modification is catalyzed by a group of enzymes known as phosphopantetheinyl transferases (PPTases). We have characterized two phosphopantetheinyl transferases that are essential for the survival of *Dictyostelium* – DiAcpS and DiSfp. We demonstrate that the two PPTases are expressed during all the stages of its life cycle. The two essential PPTases DiAcpS and DiSfp are functionally discrete and non-redundant in nature. Furthermore, biochemical studies unambiguously show that DiSfp is required for the activation of multifunctional PKS/FAS, whereas, DiAcpS can modify only the stand-alone ACP. We have elegantly resolved the recognition ability of these PPTases by using several intact multifunctional PKSs as well as mono- and di-domain protein fragments. In all the instances investigated in this study, the smaller domain fragments of type I multifunctional proteins retained their specificity to be modified by DiSfp and DiAcpS did not show activity with these engineered domains. Clearly, our work shows that the specificity of phosphopantetheinylation is not dictated by the modular architecture, but in fact involves specific recognition of the carrier domains.

The inability of DiAcpS to phosphopantetheinylate type I assembly line prompted us to search for type II ACP in Dicty. Although ACP sequences could be fairly divergent, a careful analysis of the genome using NRPS-PKS database provided DDB0184099 as the only significant hit. Notably, this ACP has been annotated as NADH dehydrogenase ubiquinone 1 in the DictyBase suggesting it to be a part of the mitochondrial respiratory chain. *Dictyostelium* stand-alone ACP (DiACP) clearly showed homology with the yeast ACP, which possesses N-terminal leader sequence of about 35 amino acids that is proposed to be toxic for its expression in *E. coli*. Interestingly, expression of complete *diacp* gene in *E. coli* yielded truncated protein with deletion at the N-terminus. Our results however show that DiAcpS and DiSfp exhibit stringent selectivity towards type II and type I ACPs respectively. In conclusion, we have shown clear demarcation in the functional roles of two PPTases in Dictyostelium. Through their action on PKS/FAS systems, these enzymes are expected to be vital in the initiation and progress of developmental pathway.

Publications

Original peer-reviewed articles

1. Arora P, Goyal A, Natarajan VT, Rajakumara E, Verma P, Gupta R, Yousuf M, Trivedi OA, Mohanty D, Tyagi A, Sankaranarayanan R* and Gokhale RS* (2009) Mechanistic and functional insights into fatty acid activation in *Mycobacterium tuberculosis*. *Nat Chem Biol* **5**:166-173. (*corresponding authors)
2. Ansari MZ, Sharma J, Gokhale RS and Mohanty D. (2008) *In silico* analysis of methyltransferase domains involved in biosynthesis of secondary metabolites. *BMC Bioinformatics* **9**:454.
3. Chopra T, Banerjee S, Gupta S, Yadav G, Anand S, Surolia A, Roy RP, Mohanty D, and Gokhale RS (2008) Novel intermolecular iterative mechanism for biosynthesis of mycoketide catalyzed by a bimodular polyketide synthase. *PLoS Biology* **6**:e163.
4. Goyal A, Saxena P, Rahman A, Singh P, Kasbekar D, Gokhale RS*, and Sankarnarayanan R* (2008) Structural insights into biosynthesis of resorcinolic lipids by a type III polyketide synthase in *Neurospora carssa*. *J Struct Biol* **162**:411-421. (*corresponding authors)

Reviews Proceedings

1. Chhabra A and Gokhale RS (2008) Novel paradigms of complex lipid biosynthetic machinery of *Mycobacterium tuberculosis*. **In**: *Mycobacterium and Cell Biology* (Eds: Parish T and Brown A), Horizon Press, 66-78.

Understanding the regulation of DNA replication

Principal Investigator: Sandeep Saxena

PhD Students: Aparna Sharma
Manpreet Kaur
Ananya Kar

We are studying DNA replication and our objective is to understand the regulation of replication proteins during normal conditions and during stress.

We propose to identify the protective machinery that ensures precise DNA replication. It is believed that when cell experiences stress such as UV and gamma irradiation it degrades its replication proteins to prevent replication initiation and we are trying to identify the replication proteins that are degraded. We have initiated this effort by identifying replication proteins and some modifications induced in upon stress utilizing mammalian cells and intracellular parasite, *Leishmania.* After characterizing the modifications, we would assess its biological consequence. We believe that some of the human cancers arise from malfunctioning of these protective pathways.

The initiation of DNA replication involves the formation of a number of protein complexes that eventually results in the formation of two replication forks at each origin. Initiation of DNA replication consists of two steps. The first step involves the loading of the six-subunit protein, origin recognition complex (ORC), Cdc6, Cdt1 and Mcm2-7 proteins on the replication origins to form the pre-replicative complex from late mitosis to early G1 phase. In the second step, Mcm10 is loaded onto chromatin which stimulates the phosphorylation of the presumed replicative helicase, Mcm2-7 complex by Dbf4-Cdc7 kinase. Once Mcm10 gets loaded it facilitates the loading of Cdc45 and GINS onto chromatin resulting in the formation of a post-replicative complex composed of Cdc45/Mcm2-7/GINS proteins. Finally, the completion of replisome formation is marked by the association of PCNA, RFC, and DNA polymerases δ and ε.

In order to understand the regulation of replication apparatus during stress, we exposed radiation stress to cells and analyzed the specific response. We have observed that after UV irradiation of mammalian cells, an essential replication protein, RP1, is rapidly proteolyzed. Downregulation of RP1 protein band was confirmed by different antibodies and siRNA. Downregulation of RP1 following UV-irradiation is specific as levels of most of the proteins remained unchanged. mRNA levels of RP1 are not altered after UV-irradiation, indicating that decrease is due to changes in protein stability. We observed that RP1 downregulation occurs specifically after UV-irradiation and is not mediated by the apoptotic pathway. Apoptotic inhibitors do not stabilize RP1 after exposure to UV radiation. We demonstrated that exogenous RP1 is downregulated after exposure to UV-radiation: stable cells expressing Cdt1-HA and RP1-HA degraded RP1 on exposure to UV radiation.

Artificial stabilization of RP1 leads to its sequestration in nucleoli

In order to understand the cellular regulation of RP1, we performed indirect immunofluorescence with an N-terminus RP1 antibody, Ab (N), and observed that in an asynchronous population around 40-50% cells retain RP1 protein, which is completely

absent from the nucleoli (Figure-1A). There was no signal with prebleed or after RP1 siRNA (Figure-1C, Figure-1D and 1E, *compare GL2 and RP1 siRNA*). Following UV-irradiation, RP1 levels reduced to very low levels (Figure-1B). Immunofluorescence was also carried out with a different RP1 antibody, Ab (FL), which confirmed the localization and degradation of RP1 post UV-irradiation. If RP1 is perceived as a detrimental molecule under stress to which the cell is intolerant, we hypothesized that any increase in its activity would be promptly counteracted. To test this, we stabilized RP1 utilizing proteasome inhibitor, MG-132 and we observed a striking regulation. RP1, which excludes nucleoli in all unperturbed cells, was completely sequestered into the nucleoli after its stabilization (Figure 1E, F). It seems that the cell could not bear enhanced RP1 activity and in an attempt to downregulate its activity, sequestered it into the nucleolus. To rule out any artifact of visualization or non-specific effects, we examined the localization of Cyclin A under similar conditions, which does not show any changes in localization with UV or MG132 treatment.

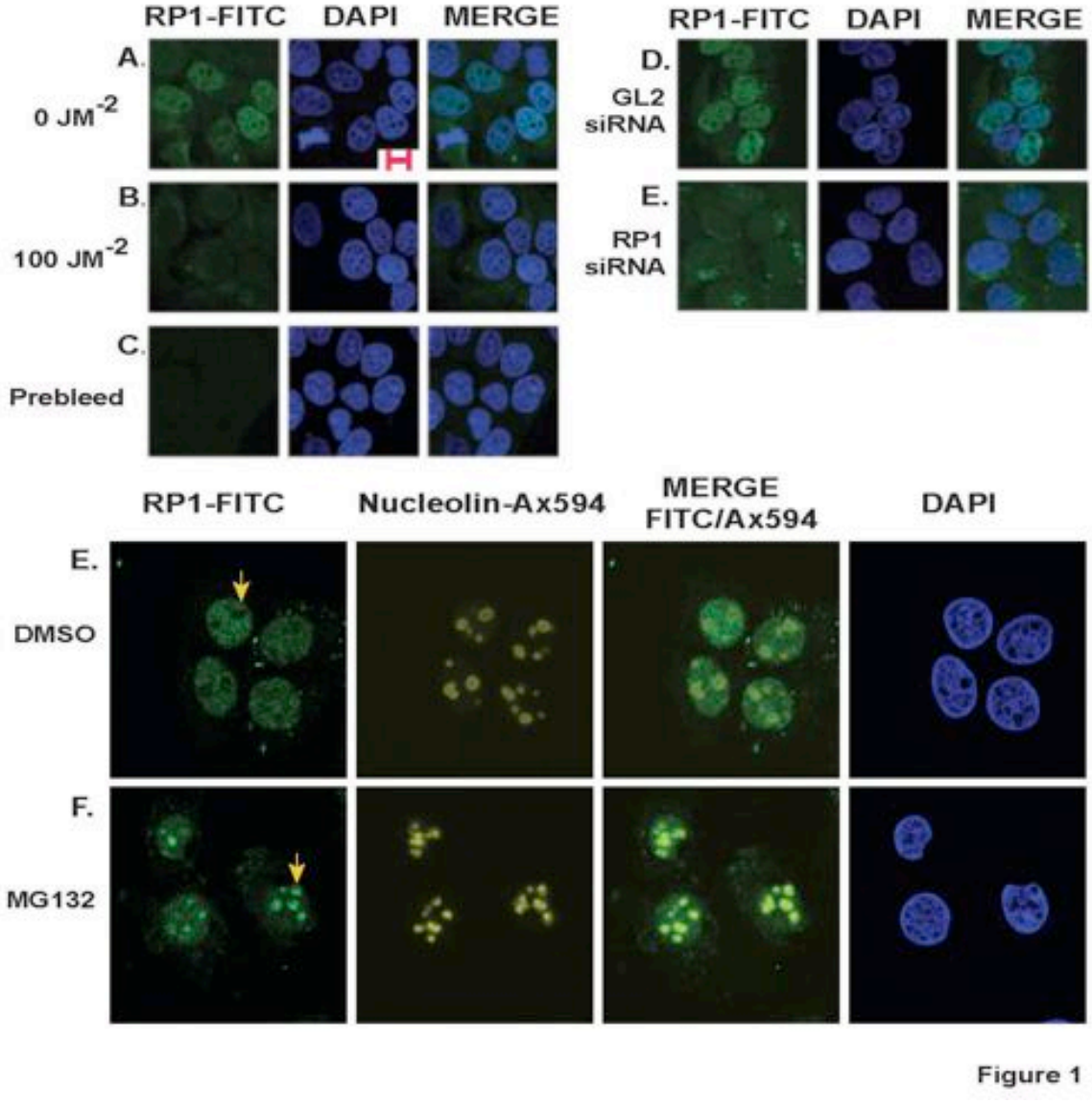

Figure-1 *Regulation of RP1 in different environments. (A-C). Indirect immunofluorescence confirms the degradation of RP1 after UV-irradiation. Unperturbed (A) and 100 JM^{-2} UV-irradiated (B) mammalian cells were fixed and immunofluorescence was performed using anti-RP1 [Ab (N)]*

antibody as described in experimental procedures. Localization of RP1 was displayed with anti-rabbit FITC secondary antibody (left panel) and DNA was stained with 4, 6-diamidino-2-phenylindole (DAPI) (middle panel). Right panel shows a merge of the images in the left and middle panels. Prebleed of anti-RP1 [Ab (N)] antibody does not show any signal (C). Scale bar is 10 microns. (D, E). RNAi confirms RP1 immunofluorescence signal. To confirm that the FITC signal is from RP1 protein, RNAi against RP1 was carried out in mammalian cells. Mammalian cells were transfected with GL2 or RP1 siRNA oligos and later processed for immunofluorescence with anti-RP1 [Ab (N)] antibody. (E, F). Stabilization of RP1 is repelled by sequestration into the nucleoli. Cells were either treated with DMSO or 50 μM MG-132 for 8 hr and processed for immunofluorescence with anti-RP1 [Ab (N)] antibody. Localization of RP1 and nucleolin was displayed with anti-rabbit FITC (left panel) and anti-mouse Alexa 594 (middle-left panel) secondary antibodies respectively. DNA was stained with DAPI (right panel). Middle-right panel shows a merge of the images in the left and middle-left panels. The arrow points to the nucleolus, visible as dense, ovoid structure in the microscope, confirmed by localization of nucleolin antibody (Note that in unperturbed cells (E), RP1 is completely absent from the nucleoli, whereas MG132 treatment (F) leads to RP1 sequestration in the nucleoli).

Therefore, utilizing two independent antibodies against the endogenous protein, we have observed that in most actively growing asynchronous population, RP1 excludes nucleoli. However, when the proteasome function was inhibited, the stabilized RP1 localized to nucleoli. It seems that the cellular machinery was intolerant to the stabilization of RP1 and repelled it by sequestration in to the nucleoli. In that case, we are looking at similar response of cell, downregulating RP1, under two different circumstances. In non-irradiated cells, normal RP1 activity is permissible but overactive RP1 (caused by MG-132 stabilization) is not and this is thwarted immediately by sequestration in nucleoli. After irradiation, cells cannot tolerate even normal RP1 levels and proteolyses it. Therefore it seems that in these two different stressed environments, the cell responded in the similar manner, by downregulating RP1 activity. We are now trying to identify the factors involved in RP1 regulation. Summing up, this work illuminates the protective machinery of the cell that targets the replication apparatus.

Identification of novel gene(s) for familial Parkinson's disease

Principal Investigator: Ramesh C Juyal

Project Fellow: Swati Verma

Collaborators: BK Thelma, *UDSC, New Delhi*
Madhuri Behari, *AIIMS, New Delhi*
Uday Muthane, *NIMHANS, Bangalore*

Parkinson's disease (PD) continues to be a major neurodegenerative disorder in the elderly, afflicting about 1.2% of all above 55years of age. A strong genetic basis of the familial forms of PD is evident from the discovery of seven genes namely α-synuclein, Parkin, UCHL1, LRRK2, DJ-1, PINK1 and ATP13A2 and five loci in the last decade. Mutations in these genes however, account for less than 10% of all familial cases tested globally, implying that more gene(s) remain to be identified. On the other hand, understanding the etiology of majority of sporadic cases has been rather limited. Further, the pathogenic mechanisms underlying the characteristic loss of dopaminergic neurons from the *substantia nigra pars compacta* of the brain leading to deficiency of dopamine in PD remains ill understood.

Only a negligible proportion of the familial cases of PD from India, recruited in our ongoing projects have shown mutations in three (Parkin, PINK1 and DJ1) of the 6 above mentioned genes (Nagar et al., 2001; Chaudhary et al, 2006., Punia et al.2006; ms. on PINK1 and DJ1 genes under preparation). Availability of both nuclear and extended families with multiple affected and unaffected members in India and absence of mutations in known genes in these families are very useful resource for genome wide scan for linkage analysis and identification of new gene(s). Thus new gene identification and unraveling the genetic basis of familial and sporadic PD is the major focus of the ongoing project in the laboratory. The proposed work is expected to make significant contributions to PD genetics research.

Mutations in seven known PD genes viz. α-synuclein, Parkin, UCHL1, LRRK2, DJ-1, PINK1 and ATP13A2 account only for a small proportion of familial PD cases screened globally implying that there are yet unidentified PD causing gene(s) in the genome.

Thus, identification of novel disease causing gene(s) using the large number of informative families with PD from India combined with currently available powerful approaches for whole genome scans and subsequent refining of the linked regions is the main objective of this project.

Novel gene(s) identification is envisaged to contribute significantly to the understanding of the pathophysiological mechanism underlying PD.

Work upon the families recruited in the 1st year and recruitment of new families with PD

Of the five families that were selected for linkage analysis based on the informativeness of the estimated power of the families in the first year of the project work, two families namely family 1 and 4 have been eliminated from linkage analysis study. It was not possible to recruit either parents/ or any additional unaffected members in one family,

and in another family, a mutation in PINK 1 gene was identified in a heterozygous state but only in one affected member and therefore these families were excluded from the study. Families 2, 5 and 6 have been taken forward for genetic analysis and progress is detailed below.

Family 03, 08, 11 and 12 which were tentatively selected for inclusion in the previous year were reviewed critically but due to inadequate sample size, these families have been dropped from the study. Remaining nine of the 18 families were also not found suitable for linkage analysis and therefore excluded from the study.

During the second year of the project, two large families with multiple members affected with PD, one from Himachal Pradesh and another from Karnataka have been identified and recruited. Detailed clinical documentation including videotaping has been made for both the affected and unaffected members from these two families. Blood samples have been collected as per study design and DNA banking has been completed. In addition to these two families, 10 more have been identified based on initial clinical assessment by the collaborating clinicians and are being followed up for possible inclusion/recruitment in the study.

Genetic Analysis

Progress of linkage analysis in the families recruited to date is summarized below:

In family 2 where over 50% of the genotyping failure was observed in the first year, regenotyping using ABI MD 10 panel is in progress. Genetic analysis on the two new families recruited this year has not been initiated yet.

Family 5 and 6: Genotyping using the ABI MD 10 panel, 400 markers for a few blanks/repeats which were recorded in these two families, (with an apparently autosomal recessive disease) at the end of the previous year, has been completed. With the complete genotyping data we have carried out two point linkage analysis using MLINK. Similar to MERLIN that we had used in the previous year, we identified several putative linked loci on different chromosomes in all these families and these are tabulated below.

Family ID	Max lod score observed	Chromosome
Family 5	0.72	1q31-41, 2p24-15, 2q23-36, **3p26-24**, 4p15.1-21,4q22-27 6q23-27, 9q22-q33, **14q11-22, 15q14-25**, 19q12-13.4
Family 6	0.99-1.09	**3p26-25**, 4p16-15.3, 4q31-32, 7p22-21, 10q21-24, 11q23-25, 13q12-13, **14q11.2-13, 15q12-21**, 17pter-p13.1, 18p11.2-22

In comparison to MERLIN (max lod score 0.6), higher lod scores were observed in MLINK (max lod score 1.19). But still, we failed to observe the acceptable lod score of ≥ 3 in these families. Considering the small size of the family, the number of informative meiosis are limited and hence observing low lod scores is not surprising.

However, since both these families belong to same geographical region and also because lod scores can be additive, we pooled the lod scores of these two families which gave us a total of approx 2. To begin with, we have selected three chromosomal regions - 3p26-24, 14q11-13.3 and 15q14-21 with informative lod scores that are shared in the two families and have initiated *in silico* analysis of the regions using bioinformatics tools. A total of 137, 220 and 63 genes are present in these linked regions on chromosomes 3, 14 and 15 respectively. Screening for the exact number of brain specific genes out of these total 420 genes is underway.

Based on that number we will either proceed with further fine mapping by using more closely spaced markers (~1 cM markers) or employ deep sequencing strategy to cover the linked regions to identify the disease causing gene(s)/mutation(s).

Alternate /Additional Linkage analysis strategy using Illumina 6200K SNP linkage panel:

Most genome wide scan for linkage analysis are carried out using ABI MD 10 panel. With the availability of the new 6200K SNP linkage panel, 6200 SNP markers Vs 400 MS markers are expected to give dense mapping profiles and therefore, smaller linked regions. With this expectation, genotyping of the two families were initiated in parallel.
We have carried out two point linkage analysis on this data set using MLINK and the results have been tabulated.

Chromosomal regions with informative lod scores were tabulated alongside the lod scores obtained using the microsatellite data. Utilising the dense SNP marker distribution available along these regions, generation of haplotypes for the family members to narrow down the boundaries of linked regions is underway.

Additional analysis done:

In the light of copy number variations being reported for PD genes, MLPA based copy number estimation for α-synuclein, Parkin, PINK and DJ 1 genes have been initiated in Family1, 5 and 6. This is essential before heavy investments are made on narrowing down the critical region, resequencing of candidate genes or deep sequencing of linked regions.

Publications

Original peer-reviewed articles

1. Sharma S, Das M, Kumar A, Marwaha V, Shankar S, Aneja R, Grover R, Arya V, Dhir V, Gupta R, Kumar U, Juyal RC and Thelma BK (2008) Interaction of genes from influx-metabolism-efflux pathway and their influence on methotrexate efficacy in rheumatoid arthritis patients among Indians. *Pharmacogenet Genomics* **18**:1041-1049.

ANCILLARY ACTIVITIES

Production of transgenic animals

Principal Investigator: Subeer S Majumdar

Project Associates/Fellows: Neerja Wadhwa
Neetu Kunj
Mohd Abul Rehan Usmani
Nirmalya Ganguli

PhD Students: Deepika Sharma

Collaborators: Vani Brahmachari, *BRACBR, Delhi*
Samit Chattopadhyaya, NCCS, Pune
Mitradas M. Panicker, *NCBS, Bangalore*
Rakesh Tyagi, *JNU, New Delhi*

Theme of the research is to produce transgenic animals for using them as a system for the study of functional genomics and mammalian development. The objective is to develop transgenic animal models using genes relevant to human health and diseases as well as to establish embryo cloning technology for making such studies more efficient.

Analysis of epigenetic regulation of CMV activity in transgenic mice: The expression of genes in transgenic mice is known to be influenced by the site of integration even when they carry their own promoter elements and transcription factor binding sites. The cytomegalovirus (CMV) promoter, a strong promoter often used for transgene expression in mammalian cells in culture, is known to be silenced by DNA methylation and histone deacetylation but there is no report on the role of histone methylations in its regulation.

Two transgenic lines from plasmid pCTGFP (transgene carrying SV40ori/EPR, 22 CTG repeats and CMV-GFP) have been generated and their analysis indicates that all lines have stable integration of the transgene and show germline transmission. In one of the two transgenic lines GFP is expressed in several tissues like liver, kidney, brain, spleen and gonads, while in second line the expression is restricted to testis only.

It has been observed that silencing of CMV promoter is dependent on the site of transgene integration, except in testis, and the nature of DNA and histone methylations strongly correlate with the expression status of the reporter. It has also been observed that silenced CMV promoter interacts *in vivo*, with Methyl CpG binding protein 2 (MeCP2), a recruiter of histone deacetylases (HDACs) and histone (H3K9) methyl transferase. Detection of H3K4 methylation in this study correlates with the ability of the promoter to get reactivated under appropriate conditions. Present study show that the CMV promoter driven expression in transgenic mice is dependent on the site of integration.

Regulation of T_H1-T_H2 decision by SMAR1: SMAR1, a matrix-associated region binding protein, have been shown to play a pivotal role in T-cell development through direct transcriptional modulation at TCRβ locus. Earlier it was shown that SMAR1 is a transcriptional repressor and recruits HDAC1 to target promoters. Now we show that SMAR1 facilitates T_H differentiation towards T_H2 lineage commitment by inhibiting T_H1-specific transcription factor T-bet, encoded by *Tbx21*. SMAR1 expression significantly increased only upon T_H2 polarization indicating a control of IFNg and T-bet

expression. We have now generated another transgenic mouse in which SMAR1 is co-expressed with GFP. Thus, the cells expressing SMAR1-GFP can directly be visualized or sorted for downstream applications. We have checked the expression of both GFP and SMAR1 in these mice. These will now be used at NCCS for understanding Th1-Th2 regulation. The *in vivo M. tuberculosis* infection studies with these mice will be performed at JALMA Institute of Leprosy, Agra. An aerosol infection with *M. tuberculosis* in SMAR1 transgenic mice will enable us to evaluate the Th2 bias and susceptibility to infection.

Generation of 5-HT2A-EGFP transgenic animals: 5-HT is a neurotransmitter known for anxiety disorders. In mammals, this neurotransmitter has a large number of G protein-coupled receptors. Transgenic mice over-expressing 5-HT2A receptors (serotonin receptor 2A) with EGFP as reporter gene were generated for understanding the role of ligand-receptor interactions *in vivo* and receptor activity in central nervous system and in the periphery. GFP expression was detected in some animals confirming the transgene integration. Homozygous line has been generated at NII. All animals are sent to NCBS for further analysis.

PXR: PXR, a human transcription factor (Pregnane and Xenobiotic Receptor) is a novel member of nuclear receptor super family which acts as a xenosensor in our body combating chemical insults. It also metabolizes several drugs in liver for ensuring their beneficial effects. The possibility of presence of various PXR isoforms in different tissues suggest utilization of combinatorial mechanisms to regulate different sets of genes under varied physiological and pathogenic conditions. This also suggests a diverse role of this receptor. To begin with, an attempt is being made to generate transgenic animals expressing luciferase driven by the promoter of PXR to detect the organs in which this transcription factor is active.

Publications

Original peer-reviewed articles

1. Mehta AK, Majumdar SS, Alam P, Gulati N and Brahmachari V (2009) Epigenetic regulation of cytomegalovirus major immediate-early promoter activity in transgenic mice. *Gene* **428**:20-24.

Publications

Original peer-reviewed articles

1. Abdullah N, Srinivasan B, Modiano N, Cresswell P and Sau AK (2009) Role of individual domains and identification of internal GAP in human guanylate binding protein-1. **J Mol Biol** 386: 690-703.

2. Alone PV and Garg LC (2008) Secretory and GM_1 receptor binding role of N-terminal end of LTB in *Vibrio cholerae*. **Biochem Biophys Res Commun** 376: 770-774.

3. Ansari MZ, Sharma J, Gokhale RS and Mohanty D (2008) *In silico* analysis of methyltransferase domains involved in biosynthesis of secondary metabolites. **BMC Bioinformatics** 9: 454.

4. Arora P, Goyal A, Natarajan VT, Rajakumara E, Verma P, Gupta R, Yousuf M, Trivedi OA, Mohanty D, Tyagi A, Sankaranarayanan R* and Gokhale RS*. (2009) Mechanistic and functional insights into fatty acid activation in Mycobacterium tuberculosis. **Nat Chem Biol** 5: 166-73. (* corresponding authors)

5. Banerjee T, Sharma SK, Surolia N, Surolia A (2008) Epigallocatechin gallate is a slow-tight binding inhibitor of enoyl-ACP reductase from Plasmodium falciparum. **Biochem Biophys Res Commun** 377: 1238-1242.

6. Bharati K, Rani R and Vrati S (2009) Evaluation of Japanese encephalitis virus DNA vaccine candidates in rhesus monkeys [*Macaca mulatta*]. ***Vaccine*** 27:10-16.

7. Bukovsky A, Caudle MR, Gupta SK, Svetlikova M, Selleck-White R, Ayala AM and Dominguez R (2008) Mammalian neo-oogenesis and expression of meiosis-specific protein SCP3 in adult human and monkey ovaries. **Cell Cycle** 7: 683-686.

8. Bukovsky A, Gupta SK, Bansal P, Chakravarty S, Chaudhary M, Svetlikova M, White RS, Copas P, Upadhyaya NB and Meter SEV (2008) Production of monoclonal antibodies against recombinant human zona pellucida glycoproteins: utility in immunolocalization of respective zona proteins in ovarian follicles. **J Reprod Immunol** 78: 102-114.

9. Campbell, C. T., Aich, U., Weier, C. A., Wang, J. J., Choi, S. S., Wen, M. M., Maisel, K., Sampathkumar, S. G., Yarema, K. J. (2008) Targeting pro-invasive oncogenes with short chain fatty acid-hexosamine analogues inhibits the mobility of metastatic MDA-MB-231 breast cancer cells. **J Med Chem** 51: 8135-8147.

10. Chaudhry A, Das SR, Jameel S, George A, Bal V, Mayor S and Rath S (2008) HIV-1 Nef induces a Rab 11-dependent routing of endocytosed immune costimulatory proteins CD80 and CD86 to the Golgi. **Traffic** 9: 1925-1935.

11. Chetnani B, Das S, Kumar P, Surolia A, Vijayan M (2009) Mycobacterium tuberculosis pantothenate kinase: possible changes in location of ligands during enzyme action. **Acta Crystallogr D Biol Crystallogr** 65: 312-325.

12. Chiu PC, Wong BS, Chung MK, Lam KK, Pang RT, Lee KF, Sumitro SB, Gupta SK and Yeung WS (2008) Effect of native human zona pellucida glycoprotein 3 and 4 on acrosome reaction and zona pellucida binding of human spermatozoa. **Biol Reprod** 79: 869-877.

13. Chiu PCN, Wong BST, Lee CL, Pang RTK, Lee K-F, Sumitro SB, Gupta SK and Yeung WSB (2008) Native human zona pellucida glycoproteins: Purification and binding properties. **Human Reprod** 23: 1385-1393.

14. Chopra T, Banerjee S, Gupta S, Yadav G, Anand S, Surolia A, Roy RP, Mohanty D and Gokhale RS (2008) Novel intermolecular iterative mechanism for biosynthesis of mycoketide catalyzed by a bimodular polyketide synthase. **PLoS Biology** 6: e163.

15. Choudhury S, Ganguly A, Chakrabarti K and Gupta SK (2009) DNA vaccine encoding chimeric protein encompassing epitopes of human ZP3 and ZP4: Immunogenicity and characterization of antibodies. **J Reprod Immunol** 79: 137-147.

16. Das J, Arora P, Gracias D, Praveen A, Raj BPJ, Martin E and Pal R (2008) Endogenous humoral autoreactive immune responses to apoptotic cells: Effects on phagocytic uptake, chemotactic migration and antigenic spread. **Eur J Immunol** 38: 3561-3574.

17. Damodaran D, Jeyakani J, Chauhan A, Kumar N, Chandra NR, Surolia A. CancerLectinDB: a database of lectins relevant to cancer (2008) **Glycoconj J** 25: 191-198.

18. Dhup S and Majumdar S (2008) Transgenesis via permanent integration of genes in repopulating spermatogonial cells *in vivo.* **Nature Methods** 5: 601-603.

19. Garg M, Kanojia D, Khosla A, Dudha N, Sati S, Chaurasiya D, Jagadish N, Seth A, Kumar R, Gupta S, Gupta A, Lohiya NK and Suri A (2008) Sperm-associated antigen 9 Is associated with tumor growth, migration, and invasion in renal cell carcinoma **Cancer Res** 68: 8240-8248.

20. Gopal PNV, Rentala S, Roy S, Wadhwa R, Sharma S, Roychaudhury PK, Mukhopadhyay A and Ray AR (2008) An artificial niche for expansion of long-term engraftable mouse hematopoietic cells. **J Stem Cells** 3: 245-254.

21. Goyal A, Saxena P, Rahman A, Singh P, Kasbekar D, Gokhale RS* and Sankarnarayanan R* (2008) Structural insights into biosynthesis of resorcinolic lipids by a type III polyketide synthase in Neurospora carssa. ***J Struct Biol*** 162: 411-21.
(* corresponding authors)

22. Gratraud P, Surolia N, Besra GS, Surolia A, Kremer L. Antimycobacterial Activity and Mechanism of Action of NAS-91 (2008) **Antimicrob Agents Chemother** 52: 1162-1166.

23. Gupta P, Gaur V and Salunke DM (2008) Purification, identification and preliminary crystallographic studies of a 2S albumin seed protein from Lens culinaris. **Acta Crystallogr Sect F Struct Biol Cryst Commun** 64:733-736.

24. Gupta G, Sinha S, Surolia A (2008). Unfolding energetics and stability of banana lectin. **Proteins** 72: 754-760.

25. Gupta G, Gemma E, Oscarson S, Surolia A (2008) Defining substrate interactions with calreticulin: an isothermal titration calorimetric study. **Glycoconj J** 25: 797-802.

26. Gupta S, Modak R, Surolia N, Surolia A (2009) Partial molar volumes of acyl carrier proteins are related to their states of acylation. **Biochem Biophys Res Commun** 380: 763-768.

27. Gupta G, Vishveshwara S, Surolia A (2009) Stability of dimeric interface in banana lectin: Insight from molecular dynamics simulations. **IUBMB Life** 61: 252-260.

28. Gupta V, Gupta RK, Khare G, Surolia A, Salunke DM and Tyagi AK (2008) Crystallization and preliminary X-ray diffraction analysis of biotin acetyl-CoA carboxylase ligase (BirA) from Mycobacterium tuberculosis. **Acta Crystallogr Sect F Struct Biol Cryst Commun** 64:524-527.

29. Gupta V, Gupta RK, Khare G, Salunke DM and Tyagi AK (2008) Cloning, expression, purification, crystallization and preliminary X-ray crystallographic analysis of bacterioferritin A from Mycobacterium tuberculosis. **Acta Crystallogr Sect F Struct Biol Cryst Commun** 64:398-401.

30. Gupta, N. and Banerjea, AC (2009) C-terminal half of HIV-1 Vif C possesses major determinant for APOBEC3G degradation. **AIDS** 23: 141-143.

31. Gupta N, Bano Aalia, Sharma Y and Banerjea AC (2008) Potent knock down of the X RNA of hepatitis B by a novel chimeric-siRNA-ribozyme construct and modulation of intracellular target RNA by selectively disabled mutants. **Oligonucleotides** 18: 225-234.

32. Gupta A, Geetha N, Mani J, Upadhyay P, Katoch VM, Natrajan M, Gupta UD and Bhaskar S (2009) Immunogenicity and protective efficacy of *Mycobacterium w* against *Mycobacterium tuberculosis* in mice immunized with live versus heat-killed *M. w* by the aerosol or parenteral route. **Infect Immun** 77: 223-231

33. Horning JL, Sahoo SK, Vijayaraghavalu S, Dimitrijevic S, Vasir JK, Jain TK, Panda AK and Labhasetwar C (2008) 3-D Tumor Model for In Vitro Evaluation of Anti-cancer Drug. **Molecular Pharmaceutics** 5: 849-862.

34. Iyer J, Kaprakkaden A, Chaudhary M and Shaha C (2008) Crucial role of cytosolic tryparedoxin peroxidase in Leishmania donovani survival, drug response and virulence. **Mol Microbiol 68**: 372-391.

35. Kanojia D, Garg M, Gupta S, Gupta A and Suri A (2009) Sperm associated antigen 9 (SPAG9), a novel biomarker for early detection of breast cancer. **Cancer Epidemiol Biomarker Prev** 18: 630-639.

36. Kar NP, Sikriwal D, Rath P, Choudhary RK and Batra JK (2008) *Mycobacterium tuberculosis* ClpC1: characterization and role of the N-terminal domain in its function. **FEBS Journal** 275: 6149–6158.

37. Kaushik S, Mohanty D* and Surolia A* (2008) Role of metal ions in substrate recognition and stability of Concanavalin A: A molecular dynamics study. **Biophys J** 96: 21-34. (*corresponding authors)

38. Khaparde SS, Roychoudhury PK, Gomes J and Mukhopadhyay A (2008) External modulation of HT-1080 human fibrosarcoma cells improves urokinase production. **Biotechnol Prog** 24: 1325-1332.

39. Khurana S and Mukhopadhyay A (2008) Hematopoietic progenitors from early murine fetal liver possess hepatic differentiation potential. **Am J Pathol** 173: 1818-1827.

40. Khurana S and Mukhopadhyay A (2008) *In vitro* transdifferentiation of adult hematopoietic stem cells: an alternate source of hepatocytes. **J Hepatol** 49: 998-1007.

41. Kumar R, Srivastava R, Singh RK, Surolia A, Rao DN. Activation and inhibition of DNA methyltransferases by S-adenosyl-L-homocysteine analogues (2008) **Bioorg Med Chem** 16: 2276-2285.

42. Kulkarni KA, Katiyar S, Surolia A, Vijayan M, Suguna K (2008) Structure and sugar-specificity of basic winged-bean lectin: structures of new disaccharide complexes and a comparative study with other known disaccharide complexes of the lectin. **Acta Crystallogr D Biol Crystallogr** D64: 730-737.

43. Li Z and Sau AK (2009) Probing the subunit-subunit interaction of the tetramer of *E. coli* KDO8P synthase by electrospray ionization mass spectrometry. **Chinese J. of Chemistry** 27: 1-10.

44. Madan R, Krishnamurthy G and **Mukhopadhyay A** (2008) SopE-mediated recruitment of host Rab5 on phagosomes inhibits salmonella transport to lysosomes. ***Methods Mol Biol*** 445: 417-437.

45. Majumdar S, Dhup S and Usmani A (2008). Deathless transgenesis: A new spermatogonia mediated *in vivo* approach for generation of transgenic mice. **Nature Protocols** DOI: 10.1038/nprot.2008.124.

46. Mishra S, Karmodiya K, Parasuraman P, Surolia A, Surolia N (2008) Design, synthesis, and application of novel triclosan prodrugs as potential antimalarial and antibacterial agents. **Bioorg Med Chem** 16: 5536-5546.

47. Mishra S, Karmodiya K, Surolia N, Surolia A (2008) Synthesis and exploration of novel curcumin analogues as anti-malarial agents. **Bioorg Med Chem** 16: 2894-2902.

48. Mehta AK, Majumdar SS, Alam P, Gulati N and Brahmachari V (2009) Epigenetic regulation of cytomegalovirus major immediate-early promoter activity in transgenic mice. **Gene** 428: 20-24.

49. Murthy BN, Sinha S, Surolia A, Indi SS, Jayaraman N (2008) SPR and ITC determination of the kinetics and the thermodynamics of bivalent versus monovalent sugar ligand-lectin interactions. **Glycoconj J** 25: 313-321

50. Naha PC, Kanchan V, Manna PK and Panda AK (2008) Improved bioavailability of orally delivered insulin using Eudragit L30D coated PLGA microparticles. **J Microencapsulation** 25: 248-256.

51. Nayak B, Panda AK, Ray P and Ray AR (2009) Formulation, characterization and evaluation of rotavirus encapsulated PLA and PLGA particles for oral vaccination. **J Microecapsulation** 26: 154-165.

52. Parikh A, Verma SK, Khan S, Prakash B* and Nandicoori VK* (2009) PknB-mediated phosphorylation of novel substrate, N-Acetylglucosamine-1-Phosphate Uridyltransferase, modulates its acetyltransferase activity. **J Mol Biol** 386: 451-464. (* corresponding authors)

53. Premi S, Srivastava J and Ali S (2009) Unique signatures of the natural background radiation on the human Y chromosome from Kerala (INDIA). **PLoS One** 4: e4541.

54. Premi S, Srivastava J, Panneer G and Ali S (2008) Startling mosaicism of the Y chromosome and tandem duplication of SRY and DAZ genes in patients with Turner Syndrome **PLoS One** 3: e3796

55. Purushothaman S, Gupta G, Srivastava R, Ramu VG, Surolia A. Ligand specificity of group I biotin protein ligase of Mycobacterium tuberculosis (2008) **PLoS ONE** 3: e2320.

56. Rohatgi S, Ganju P and Sehgal D (2008) Systematic design and testing of nested RT-PCR primers for specific amplification of mouse rearranged/expressed immunoglobulin variable region genes from small number of B cells. **J Immunol Methods** 339: 205-219.

57. Roy S, Gupta N, Nithya S, Mondal T, Banerjea AC and Das S (2008) Sequence specific cleavage of Hepatitis C virus RNA by DNA-enzymes: Inhibition of viral RNA translation and replication. **J Gen Virol** 89: 1579 -1586

58. Srivastava J, Premi S, Kumar S and Ali S (2008) Organization and differential expression of the GACA/GATA tagged somatic and spermatozoal transcriptomes in buffalo *Bubalus bubalis.* **BMC Genomics** 20: 132.

59. Sharma S, Das M, Kumar A, Marwaha V, Shankar S, Aneja R, Grover R, Arya V, Dhir V, Gupta R, Kumar U, Juyal RC and Thelma BK (2008) Interaction of genes from influx-metabolism-efflux pathway and their influence on methotrexate efficacy in rheumatoid arthritis patients among Indians. ***Pharmacogenet Genomics*** 18: 1041-1049.

60. Singh V and Srivastava M (2008) Enhancer blocking activity of the insulator at *H19-ICR* is independent of chromatin barrier establishment. **Mol Cell Biol** 28: 3767-3775.

61. Sharma SK, Kumar G, Kapoor M, Surolia A (2008) Combined effect of epigallocatechin gallate and triclosan on enoyl-ACP reductase of Mycobacterium tuberculosis. **Biochem Biophys Res Commun** 368: 12-17.

62. Sood V, Ranjan R and Banerjea AC (2008) Functional analysis of HIV-1 subtypes B and C HIV-1 Tat Exons and RGD/QGD motifs with respect to Tat mediated transactivation and apoptosis. **AIDS** 22: 1683-1685.

63. Singh SM, Upadhyay AK and Panda AK (2008) Solubilization at high pH results in improved recovery of proteins from inclusion bodies of *E. coli.* **J of Chemical Technology and Biotechnology** 83: 1126-1134

64. Suri A (2009) Report on the first international symposium on cancer biology (ISCB), November 14–16, 2007, at the National Institute of Immunology, New Delhi, India. **Cancer Immunology, Immunotherapy** 58: 311-316.

65. Sikriwal D, Ghosh P and Batra JK (2008) Ribosome inactivating protein saporin induces apoptosis through mitochondrial cascade, independent of translation inhibition. **International Journal of Biochemistry and Cell Biology** 40: 2880-2888.

66. Sikriwal D, Seth D and Batra JK (2009) Role of catalytic and non-catalytic subsite residues in ribonuclease activity of human eosinophil-derived neurotoxin. **Biological Chemistry** 390: 225-234.

67. Tupperwar N, Vineeth V, Rath S and Vaidya T (2008) Development of a real-time polymerase chain reaction assay for the quantification of Leishmania species and the monitoring of systemic distribution of the pathogen. **Diagn Microbiol Infect Dis 61:** 23-30.

68. Ujjwal Neogi, Vikas Sood, Nidhi Goel, Ajay Wanchu and Banerjea AC (2008) Novel HIV-1 Long terminal Repeat (LTR) sequences of subtype B and mosaic intersubtype B/C recombinants in North India. **Arch Virol** 153: 1961-1966.

69. Vashist S, Anantpadma M, Sharma H, and Vrati S (2009) La protein binds the predicted loop structures in 3'-noncoding region of Japanese encephalitis virus genome: role in virus replication. ***Journal of General Virology*** (In press).

70. Vomastek T, Iwanicki MP, Burack WR, Tiwari D, Kumar D, Parsons JT, Weber MJ* and Nandicoori VK* (2008) ERK2 phosphorylation sites and docking domain on the nuclear pore complex protein Tpr cooperatively regulates ERK2-Tpr interaction. **Mol Cell Biol** 22: 6954-6966. (* corresponding authors)

71. Vyas HK, Pal R, Vishwakarma R, Lohiya NK, Talwar GP (2009) Selective killing of leukemia and lymphoma cells expressing ectopically hCGβ by a conjugate of curcumin with an antibody against hCGβ subunit. **Oncology** 76: 101-111.

Reviews / Proceedings

1. Bal V, Subramanian V and Murthy L (2008) In 'Contraceptive research: Is there a gender-neutral approach? In 'Women's studies in India: a reader' (Ed) Mary E John, Penguin Books India, pp371-380.

2. Bal V and Sharma V (2008) Women scientists meet in Delhi on international women's day. **Current Science** 95: 709-711.

3. Bal V (2008) Why women scientists in India need affirmative action. **Nature India** doi:10.1038/nindia.2008.322; Published online 20 November 2008.

4. Bharati K and Vrati S (2008) Development of recombinant vaccines against Japanese encephalitis. In: Arthropode-borne viral infections: Current status and research (Eds) Raghunath D and Durga Rao C. Tata McGraw-Hill, New Delhi, pp 259-283.

5. Bukovsky A, Gupta SK, Virant-Klun I, Upadhyaya NB, Copas P, Van Meter SE, Svetlikova M, Ayala ME and Dominguez R. Study origin of germ cells and formation of new primary follicles in adult human and rat ovaries. **Methods Mol Biol** 450: 233-265 (2008).

6. Chhabra A and Gokhale RS (2008) Novel Paradigms of Complex Lipid Biosynthetic Machinery of *Mycobacterium tuberculosis*. In: Mycobacterium Genomic and Cell Biology (Eds) Parish T and Brown A, pp 66-78.

7. Doerig C, Billker O, Haystead T, Sharma P, Tobin AB and Waters NC (2008) Protein kinases of malaria parasites: an update **Trends In Parasitology** 24: 570-7.

8. Kaushik DK and Sehgal D (2008) Developing antibacterial vaccines in genomics and proteomics era. **Scand J Immunol** 67: 544-552.

9. Shaha C (2008) Estrogens and Spermatogenesis. In: Molecular Mechanisms of Spermatogenesis Ed: C.Y.Cheng, Landes Bioscience, Austin, Texas. pp 42-56.

Patents

1. Shaha C, Jain R and Mandal C (2009) Detection of pathogen using antigenic prohibitin peptide. Patent application # 474/DEL/2009.

2. Suri A (2009) Inhibition of SPAG9 expression with siRNAs. European patent granted (Application No: 06710485.1).

3. Vrati S and Appaiahgari MB (2009) DNAzymes for inhibition of Japanese encephalitis virus replication. US patent application no. US-2009-0010907-A1 published on January 8, 2009.

5. Sehgal D and Rohatgi S (2009) Immunoglobulin gene specific oligonucleotides and uses thereof. Indian Patent Application # 634/DEL/2008.

6. Sehgal D and Rohatgi S (2009) Immunoglobulin gene specific oligonucleotides and uses thereof. Eurpoean Patent Application filed on 13.3.09.

7. Sehgal D and Rohatgi S (2009) Immunoglobulin gene specific oligonucleotides and uses thereof. United States of America Patent Application filed on 13.3.09.

Technology transfer

1. Garg L and Mathur D. Technology for the recombinant epsilon toxin based vaccine against *Clostridium perfringens* D transferred to Indian Immunologicals Limited, Hyderabad.

2. Garg L and Panda A. Technology for solubilization of recombinant proteins expressed as inclusion body transferred to Therapus, Chennai.

Trademark product

1. Panda A. Artskinii ^{TM} (A product for wound healing and burn treatment)